

Switch Panel Structural Performance (SP2)

Hiensch, Martin

DOI

[10.4233/uuid:99d6611c-ad5a-4eaa-b915-f6834fddd1f5](https://doi.org/10.4233/uuid:99d6611c-ad5a-4eaa-b915-f6834fddd1f5)

Publication date

2019

Document Version

Final published version

Citation (APA)

Hiensch, M. (2019). *Switch Panel Structural Performance (SP2)*. [Dissertation (TU Delft), Delft University of Technology]. <https://doi.org/10.4233/uuid:99d6611c-ad5a-4eaa-b915-f6834fddd1f5>

Important note

To cite this publication, please use the final published version (if applicable).
Please check the document version above.

Copyright

Other than for strictly personal use, it is not permitted to download, forward or distribute the text or part of it, without the consent of the author(s) and/or copyright holder(s), unless the work is under an open content license such as Creative Commons.

Takedown policy

Please contact us and provide details if you believe this document breaches copyrights.
We will remove access to the work immediately and investigate your claim.

19/8/2019



THESIS

SWITCH PANEL STRUCTURAL PERFORMANCE (SP2)

Proefschrift

ter verkrijging van de graad van doctor

aan de Technische Universiteit Delft,

op gezag van de Rector Magnificus, prof.dr.ir. T.H.J.J. van der Hagen

voorzitter van het College voor Promoties,

in het openbaar te verdedigen op

woensdag, 25 september, 2019 om 12:30 uur

door

Evert Jacob Martien HIENSCH

ingenieur, Hogeschool Utrecht, Nederland

Geboren te Rhenen, Nederland

Dit proefschrift is goedgekeurd door de

promotor: Prof. dr. ir. R.P.B.J. Dollevoet
copromotor: Dr. ir. M.J.M.M. Steenbergen

Samenstelling promotiecommissie bestaat uit:

Rector magnificus,	voorzitter
Prof. dr. ir. R.P.B.J. Dollevoet	TU Delft, promotor
Dr. ir. M.J.M.M. Steenbergen	TU Delft, copromotor

Onafhankelijke leden:

Prof. dr. ir. R.H. Petrov	Universiteit Gent
Prof. dr. D.I. Fletcher	Sheffield University
Prof. dr. ir. E. van der Heide	University of Twente
Dr. I. Shevtsov	ProRail
Dr. ir. J. Horst	DEKRA Rail
Prof.dr.ir. Z. Li	TU Delft, reservelid

Contents

Contents	3
Abstract	4
Samenvatting	6
Thesis	9
Review and summary	10
1 Introduction	10
1.1 Switch panel structural performance	10
1.2 Research aim, objective and scope	11
2 Research Approach	11
3 State-of-the-art review	12
4 Results and evaluation	13
4.1 Switch panel loading	13
4.1.1 Switch panel loading assessment; vehicle dynamics	13
4.1.2 Track friendliness of vehicles at the switch panel	15
4.1.3 FSS validation and implementation	17
4.1.4 Track friendliness of the freight bogie design	19
4.1.5 Governing train operational factors	21
4.2 Switch panel loading response	22
4.2.1 RCF damage model development from field data	22
4.2.2 Damage function development from two-disc testing	26
4.2.3 Rail grade selection	28
5 Thesis contribution	30
5.1 Reducing S&C loading levels	30
5.2 Switch panel loading response (fit-for-purpose)	32
5.3 Practical implementations of results	33
6 Concluding remarks and future work	35
6.1 Switch Panel loading levels	35
6.2 Switch panel loading response	36
6.3 Future work	36
Acknowledgements	38
References	39
Curriculum vitae	43
Appended papers	44

Abstract

Switches and crossings (S&C), also addressed as turnouts, are key elements in the railway network operation as they enable trains to change between tracks. At the same time, S&C are known to be vulnerable assets from the viewpoint of maintenance and failure. The vulnerability of S&C can be explained by the nature of its function, design, and the complex dynamic behaviour of a railway vehicle when negotiating an S&C.

Thus, as a pivot component S&C have a strong impact on the vulnerability of the railway system. In the Netherlands in the year 2010, train delays due to turnout failure were responsible for 55% of the total disruption time (source: ProRail). In view of its impact on cost, switch maintenance has claimed a disproportionate amount of the overall track maintenance budget (in the Netherlands in 2014 this amounted to 40%, source: ProRail). It is significant that European infrastructure managers put 'switch rail wear' in the top three of main reported track problems (source: EU project INNOTRACK, 2010). Improved structural behaviour of the switch panel is, therefore, expected to significantly support robustness of the railway system.

This thesis describes the development of measures and tools that support the structural behaviour of the railway switch panel. The work research project has improved our understanding of the root causes of switch panel rail damage and has identified potential mitigation measures. Improved engineering models have been developed, aiding switch maintenance and design. This research was performed on the basis of simulations of dynamic train-track interaction, inspections and measurements in track, measurements in trains, and laboratory testing. Achieving sustainability of the switch panel was investigated using a two-fold approach: one aiming at reducing the switch panel loading levels, the other at improving the switch panel response to loading resulting into a 'fit-for purpose' design.

Switch panel wear and Rolling Contact Fatigue (RCF) damage development are governed by the tangential (shear) forces and slip at the wheel-rail interface. The level of shear forces and slip can be represented by the calculated 'wear number' T_y , providing a parameter to quantify the occurring loading level as well as expected damage response. In this thesis the T_y approach therefore was central to the assessment of the study outcomes. From previously performed vehicle design evaluations it was recognised that operational levels of T_y and hence wear and RCF loading are significantly determined by the resistance the wheelset experiences when rotating around the yaw axis within the bogie frame, the so-called primary yaw stiffness. Studies conducted in this thesis aiming at lower levels of switch panel loading by optimizing vehicle design therefore focus on the primary suspension.

The concept of 'frequency selective stiffness' of the railway vehicle primary suspension design is evaluated in relation to switch panel negotiation. In conclusion, this concept can significantly contribute to a reduction of switch panel loading levels, improving the so-called track friendliness of the vehicle. For the assessed configuration, a significant reduction in switch panel wear loading is achieved (up to 50%) together with a significant reduction in the operational cost for the switch panel (with marginal cost reduced up to 60%).

Switch panel damage was further investigated for the 'as-is' situation in Dutch railway operation, based upon its current track and train characteristics. To understand how track engineers may reduce the development of switch rail damage, a sensitivity study was conducted with regard to

the dominant operational factors that influence switch loading and related damage development. For the assessed S&C configuration (being the most common type of turnout applied in Dutch track with crossing angle 1 in 9 and normal grade rail R260Mn) only (flange)lubrication is seen to reduce wear loading to levels preventing abnormal lateral switch wear. It was found that other investigated parameters did not play a decisive role (e.g. vehicle type, vehicle speed, direction of traffic, axle load, yearly tonnage, traction or mode of operation: push-pull vs. pull).

In order to support future optimisation of the S&C design and maintenance, work was carried out to understand the operational performance of different rail grades in terms of surface degradation with respect to occurring loading levels using the concept of rail damage function. This thesis defines the individual rail grade damage response to operational loading levels and further discusses and illustrates the potential of the RCF-damage function to support the process of rail grade selection and track maintenance. Using these damage functions/models, the damage response of different rail grades can be predicted given the dynamic loading conditions. This thesis extends the concept of rail damage function from the conventional rail grade to premium pearlitic rail. Rolling Contact Fatigue (RCF) damage index values for the normal R260Mn and the premium R370CrHT grade rail are established, describing the behaviour of the associated damage functions. The R370CrHT RCF damage function has implications with respect to rail grade selection in design situations. Compared to the normal grade, the increased fatigue crack initiation limit value of the R370CrHT damage function indicates a reduction in RCF susceptibility, preventing RCF initiation for an extended range of track curving conditions. Under equal loading conditions, the reduced slope of the ascending part of the R370CrHT damage function will result in a significant increase in expected time to until visible RCF damage initiation occurs as compared to normal grade rail.

It is shown that the concept of the rail damage function provides vital understanding of the operational performance of rail grades in terms of surface degradation. However, from the occurring wide range in track loading conditions it is difficult to achieve clear characterization results from track data only. To reach more controlled loading conditions, a rolling-sliding two-disc laboratory set up to define rail/wheel interface wear and RCF response was designed and validated here. The validation result suggest that the presented two-disc approach can be used to support future work to establish RCF-damage functions within a well-defined laboratory environment.

The RCF damage functions have significant engineering relevance. Their application allows for a dedicated rail grade selection, adapted to site-specific operational conditions. This can be expected to significantly affect the life-cycle costs as well as availability of track.

The work carried out in this thesis clearly shows how switch loading levels can be managed and how switch robustness to these loading levels can be improved. This work provides new tools and insights supporting switch panel structural performance, which is of great relevance for the achievement of high train punctuality and customer satisfaction at minimum life cycle costs. The research has directly contributed to the design and redesign of bogie components of the Dutch NS intercity fleet and to the ongoing discussion about the system of track access charging for the Dutch rail infrastructure.

Keywords: switch panel, wear, rolling contact fatigue (RCF), rail, damage model, track friendliness.

Samenvatting

Wissels zijn essentieel voor een goed functionerend spoorstelsel. Het wissel stelt een spoorvoertuig in staat veilig van rijweg te veranderen. Tegelijkertijd staan wissels bekend als kwetsbare onderdelen vanuit het oogpunt van falen en onderhoud. Deze kwetsbaarheid wordt verklaard door de aard van de functie, het ontwerp en het complexe dynamische gedrag van een voertuig tijdens de passage van een wissel.

Mede door hun knooppuntfunctie zijn wissels verantwoordelijk voor een substantieel deel van de storingen op het spoorwegnet. Dit is hinderlijk voor zowel reizigers als spoorbeheerders. In het jaar 2010 waren de treinvertragingen als gevolg van wisselstoringen verantwoordelijk voor ca. 55% van de totale verstoringstijd op het Nederlandse spoor (bron: ProRail). De impact op kosten wordt zichtbaar door het onderhoudsbudget voor wissels, dat een onevenredig groot deel van het totale onderhoudsbudget voor het spoor claimt (in Nederland bedraagt dit in 2014 ca. 40%, bron: ProRail). Het EU project INNOTRACK stelde in 2010 vast dat slijtage van de tongbeweging zich in de top drie bevindt van de gerapporteerde belangrijkste problemen van Europese infrastructuurbeheerders. Er mag dan ook worden verwacht dat een structurele verbetering van het gedrag van het wissel de robuustheid van het spoorwegsysteem aanzienlijk ten goede zal komen.

Dit proefschrift beschrijft de ontwikkeling van maatregelen en hulpmiddelen gericht op een structurele verbetering van het gedrag van het wissel, met name van de tongbeweging binnen het wissel (de wisseltong en aanslagspoorstaaf). Het uitgevoerde werk richt zich op de fundamentele oorzaken van spoorstaafschade binnen de tongbeweging en onderzoekt mogelijke beheersmaatregelen. Het onderzoek binnen dit proefschrift is uitgevoerd op basis van simulaties van dynamische interactie tussen voertuig en baan, inspecties en metingen in het spoor, metingen uitgevoerd aan treinen en laboratoriumtests van componenten. Om te komen tot een toename van de duurzaamheid van het wissel is een tweevoudige benadering toegepast. Eén gericht op het verminderen van de door de trein opgelegde belasting, de andere op het verbeteren van de weerstand van de tongbeweging tegen de opgelegde belasting, gericht op een 'fit-for-purpose' wisselontwerp.

Tangentieële krachten en slip in het wiel-railcontact bepalen in sterke mate de optredende slijtage en RCF binnen de tongbeweging. Het niveau van deze schuifkrachten en slip kan worden gekwantificeerd aan de hand van de berekende 'wear number' T_y . Eerder uitgevoerde evaluaties van voertuigontwerpen laten zien dat operationele niveaus van T_y (en dus de intensiteit van slijtage en RCF) sterk worden bepaald door de weerstand die het wielstel ondervindt bij een rotatie rond de verticale as binnen het draaistelframe (een verandering van bewegingsrichting); de zogenoemde primaire uitdraaistijfheid. Deze primaire uitdraaistijfheid hangt af van het ontwerp van de primaire vering. In het streven naar een verlaging van de optredende belasting door middel van optimalisatie van het voertuigontwerp richt deze thesis zich daarom op de primaire vering.

Met betrekking tot de primaire vering van voertuigen is het concept van frequentieafhankelijke stijfheid onderzocht in relatie tot de belastingen die optreden tijdens het doorrijden van een tongbeweging. Geconcludeerd wordt dat dit concept aanzienlijk kan bijdragen aan de zogenoemde 'spoorvriendelijkheid' van het voertuig. Voor de beoordeelde configuratie wordt een aanzienlijke vermindering van de slijtagebelasting van de tongbeweging bereikt (tot 50%) wat resulteert in een significante verlaging van de samenhangende verwachte operationele kosten (tot 60%).

Tevens is de spoorstaafschade in de tongbeweging onderzocht zoals deze momenteel optreedt binnen van het Nederlandse spoorvervoer, gebaseerd op de huidige infra- en

voertuigeigenschappen. Om te begrijpen welke beheersmaatregelen de baanspecialist effectief kan inzetten omtrent de instandhouding van zijn wissels is een gevoeligheidsonderzoek uitgevoerd waarbij de meest dominante operationele factoren zijn geïdentificeerd die van invloed zijn op wisselbelasting en gerelateerde schadeontwikkeling. De beoordeelde configuratie betreft het type wissel dat binnen het Nederlandse spoor het meest wordt toegepaste (wisseltype met hoekverhouding 1:9). Voor deze configuratie geldt dat enkel de inzet van (flens) smering de slijtagebelasting in afbuigende richting dusdanig kan verlagen dat abnormale zijdelingse slijtage wordt voorkomen. Andere onderzochte parameters blijken geen bepalende factor te zijn (bijvoorbeeld voertuigtype, voertuigsnelheid, rijrichting, aslast, jaarlijkse tonnage, tractie noch type operatie: trek-trek vs. trek-duw).

Om toekomstige optimalisatie van het ontwerp en onderhoud van wissels te faciliteren is inzicht verkregen in de operationele prestaties van verschillende spoorstaafkwaliteiten in termen van degradatie van het loopvlak in relatie tot optredende belastingniveaus. Dit gedrag is beschreven vanuit het concept van materiaal-afhankelijke schademodelen. Met behulp van de hierin vastgelegde functies kan de verwachte schadeontwikkeling voor verschillende spoorkwaliteiten worden afgeleid in relatie tot de specifieke belastingomstandigheden. Dit proefschrift breidt dit concept uit van de standaard perlitische kwaliteit spoorstaaf naar die van de premiumkwaliteit. Rolling Contact Fatigue (RCF) schade-indexwaarden voor de normaalkwaliteit R260Mn en de premium R370CrHT kwaliteit spoorstaaf zijn vastgesteld. Deze waarden beschrijven het gedrag van de bijbehorende schadefuncties. De vastgestelde grenswaarde voor initiatie van vermoeiingsschade ligt voor de R370CrHT-schadefunctie duidelijk boven die voor het R260Mn spoorstaafmateriaal. Dit duidt op een afname in RCF-gevoeligheid voor het R370CrHT materiaal en op een toename van het bereik van belastingcondities waaronder RCF-initiatie wordt voorkomen. De verminderde helling van het opgaande deel van de R370CrHT-schadefunctie zal, onder gelijke belastingcondities, resulteren in een aanzienlijke toename van de verwachte tijd tot zichtbare RCF-schadeinitiatie.

Aangevoerd wordt dat het concept van de schadefunctie een vitaal begrip biedt van de operationele prestaties van spoorstaafkwaliteiten in termen van loopvlakdegradatie. Schadefuncties zijn in het verleden opgesteld op basis van observaties in het spoor in combinatie met voertuig-baan simulaties. Echter, vanuit het voorkomende brede bereik in belastingomstandigheden is het moeilijk om enkel vanuit praktijkobservaties te komen tot een eenduidige karakterisering. Om te komen tot meer gecontroleerde belastingstoestanden is in deze thesis een twee-schijven laboratoriumbeproeving ontworpen om de RCF- responsie te definiëren. Het resultaat van de validatie laat zien dat de gepresenteerde aanpak kan worden gebruikt ter ondersteuning van toekomstige werkzaamheden om RCF-schadefuncties vast te stellen binnen een gedefinieerde laboratoriumomgeving.

De RCF-schadefuncties zijn van groot operationeel belang. Hun toepassing biedt de onderbouwing voor een gerichte spoorstaafkeuze, aangepast aan locatie-specifieke operationele omstandigheden. Verwacht mag worden dat deze wijze van spoorstaafselectie zal bijdragen aan het terugdringen van de onderhoudskosten van het spoor evenals een verbetering van de beschikbaarheid van de infra.

De werkzaamheden in dit proefschrift laten duidelijk zien hoe de belastingniveaus die optreden binnen de tongbeweging kunnen worden beheerst en hoe de robuustheid van de tongbeweging voor deze belastingniveaus kan worden verbeterd. Het onderzoek heeft direct bijgedragen aan het (her)ontwerp van draaistelcomponenten van de intercityvloot van de

Nederlandse Spoorwegen (NS) en aan de discussie rondom de invulling van de gebruikersvergoeding van de Nederlandse railinfra.

Trefwoorden: tongbeweging, slijtage, RCF, spoorstaaf, schademodel, baanvriendelijkheid.

Thesis

This thesis consists of an extended summary and the following appended papers:

1. Hiensch, E.J.M. Wiersma, P. Reducing switch panel degradation by improving the track friendliness of trains, *Wear* 366-367 (2016) 352–358, <http://dx.doi.org/10.1016/j.wear.2016.03.031>
2. E.J.M. Hiensch & N. Burgelman (2017): Switch Panel wear loading – a parametric study regarding governing train operational factors, *Vehicle System Dynamics*, <http://dx.doi.org/10.1080/00423114.2017.1313435>
3. Hiensch M. Burgelman N. Hoeding W. Linders M. Steenbergen M. Zoeteman A. Enhancing rail infra durability through freight bogie design. *Vehicle System Dynamics* (2017). DOI: <http://dx.doi.org/10.1080/00423114.2017.1421766>
4. Martin Hiensch and Michaël Steenbergen, Rolling Contact Fatigue on premium rail grades: Damage function development from field data, *Wear* 394–395 (2018) 187–194, <https://doi.org/10.1016/j.wear.2017.10.018>
5. Martin Hiensch and Nico Burgelman, Rolling Contact Fatigue: damage function development from two-disc test data, *Wear* 430-431 (2019) 376-382, <https://doi.org/10.1016/j.wear.2019.05.028>

Contribution to co-authored papers

As the first author of all publications listed above, I initiated and designed the research approach and was responsible for the acquisition, analysis, and interpretation of the data. I have carried out multiple track inspections, field measurements and laboratory tests, also designing the train-track simulations required to gain further understanding in switch panel loading. I independently drafted the work and revised it critically for important intellectual content. I have written all the articles myself. I am also responsible for the approval of the published final version of each paper. During peer review, I ensured that questions related to the accuracy or integrity of any part of the work were appropriately investigated and resolved.

My co-authors primarily supported activities related to the use of the simulation software VAMPIRE® Pro 6.30 to simulate vehicle dynamics. This consisted of setting up new and adjusting existing vehicle and track models together with the preparation and execution of simulation run files according to the author's specifications. The co-authors further contributed through discussions and reviews of article draft versions.

Review and summary

1 Introduction

The work presented in this thesis is part of the integrated project ‘Sustainable Switches’, more specifically the research line covering the ‘Structural Performance of the Switch Panel’. This research was carried out by the author under the project number T91.1.12475a in the framework of the Research Programme of the Materials innovation institute M2i. The structure of this extended summary is the following. Within chapter 1 the scope, aim and objective of the research is presented, followed in chapter 2 by a description of the research approach. An overview of the state of the art of the relevant research area is presented in chapter 3. Chapter 4 presents the results and evaluation of the performed work, with the contribution of this thesis to the improvement of switch panel structural performance presented in chapter 5. Concluding remarks and suggestions for future work are presented within chapter 6.

1.1 Switch panel structural performance

Switches and crossings (S&C), also addressed as turnouts, are key elements in the railway network operation as they enable trains to change between tracks. Allowing trains to reach their targeted platform, the number of railway switches per route length is especially high at and around railway stations. A railway turnout consists of a switch panel and a crossing panel connected by a closure panel. The designated areas in turnout negotiation are indicated in figure 1.

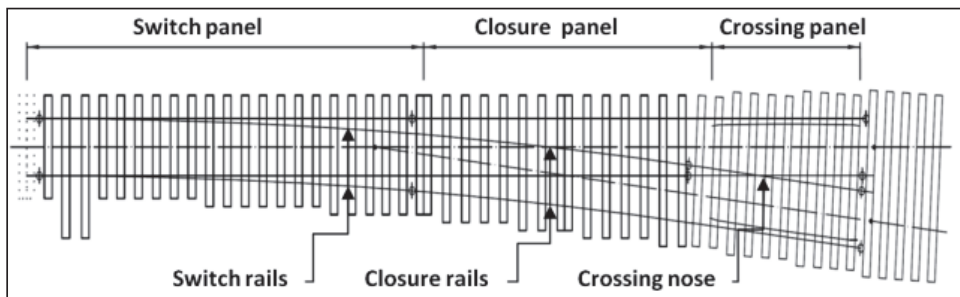


Figure 1: Designated areas in turnout negotiation

Railway switches are heavily loaded by trains. Resulting damages lead to urgent and unplanned replacements, non-availability of tracks, and high maintenance and replacement costs. The increasing use of rail by both passenger and freight traffic demands an increasing effort and costs for the maintenance of tracks and, if unchallenged, could become a major constraint in the development of overall railway productivity. Issues with track availability and cost related to maintenance will present themselves first at the more vulnerable bottlenecks in the railway network. From this viewpoint, S&C clearly stand out; thus, improving the reliability of switches will be bound to have a positive effect on railway performance.

The turnout ‘Switch panel’ determines the resulting route of vehicles and consists of switch and stock rails. As already mentioned it is known to be a vulnerable part of turnout design. The EU research project INNTRACK (Concluding Technical Report), aiming to reduce cost and improve the reliability of track systems, concludes that ‘switch wear’ is one of the top three main reported track problems. Apart from wear, Rolling Contact Fatigue (RCF) damage (the initiation and growth of fatigue cracks on

the rail running surface) also influences switch panel performance negatively. The work carried out in this thesis concerns the improvement of the structural performance of the switch panel in two ways: on the one hand by reducing the forces imposed on it and on the other hand by improving its response to these forces.

1.2 Research aim, objective and scope

The general aim of this work is to obtain an interdisciplinary understanding of damage mechanisms of the switch panel (switch and stock rail) and to identify possibilities for the optimisation of the switch panel long-term behaviour. The research is situated in the disciplines of vehicle-track interaction, contact mechanics, and metallurgy. The practical application of this general research aim leads to the decrease of life cycle cost (LCC) of switches both by an improved design and appropriate maintenance strategies, resulting in a reduction of operational disturbances on the railways due to uncontrolled switch damage.

The research objective is to improve the understanding of the root causes of switch panel rail damage and potential mitigation measures and to develop improved engineering models to support optimisation. The research specifically focuses on the dynamic interaction between a railway vehicle and track. Switch panel loading levels, the resulting stresses and forces acting within the wheel-rail contact, and rail material damage response are of special interest here. To achieve the mentioned objective, the following four sub-objectives have been defined:

- 1) On the basis of simulations of dynamic train-track interaction, switch panel loading levels should be evaluated in relation to measures aimed at improving the so-called track friendliness of the vehicle;
- 2) Classifying observed switch panel damage, deterioration of the switch panel running surface is to be further understood;
- 3) On the basis of track inspections and train-track simulations, switch panel damage development should be studied in dependence to train and track operational factors;
- 4) Design rules/models should be developed that provide new tools and insights supporting switch panel structural performance.

2 Research Approach

Different methods of investigation were used for this research project: literature studies, dynamic modelling, field testing and laboratory testing. **The first part** of the work focused on the loading levels imposed on the switch panel and the ways in which these levels can be influenced. Through track-train simulations, switch panel loading levels were established with regard to conventional trains and so-called 'track-friendly' trains which produce low or moderate forces on the track with an emphasis on the impact of vehicle primary suspension design modifications (**paper 1** and **paper 3**). Validation of the applied track-friendly vehicle model and functionality of the novel primary suspension design was carried out by means of measurements at vehicles in service and laboratory component tests. Furthermore, a sensitivity analysis was carried out to investigate switch panel loading levels with regard to train and track operational factors e.g. direction of traffic, vehicle speed, lubrication, and traction (**paper 2**).

The second part of the study aimed to optimise the switch panel damage response to the occurring loading levels. On the basis of performed train-track simulations in combination with track inspections, Rolling Contact Fatigue (RCF) damage index values for the normal and premium grade rail were established, describing the course of the damage functions (**Paper 4**). This part of the work

greatly improved the understanding of rail grade performance towards (switch panel) loading conditions. From the occurring wide range in track loading conditions it is difficult to achieve clear characterization results from track data only. To reach more controlled loading conditions, a rolling-sliding two-disc laboratory set up can be applied. To this end a two-disc test approach to define rail/wheel interface wear and RCF response was designed and validated (**Paper 5**).

3 State-of-the-art review

The design of railway turnouts has traditionally been based on the assessment of vehicle response using kinematic equations, evaluating the maximum values of lateral acceleration, rate of acceleration change, and jerk. According to Oswald and Bishop (2001), it is a clear shortcoming of traditional design methods that they have not taken dynamic vehicle response into account. This was illustrated by field measurements confirming lateral accelerations in turnouts to be up to twice the kinematic values. Therefore, to improve the understanding of vehicle running behaviour at a turnout and to identify possible optimisation of turnout design, an evaluation of the dynamic interaction between vehicle and track, wheel and rail is essential. Since the railway switch panel is characterized by a gradually changing rail profile with changing wheel-rail contact conditions, the dynamic interplay between vehicle and switch panel is even more complex.

In recent years, multi-body simulation packages have been used for the prediction of railway vehicle dynamics, with the associated wheel-rail contact forces used as input to material degradation models. Oswald and Bishop (2001) and later Kassa (2006) were among the first to investigate the railway switch by simulation of dynamic interaction between train and railway turnout using multi-body software. Oswald and Bishop (2001) studied different curve geometries for the diverging route and concluded that, compared to constant radius geometries, turnouts with clothoid type geometry result in improved vehicle performance. Comparing perfect geometry response to simulations made with varying random track defects, Oswald and Bishop (2001) have shown that design geometry calculations can predict net or average improvements. Kassa and Johansson (2001) studied the switch rail at the diverging route with respect to vehicle characteristic such as wheel profile, axle load, and vehicle speed in relation to contact pressure and wear. They showed that the large contact pressure on the switch rail mainly results from poor contact geometry conditions. Further research on train operational parameters which are potentially important regarding accumulated damage development is required. The possible contribution of novel running gear design on track loading was studied e.g. by Iwnicki (2013) and Tunna (2009); however, until now these studies have focussed on the running behaviour at plain track. Regarding the design of the vehicle, they concluded that the characteristics of the Primary Yaw Stiffness (PYS) significantly influence the resulting rail surface damage. The impact of improved track friendliness of trains regarding switch panel negotiation has not been studied yet. Öberg and Andersson (2009) established a cost calculation system for determining the deterioration cost for railway tracks. This allows the effect of track friendliness to be quantified in terms of cost.

Concentrating on track characteristics, further improvement of the switch panel design for the through route was studied by Nicklisch (2010) and Bugarín (2002). Based on a parametric study, dynamic track gauge optimisation by geometry gauge variation resulted, for the analysed configuration, in a significant reduction of wear and improved behaviour in terms of rolling contact fatigue. The suggested gauge widening can be successful for the through route; it is, however, not effective in mitigating problems in the diverging route. Investigating the effect of track stiffness, Nicklisch (2010) concluded that a considerable reduction in wear index is obtained when varying the

rail pad stiffness and ballast/subgrade stiffness to smoothen the large change in track stiffness along the switch panel. Pålsson and Nielsen (2012) further studied switch rail profile design, optimising rolling radius characteristics to improve switch kinematics.

An alternative approach to improving the structural behaviour of the switch panel lies in the improvement of the material resistance to the imposed stress and slip levels. Here rail damage models can be used as an asset management tool to analyse specific track sections, assessing the likelihood of RCF crack initiation and wear on the basis of given loading conditions. Burstow (2003, 2004) investigated the damage response of the R220 normal rail grade, characterising this material in terms of the loading history and related RCF damage development. Understanding the performance of further rail grades, as a function of operational loading conditions, is vital to support the process of rail grade selection. The level of achieved knowledge and development in the research domain of switch panel loading and damage response was further discussed in the published **papers 1 to 5**.

4 Results and evaluation

This chapter discusses the performed work regarding switch panel loading levels, obtaining an improved understanding of the ways in which these loading levels can be influenced and of the associated rail damage response.

4.1 Switch panel loading

4.1.1 Switch panel loading assessment; vehicle dynamics

The vulnerability of S&C is determined by the nature of its function, design, and resulting forces. The dynamic behaviour of a railway vehicle in S&C is complex. From the switch toe (figure 2), moving down the switch panel, switch- and stock rail profiles are gradually changing. This has an ongoing effect on the contact positions between wheel and rail, the occurring rolling radius difference, and resulting (tangential) wheelset steering forces. To calculate these forces and stresses acting within the wheel-rail contact patch, relative motion of the two contacting bodies, elastic deformations, and friction processes need to be accounted for. To solve the wheel-rail contact problem, Kalker (1991) developed numerical methods for rolling contact, making these available through his programme CONTACT and later the fast algorithm FASTSIM. Within vehicle system dynamics packages, multi-body software is used to describe both track and vehicles by a number of interconnected rigid or flexible bodies. System behaviour is obtained through the analysis of the equations of motion, computing the dynamic movement of the different components, allowing the rail-wheel contact slip and locations to be determined. Then normal contact forces can be determined by using, for example, Herizian formulas and FASTSIM for the tangential direction.

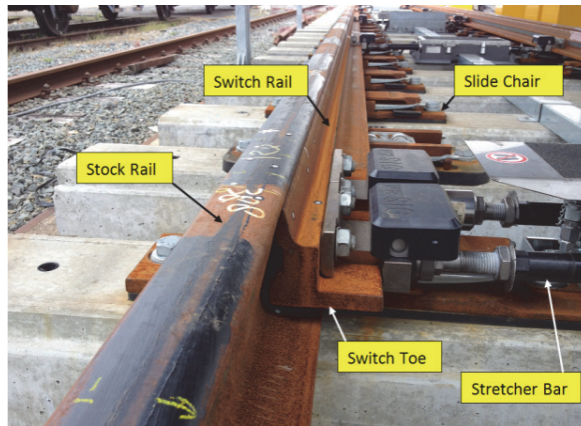


Figure 2: Switch panel components

The use of dynamic simulation tools provides the railway engineer with the ability to quantify the impact of changes in design and operational parameters, by considering the complete interaction between vehicle and track. This work requires track and vehicle models to be set up, as well as operational inputs such as speed and loading profiles. The simulation software VAMPIRE® Pro 6.30 was used to simulate vehicle dynamics for traffic at the diverging route. Each multi-body model of a turnout (switch and closure panel) is based upon a mass-spring-damper system. This track model consists of two rails, each attached to the rigid, massless sleeper by spring-damper elements in the lateral direction. The sleeper is connected with two vertical spring-damper elements to the rigid ground. The track model is coupled to each wheelset in the vehicle model (moving track model). The S&C track models set-up in this research project describe the diverging route through the switch panel of the most common type of turnout applied in Dutch track: crossing angle 1:9, as well as the ProRail New Generation (NG) type switches NG1:18 and NG1:29. The cross-sectional geometry through the complete switch panel of each type was built up from over 120 transverse rail profiles, measured in track, using the MiniProf measurement system. The left and right rail profiles were measured individually. For the switch panel only nominal track geometry design values were applied (gauge, alignment, level and cant). For the work in this thesis, three different vehicle models were applied, together sufficiently representative to assess overall ProRail infra loading conditions. Two types of applied vehicle models were already partly available and one type was built from scratch. Two of these vehicle models were extended in order to evaluate the impact of bogie design variations.

Evaluating the output from the vehicle dynamic simulations, expected wear and Head Check damage development can be derived from the RCF damage function as first proposed by Burstow. The RCF damage function describes the relationship between the wear energy number T_γ and RCF crack initiation fatigue damage. The parameter T_γ represents the work performed by the frictional shear stresses in the moving wheel-rail contact patch, usually considered per travelled unit distance along the track. This work is equivalent to energy dissipated in the contact patch, and is commonly expressed for a unit length of 1 m, giving rise to T_γ being expressed in the unit [J/m] or [N]. The wear number T_γ is calculated from the sum of the lateral and longitudinal products of shear forces (T_x and T_y) and creepages (γ_x and γ_y) at the wheel/rail interface. The wear number is a standard output from

vehicle dynamics software. From the model the calculated T_y is translated into a fatigue damage index, indicating the number of loading cycles to visual crack initiation. This 'RCF damage index' expresses the number of cycles before visible RCF cracks can be expected on the rail head. In the case of switches, the assessment of T_y loading distinguishes two contacting areas: the running surface (rail crown/ shoulder) and flange. Further assessment of vehicle running behaviour by means of track-train simulations is aimed at the evaluation of running stability, dynamic track loading, and passenger comfort.

4.1.2 Track friendliness of vehicles at the switch panel

Tangential forces and slip govern the wear and rolling contact fatigue of the switch panel. As explained in the previous paragraph the level of shear forces and slip at the wheel/rail interface can be represented by the calculated 'wear number' T_y . Vehicle design evaluations show that operational levels of T_y (and hence the intensity of wear and RCF) are strongly determined by the resistance the wheelset experiences when rotating around the yaw axis within the bogie frame (changing the direction of motion), the so-called primary yaw stiffness. In line with the objectives in par. 1.2, this thesis aims at a reduction of the switch panel loading through vehicle design optimisation and therefore focuses on the primary suspension.

Recent developments within bogie design are aiming, among other things, at the application of new elastic components with a characteristic that is dependent on the frequency of loading. These so-called **Frequency Selective Stiffness (FSS)** elements can, when applied at the primary yaw suspension, provide the required high stiffness at high loading frequencies to ensure stable running, together with low stiffness at low frequencies, resulting in moderate loading when negotiating a curve or switch. **Paper 1** presents the performance of primary suspension elements with Frequency Selective Stiffness (FSS) behaviour in bogies with respect to the ability to reduce wear and fatigue damage at the wheel-rail interface, thus enhancing the so-called 'track friendliness' of trains. Vehicle behaviour during the negotiation of a turnout is evaluated in a case study with the Dutch double stock VIRM-4 train. The impact of FSS suspension elements is quantified in relation to wear and rolling contact fatigue damage (RCF) in the wheel-rail interface and regarding ride quality.

For the application studied in this thesis, FSS behaviour is achieved by redesigning the classic steel-rubber component, adding internal chambers filled with hydraulic liquid. Connecting these chambers through a channel, serving as a flow control, adds a damper function to the component. The component stiffness becomes sensitive to the speed at which the fluid is transported from one chamber to another, resulting in a frequency-dependent stiffness (figure 3). This type of component, also addressed as '**hydro bush**', can often be retro-fitted within the existing train concept by simply replacing the conventional bush.

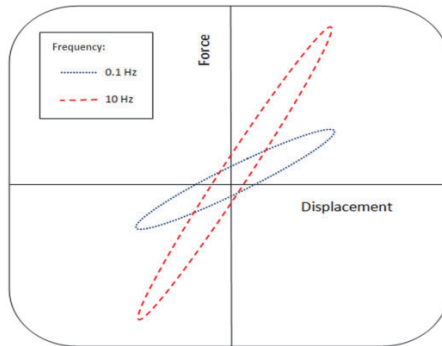


Figure 3: Typical FSS stress-strain behaviour depending on loading frequency

The research shows that with the application of FSS elements at the primary suspension, wear loading of switch and closure rail can be reduced significantly, increasing expected maintenance intervals and rail life. Simulation results demonstrate that passenger comfort levels are not influenced negatively.

4.1.3 FSS validation and implementation

Following the promising simulation results, a field test programme was set up for further ascertainment of the impact of FSS on vehicle behaviour. For this trial stage, three bogies of VIRM-4 vehicle were equipped with FSS radial arm bush elements; the other bogies retain their conventional bushing (in total the test train consisted of four wagons, with two motor and six trailing bogies in total – figure 4).

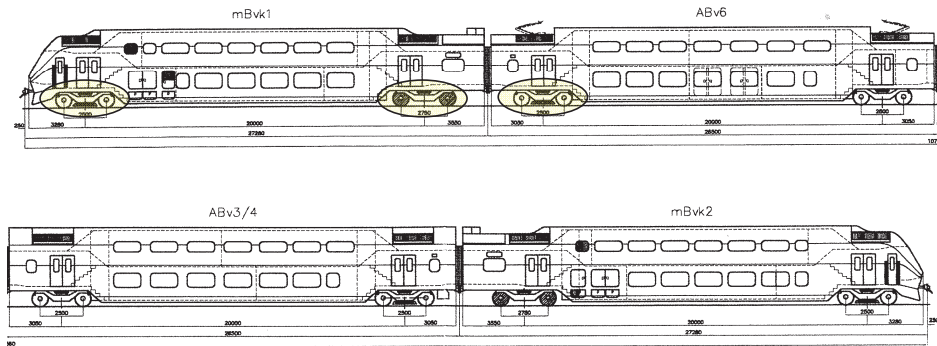


Figure 4: VIRM-4 vehicle. Bogies fitted with FSS are marked yellow (dark wheels are motored)

Test train operation was carried out in accordance with normal service conditions, covering in total about 500 km of track. On-board measurements (displacements, accelerations and forces) were performed to assess the impact of FSS application on curving behaviour, switch negotiation, running behaviour, and passenger comfort. Halfway through the testing programme, the facing direction of train was reversed (front side became back). Measuring the same track without a change in running direction with respect to the track allowed for a direct comparison e.g. between the behaviour of both motor bogies. These test results also provided the opportunity for further validation of the simulation vehicle model.

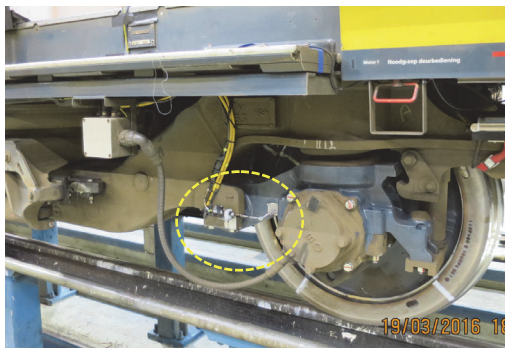


Figure 5: Instrumented VIRM-train motor bogie with FSS component installed at the radial arm (circled).



Figure 6: Detail - instrumented radial arm (measuring displacement)

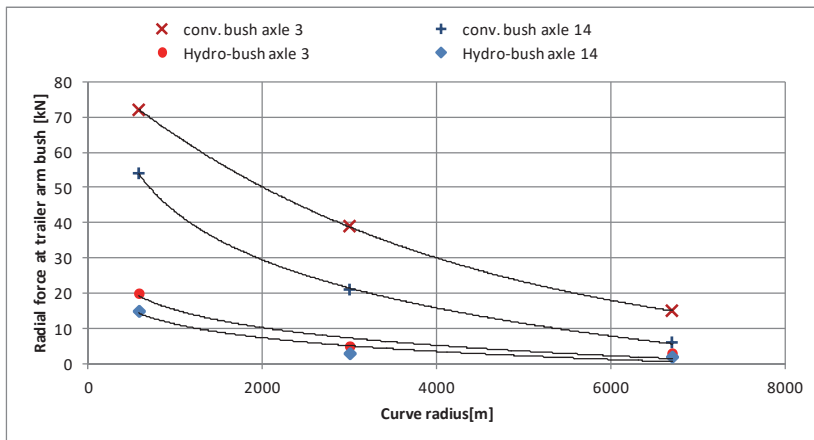


Figure 7: Average radial force at the trailer arm bush in dependence to curve radii

The measurement results further confirmed the expected beneficial behaviour of the FSS component. The axle numbers in figure 7 correspond to the position in the train. Axle 3 represents the first axle of the leading motor-bogie at the front end of the train; axle 14 represents the second axle of the motor bogie at the rear end of the train. Figure 7 clearly shows the level of the average radial force resulting from the longitudinal displacement of the trailer arm to be significantly lower for the bogie equipped with Hydro-bush compared to the conventional design. This is mainly related to the lower quasi-static stiffness of the hydro-bush elements. Moreover, the measured dynamic force variations during curving are smaller for the hydro-bush elements. These results further confirm the application of the hydro-bush to result in a significant reduction of wheel-rail forces at curving as was also concluded from the simulation work.

Comparing the calculated running behaviour from simulations with the measured values showed good agreement. Judging from the simulation results, the application of the hydro-bush with 15kN/mm radial high frequency stiffness should not lead to higher levels of lateral accelerations and, thus, should have no consequences for passenger comfort. This was confirmed by the field test measurements.

Component lifetime

Apart from its effect on vehicle behaviour, the expected lifetime of the FSS component is also an important feature when considering the replacement of the conventional bush by a hydro-bush. This should not lead to a shortening of the current bogie overhaul interval. To determine the expected lifetime, a representative load collective was established from the field measurements. Parallel to the field experiments a second load collective was established on the basis of train-track simulations, assessing over 200 km of measured track geometry, representing a VIRM dominated route. The load collectives derived from the field measurements and from the simulations showed good agreement, providing a valid base to perform the life time calculation. It can be concluded from this calculation that under these operational conditions the required minimum lifetime of 2,4 million km will be achieved. From additional laboratory testing the lifetime development of the frequency dependent characteristics of the hydro-bush were further evaluated. To this end two loading sequences were derived from the rain-flow analysis of the measured load collective: one representing moderate

loading, the other excessive overload. These sequences were applied to a number of hydro bushes by means of a servo-hydraulic test bench (figure 8). During these endurance tests no severe changes in force or stiffness were measured, indicating that no internal fracture or defect occurred.



Figure 8: Hydro-bush dynamic testing at 100KN servo-hydraulic test bench

4.1.4 Track friendliness of the freight bogie design

Based on the demonstrated positive effect in **Paper 1**, an additional study was performed to provide further insight into potential contributions to track friendliness. This assessment was carried out in relation to track deterioration mechanisms and cost in order to improve the understanding of how potential benefits are best to be utilized. To this end, six proposed freight bogie design measures were evaluated with respect to the improvement in curving behaviour, switch negotiation, and related track degradation mechanisms. Additionally, the impact on track deterioration costs was calculated for those track-friendly design modifications identified as most promising (**Paper 3**).

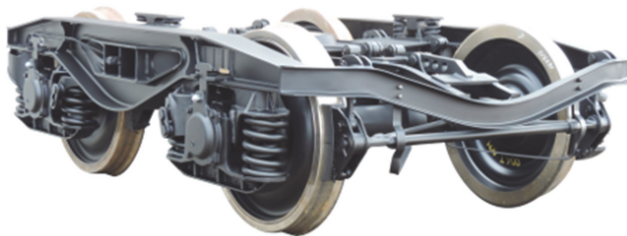


Figure 9: The bogie Y25L is admitted for axle loads up to 22,5 ton (picture by courtesy of Transwagon AD)

Economic evaluation

Öberg and Andersson's (2009) track deterioration cost calculation model is able to differ between vehicle types based on their characteristics and tendency to deteriorate tracks. The model applies the marginal cost methodology, aiming to determine the additional cost per extra vehicle unit by determining the impact of that vehicle. This model is applied in **Paper 3**, which assesses the impact of the proposed track-friendly designs regarding track deterioration costs. As case study we selected a dedicated freight corridor. The first step in calculating the deterioration cost is to determine the marginal cost level currently in place for infrastructure in the Netherlands (marginal cost is the cost related to one additional unit, in this case an additional freight wagon across the corridor). A set of VAMPIRE® tracks models was subsequently set up, representative of the studied corridor. From the executed simulation runs, input data to the deterioration model is acquired, consisting of Ty wear numbers, guiding forces, and dynamic wheel loads. Finally the deterioration cost per ton-km for each vehicle concept is calculated.

From **Paper 3** it is concluded that the standard Y25L freight bogie design displays rather track-friendly behaviour. For the assessed operational conditions, the reference Y25L bogie displays excellent curving behaviour for curves with radii >750m, keeping operational Ty levels below the RCF damage threshold. At switches and narrow radius curves, the track-friendliness for the standard Y25 reference situation is seen to decrease sharply, causing the related marginal cost to significantly increase. The calculated marginal cost at switches is about 12 times the cost at tangent track. Tuning the primary yaw stiffness shows a high potential for a further improvement of track-friendliness, significantly reducing track deterioration cost at narrow radius curves and switches (by respectively 30 and 60%). However, since narrow radius curves and switches only represent a small part of the total route, the resulting marginal cost in the executed corridor study is dominated by tangent track and large radius curve sections. Although not significantly contributing to the calculated overall cost, measures decreasing the track deterioration for switches and narrow radius curves, as the more vulnerable track elements, are expected to be beneficial from the viewpoint of track availability and overall performance. Currently this seems to be insufficiently reflected in the overall assessment result. When calculating the overall deterioration cost for the travelled route, the calculation model should include a well-balanced representation of switches and narrow radius curves. This will support the development of future track access charging systems, stimulating the design and introduction of vehicles with improved track-friendliness.

Within Europe, the infrastructure providers of Switzerland (SBB) and the United Kingdom (Network Rail) have introduced a system of Track Access Charging (TAC) taking into account the level of train track friendliness. Their objective is to achieve a more transparent and fair system allocating direct costs at train level to the 'polluter pays' principle and to stimulate the introduction of more track friendly vehicles. Both the Swiss and the UK infrastructure charging system aim to recover the cost related to the use of the infrastructure from the train operator. Both systems try to quantify the contribution of individual vehicles to infrastructure degradation on the basis of recognized damage models. The UK system assesses track friendliness of rolling stock mainly on the basis of the RCF damage index. Compared to the UK, the Swiss use a more extensive set of damage parameters in their assessment and take account of multiple degradation mechanisms. This assessment concerns not only the RCF damage index, but also the degradation of the track geometry and fatigue of infrastructure components.

Vehicle specific cost are established from the calculated individual damage parameters combined with the established cost factors regarding track maintenance. This results in a table with rates per vehicle class (€ / veh-km), with speed-dependent and (for freight wagons) load-dependent values (see figure 10). The Swiss TAC calculation method uses a classification of the entire network in curve or speed sections. For the Swiss situation, with a network containing both routes with relatively many curves and routes with relatively few curves, the adopted system leads to a more fair allocation of costs. The division into categories of curve radii and infra-assets may also have the advantage that possible track-related optimisations can be taken into account. SBB expects that the newly introduced TAC system will lead the total TAC to be build-up of around 60% by the set basic price for the route (governed by train kilometres, demand, and priority of the requested train path). Around 40% of the TAC will be determined by the vehicle specific contribution to track degradation. It is expected that this will lead to a slight decrease in the infrastructure charge for freight stock and an increase for intercity and regional traffic. Given the Dutch situation with a relatively weak subsoil and associated problems with degradation of the track geometry and fatigue of runway components, the Swiss method with regard to the determination of variable costs seems more appropriate.



Figure 10: TAC established on the basis of vehicle type, speed and for freight wagon the individual load. For example: loco class x – 80 km/h, three wagons class y -full, three wagons class z-empty (source: SBB).

4.1.5 Governing train operational factors

The acting forces and resulting material degradation at the running surfaces of wheels and rail are determined by vehicle, track, interface, and operational characteristics. Vehicle and track characteristics are addressed in **Paper 1 and 3**. The interface and operational characteristics are covered by performing a sensitivity analysis of interface and operational factors and their impact on expected switch panel wear loading (**Paper 2**). To this end, a parametric study was carried out by means of vehicle-track simulations. Additionally, theoretical concepts were cross-checked with operational practices by means of a case study in response to a dramatic change in lateral rail wear development at specific switches in Dutch tracks.



Figure 11: Example of excessively worn and spalled switch rail

Data from train operation, track maintenance, and track inspection was analysed, providing further insight into operational dependencies. The simulations performed in this study have shown that switch rail lateral wear loading in the diverging direction of a 1:9 type turnout, is significantly influenced by the level of wheel-rail friction and to a lesser extent by the direction of travel. The other studied operational parameters (vehicle speed, traction, gauge widening, and track layout) showed no significant impact on the expected wear loading. The significance of the wheel-rail friction coefficient regarding wear development was further underpinned by the case study results. The one distinct difference between the investigated 'severe' and 'mild' wearing switches is the presence of lubrication at the latter. Another interesting case study result shows that it is not the annual tonnage that is the switch rail life defining parameter here, but much more the occurring wear regime. For the modelled setup a change in wear regime from severe to mild could only be reached with decreased wheel-rail friction. Judging from the switch rail life development at the inspected site, the mode of operation (push-pull vs. pull) also did not show to have a significant effect on the switch rail wear rate, nor did worn wheel or rail profiles.

4.2 Switch panel loading response

Aiming to prevent or reduce damage development, controlling measures may target the occurring wheel-rail forces, limiting these e.g. through optimising the wheel-rail interface geometry or stimulating the use of track-friendly vehicles which produce low or moderate forces on track. An alternative approach may be to improve the material's resistance to the imposed stresses and slip. Careful consideration of track geometry, operating conditions, and traffic is important when selecting the most appropriate rail grade for use at a given location. To determine rail grade selection criteria, rail damage models can be used as an asset management tool to analyse sites which are to be re-railed, assessing the likelihood of RCF crack initiation and wear. Burstow (2003, 2004) presented a specific material damage function based on track inspections in combination with related vehicle-track simulations, describing the relationship between the wear energy number and RCF crack initiation fatigue damage. With available damage functions for a range of rail grades and known wear number window and distribution for a specific site, rail grade selection can take place in terms of fit-for-purpose (FFP). The RCF damage function is, however, currently only available for one normal grade of rail (R220). Enabling this approach, therefore, requires the development of damage models for further rail grades. To this end further material specific damage functions have been derived from measurements in track combined with vehicle-track simulations, presented within paragraph 4.2.1. and **paper 4**. However, from the occurring wide range in track loading conditions it is difficult to achieve clear characterization results from track data only. To reach more controlled loading conditions towards damage function development a rolling-sliding two-disc laboratory set up was investigated and presented within paragraph 4.2.2 and **paper 5**.

4.2.1 RCF damage model development from field data

The shape of the RCF damage function is determined by the individual linear damage functions regarding wear and fatigue (figure 12). The behaviour of the overall RCF damage function (function at the bottom in figure 12) is determined by the individual linear damage functions regarding both wear and RCF (functions at the top in figure 12). No RCF develops at damage levels below the fatigue threshold (zone a). For the rising slope of the damage function (zone b), RCF damage develops due to plastic ratchetting. At higher levels of energy dissipation, the wear rate is seen to increase, removing

RCF damage as indicated by the descending slope (zone c). When the damage function becomes negative (zone d), initiation of RCF damage is entirely suppressed by wear.

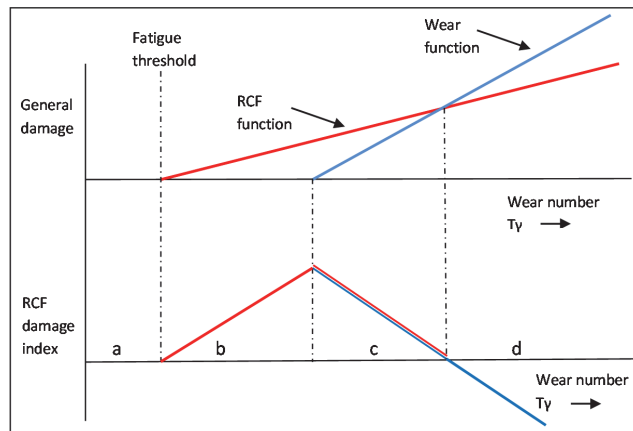


Figure 12 : Wear and RCF as competing mechanisms of surface degradation.

Wear mechanisms and transitions shape the geometry of the damage function. The wear of rail materials has been studied by Bolton and Clayton (1984) with the help of two-disk testing. From the occurring wear rate, the contact surface appearance and the amount of wear debris during the two-disk testing three different wear regimes were identified. They were referred to as type I, II and III, associated to increasing contact pressure and slip percentage.

- [I] Type I (mild) involves a combination of two wear modes. Oxidative wear occurs at low contact pressure and partial slip conditions; the mechanical breakdown of an oxide layer results in debris containing mainly oxide. When full slip conditions are reached, metal flakes are formed, also indicating wear from deformation;
- [II] Type II (severe) is fully characterized by thin metallic flake-type wear debris from the deformation process and the fracture of delaminating surface particles;
- [III] Type III (catastrophic) produces a large variation in debris size, often showing score marks on the larger particles, suggesting an abrasive wear regime.

Examining side-worn rail samples from curved track sections, Bolton and Clayton conclude that the type II wear regime is most closely related to the rail crown and the gauge corner region, whereas type III wear is concentrated at the gauge face. Burstow (2003) associated mild wear to the RCF-dominated regime (the rising part of the damage function in figure 12), with the transition from mild to severe wear to the change to the wear-dominated regime (the falling part). Lewis et al suggest that this mild to severe transition can be associated with the onset of contact conditions of full sliding.

In this thesis, new RCF damage functions were derived for different rail grades (figure 13). For this purpose results from track inspections have been assessed in combination with vehicle-track simulations for the considered case. Damage index values have been determined from the accumulated damage to the first visible RCF cracks (**paper 4**).

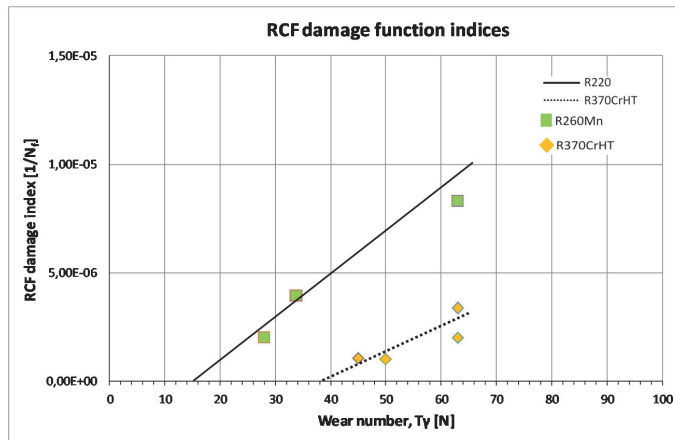


Figure 13: RCF damage index values for the normal R260Mn and premium R370CrHT grade rail. The black line represents the R220 damage function from Burstow (2003). The dotted line represents the established R370CrHT linear damage function within this zone.

The R370CrHT RCF damage function has implications with respect to rail grade selection in design situations. Compared to the normal grade, the increased fatigue crack initiation limit value of the R370CrHT damage function indicates a reduction in RCF susceptibility, preventing RCF initiation for an extended range of track curving conditions. The reduced slope of the ascending part of the R370CrHT damage function will, under equal loading conditions, result in a significant increase in expected time to visible RCF damage initiation as compared to normal grade rail.

The expectation for the remaining part of the damage function is based on the work performed by Bolton and Clayton (1984) regarding rolling-sliding wear damage. Burstow associates the change of the RCF-dominated regime (the ascending part) to the wear-dominated regime (the descending part) with the transition from mild to severe wear. Bolton and Clayton present mild to severe wear transition zone creepage values at contact stresses typical for moderate curving. These show little to no difference for the different rail materials, indicating the damage function peak for all examined rail grades to be positioned at a similar wear number under these conditions. According to Bolton and Clayton the slope of the descending wear function is proportional to the material hardness. Figure 14 presents the R220 damage function from Burstow (2003) together with the interpolated and extrapolated course of the R370CrHT damage function. Since the type II wear function has not been defined yet, the starting point and geometry of the descending branch of the R370CrHT damage function remain speculative.

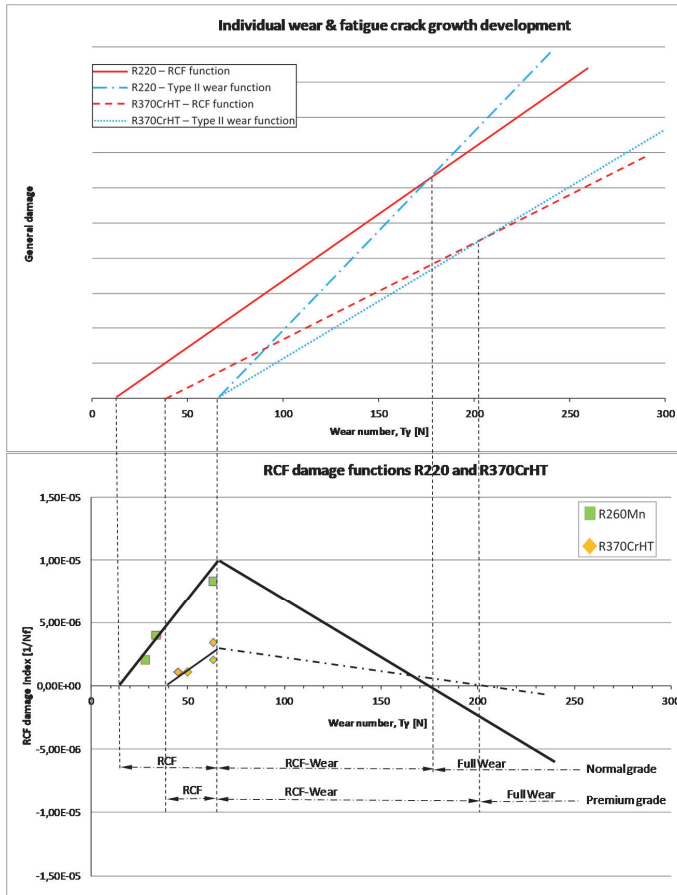


Figure 14: The individual wear and fatigue crack growth development for R220 as derived from Burstow [6], together with those for R370CrHT as determined in this study (top); RCF damage functions for both R220 and R370CrHT rail grades (bottom). The starting point and development of the downward slope of the R370CrHT damage function (stripe-dotted line) remain speculative.

The R370CrHT RCF damage function can be further discussed together with its implications regarding rail grade selection. Compared to the normal grade, the increased fatigue crack initiation limit value of the R370CrHT damage function indicates a reduction in RCF susceptibility, preventing RCF initiation for an extended range of track curving conditions. The reduced slope of the ascending part of the R370CrHT damage function will, under equal loading conditions, result in a significant increase in expected time to visible RCF damage initiation as compared to normal grade rail. Although not validated, the reduced RCF index peak value will have a further beneficial effect on the loading frequency until visible RCF. Compared to the normal rail grade, the increased R370CrHT transition value to the regime of full wear, at the intersection with the horizontal axis, implies an extension of RCF susceptibility (figure 14, the regime of RCF-wear). At loading conditions within this extended area, replacing normal rail by premium rail is expected to result in a transition from a wear-dominated damage mechanism to a regime of RCF-wear. However, together with the expected low rate of RCF development and depending on preventive rail grinding intervals this should not necessarily cause problems.

4.2.2 Damage function development from two-disc laboratory testing

To reach more controlled loading conditions towards damage function development a rolling-sliding two-disc laboratory set up was investigated (figure 15). The design and validation of a two-disc test approach in order to define rail/wheel interface wear and RCF response is presented in **paper 5**. The validation result suggest that the presented two-disc approach can be used to support future work to establish RCF-damage functions within a well-defined laboratory environment.

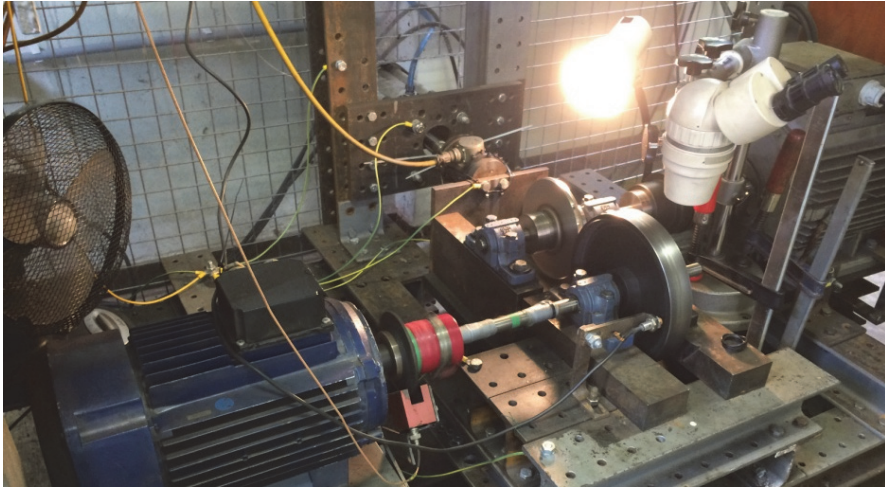


Figure 15: Two-disc testing machine overview; rail disc (rear) and wheel disc (front).

RCF-damage function indices are established using a rolling-sliding two-disc laboratory set up. The applied test rig configuration allows both longitudinal and lateral slip to be introduced into the contact, corresponding to the dynamic conditions between wheel and rail when negotiating a curve. For purpose of laboratory set-up validation, performed tests investigate the damage response of the normal rail grade R220. For this rail grade the RCF-damage function already is available from field observations by Burstow (2003,2004). Starting from the level of friction coefficient, creepages, normal load and disc curvature, the resulting value of wear index T_γ can be calculated using the FASTSIM algorithm for wheel-rail contact evaluation from Kalker (1990). As Jaschinsky (1990) concludes T_γ to scale proportional to the normal force an equivalent T_γ for a full size wheel is calculated from the T_γ for the two disc set up (figure 16).

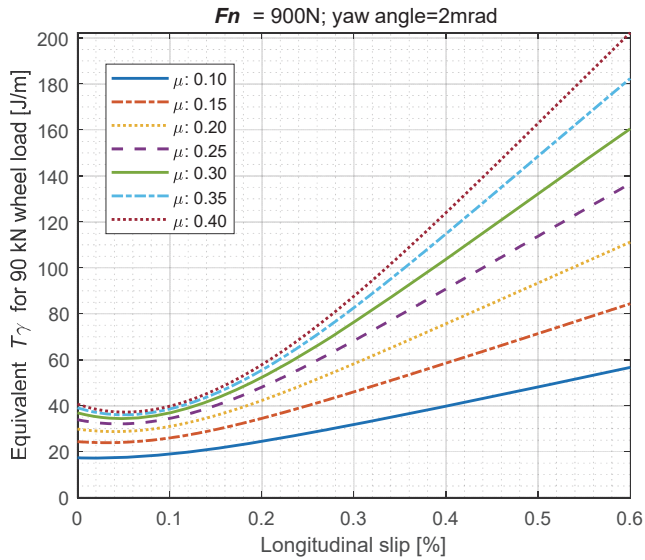


Figure 16: Equivalent T_γ for 90 kN wheel load as a function of longitudinal slip and friction coefficient. The graph is valid for a set angular rotation between the two discs of 2 mrad.

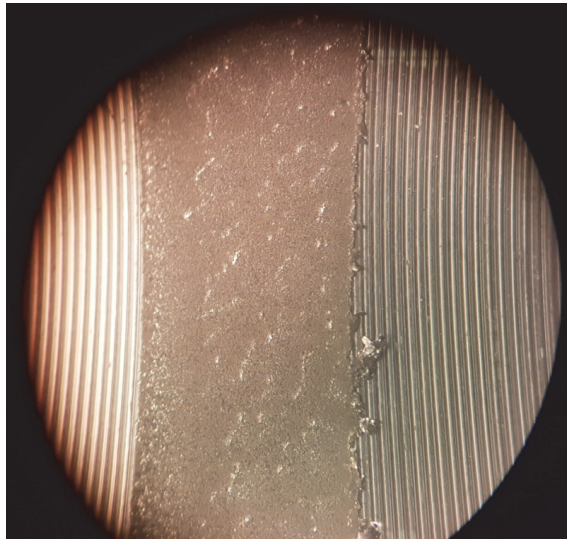


Figure17: Monitoring of the running surface consists of visual inspection using a stereo microscope (running band width approx. 2.5 mm).

Damage function indices for the different T_γ loading levels are determined from the observed cycles to the initiation of visual surface cracks (figure 17). The resulting indices are presented in figure 18. The RCF damage function of the R220 rail grade as established by Burstow is shown by the black line.

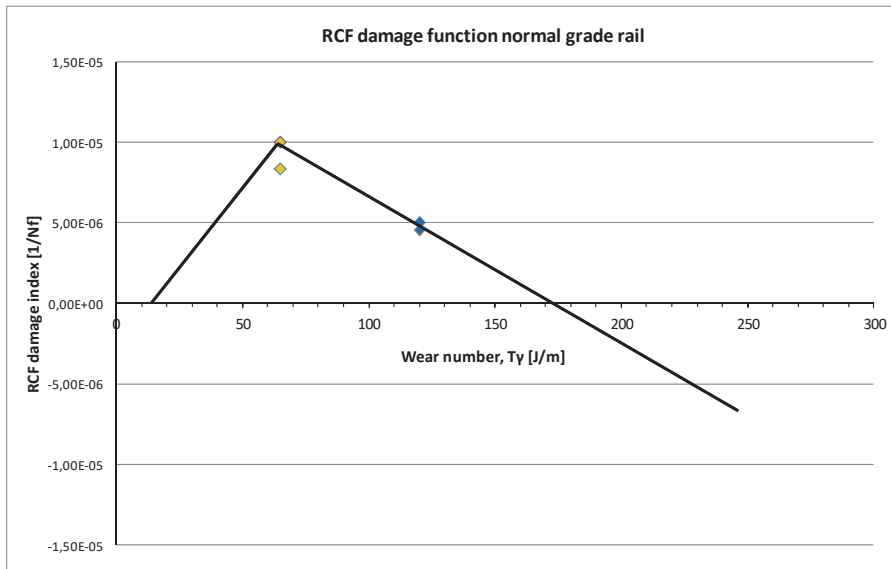


Figure 18: Damage function indices at loading levels T_y 65 (yellow diamonds) and 120 J/m (blue diamonds) established with two-disc testing, depicted within the RCF damage function of normal grade rail as established by Burstow (black line).

For the examined wear numbers the RCF damage function indices established by two-disc testing can be observed to be in the same order of magnitude as that of the normal grade RCF damage function as established from field observations. The validation result suggest that the two-disc approach can be used to support future work to establish RCF-damage functions within a well-defined laboratory environment.

4.2.3 Rail grade selection

Wear number (T_y) loading levels and frequencies for any particular site are required in order to apply the RCF damage function, selecting the optimal rail grade to be installed or to forecast headcheck development. A daily fatigue index as suggested by Zacher (2009) can be used by the track engineer, to consult for instance look up tables. The T_y magnitude is found to depend strongly on the curve radius together with vehicle curving characteristics. Especially at the in paper 4 examined larger radius curve ($R=2500$ m), the operating T_y levels and contact patch distribution are significantly influenced by the intensity of track geometry variation. This behaviour needs to be reflected within the track-train specific look up tables and can be addressed for example by taking into account the (mean) track quality number as obtained by the track geometry recording train. Due to the wide range of influencing factors (e.g. wear of wheel profiles, friction conditions), the accuracy of the theoretical model is valuable only to a certain extent. To support rail grade selection in practice, an overall description of the RCF damage function for the different rail grades seems to be sufficient therefore.

The application of the RCF damage model regarding rail grade selection is illustrated by reviewing different switch types in relation to a VIRM passenger train (figure 19, IC1) and a freight

wagon type equipped with Y25 bogies. Among others vehicle-track simulations were carried out at switch type NG1:18, negotiating the diverging route at allowed maximum speed of 80km/h. Applied rail profiles were derived from profile measurements at new unworn turnouts. Calculated T_γ values were separately issued for the contacting areas at rail shoulder/gauge corner and gauge face. Contacting the wheel tread/ flange root at the high rail in curves, RCF damage is seen to initiate predominantly at the rail shoulder/ gauge corner. The gauge face area, when in contact with the wheel flange, experiences high contact stresses and especially high sliding velocities and is, therefore, more prone to wear. Figure 19 shows the wear number development along the switch and closure panel.

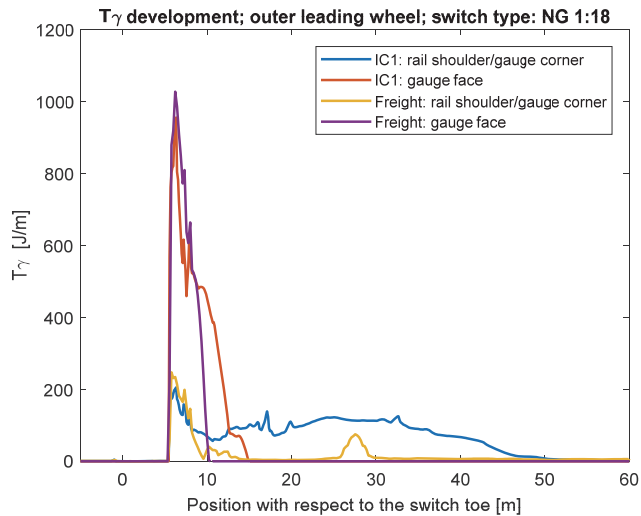


Figure 19: T_γ development for the leading wheel negotiating the switch type NG 1:18 at the diverging route. The switch toe is located at position 0m; the closure panel starts a position 15m, ending at position 40m.

Calculated wear numbers at the switch panel rail shoulder/ gauge corner are close to 100N. Based on the RCF damage functions from figure 14, the application of R370CrHT premium rail will lead to an expected increase in loading cycles to visible RCF damage initiation compared to normal grade rail. At those positions where flange contact occurs, calculated T_γ levels suggest the operational regime to be in full wear. Here the application of premium grade rail at the switch panel can also prove to be beneficial from the viewpoint of improved wear resistance. From the calculated rail shoulder/ gauge corner T_γ , the NG 1:18 closure panel is also expected to benefit from premium rail application towards the reduction of RCF damage initiation. This illustrates how the further development of RCF damage models for premium rail grades can support future switch design and switch maintenance.

5 Thesis contribution

Achieving sustainability of the switch panel was investigated using a two-fold approach: one aimed at reducing the switch panel loading levels, the other at improving the switch panel response to loading resulting into a 'fit-for purpose' design.

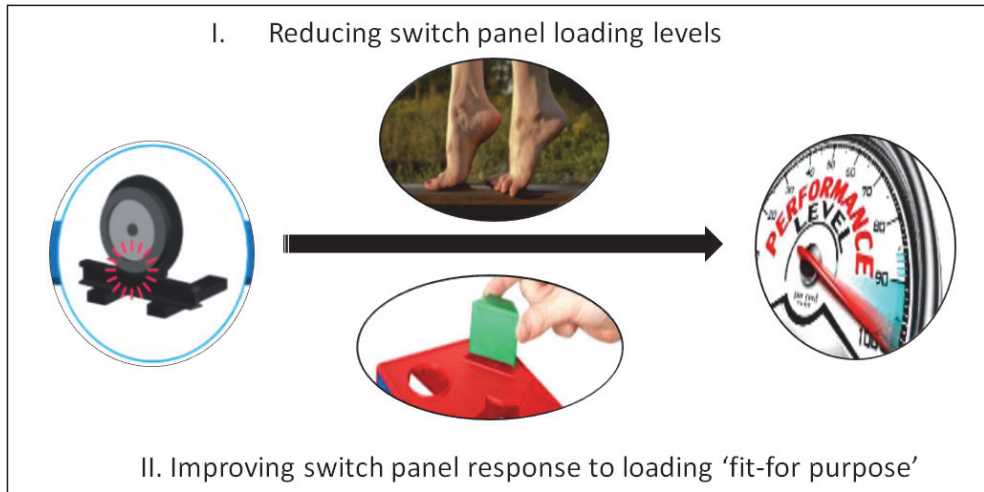


Figure 20: achieving sustainability of the switch panel by using a two-fold approach.

As concluded by the EU research project INNTRACK the main threats to the sustainability of the switch panel are rail head wear and initiation and growth of fatigue cracks at the rail running surface. Wear and RCF damage development is governed by the tangential (shear) forces and slip at the wheel-rail interface. The level of shear forces and slip can be represented by the calculated 'wear number' T_y , providing a parameter to quantify the occurring loading level as well as expected damage response. In this thesis the T_y approach therefore is central to the assessment of study outcomes.

5.1 Reducing S&C loading levels

Track friendliness

The design of railway turnouts has traditionally been based on the assessment of vehicle response using kinematic equations, not taking into account the dynamic vehicle response. However, to improve the understanding of vehicle running behaviour at a turnout and to identify possible optimisation of turnout negotiation, an evaluation of the dynamic interaction between vehicle and track, wheel and rail, is essential and therefore is key in the here presented work. Oswald and Bishop (2001) and later Kassa (2006) were among the first to investigate the railway switch by simulation of dynamic interaction between train and railway turnout. Using multi-body software, switch design parameters such as curve radius, track stiffness, dynamic gauge variation and rail profile have been assessed by different researchers. However, the design of the vehicle in relation to switch loading is

much less investigated and understood. The impact of vehicle design optimisations, aimed at improving track friendliness of the vehicle, towards degradation of the running surface and associated cost previously has only been investigated for plain track.

The here performed research has extended this work to the railway switch panel, quantifying the effect of vehicle design optimisations towards switch panel loading levels and related damage development as well as the impact regarding the cost of maintenance and availability. Vehicle design evaluations show that operational levels of $T\gamma$ (and hence the intensity of wear and RCF) are strongly determined by the resistance the wheelset experiences when rotating around the yaw axis within the bogie frame (changing the direction of motion), the so-called primary yaw stiffness. The primary yaw stiffness is determined by the design of the primary suspension. In line with the objectives in par. 1.2, this thesis aims at a reduction of the switch panel loading through vehicle design optimisation and therefore focuses on the primary suspension. The concept of 'frequency selective stiffness' of the railway vehicle primary suspension design was evaluated in relation to switch panel negotiation. In conclusion, this concept can significantly contribute to a reduction of switch panel loading levels, improving the so-called track friendliness of the vehicle.

The work presented in this thesis contributes to research on switch panel loading levels. It provides insight into the effect of vehicle design optimisation to reduce switch loading and related wear and RCF damage, quantifying the expected reduction in terms of track loading ($T\gamma$) as well as in track degradation cost. The presented work has provided transparency with regard to the benefits of track friendly vehicle design towards S&C sustainability. When stimulating track friendly design measures e.g. through the system of Track Access Charging (TAC), improvements in cost and availability for S&C can be fully appreciated.

Operational factors

Additionally, loading levels at the switch panel have been investigated with regard to train and track operational factors. Before taking effective mitigating measures when confronted with abnormal degradation of the switch panel running surface, the responsible track engineer needs to understand the impact of the individual parameters contributing to the observed damage. However, many of these parameters within the vehicle-track system are closely connected but this interconnection is not always obvious. Previously Kassa and Johansson (2006) have investigated the influence of the wheel profile, axle load and speed with regard to plastic deformation of rail profiles within the turnout. However, other operational parameters possibly influencing degradation of the switch panel such as direction of traffic or lubrication, need further investigation. Therefore, within this thesis a sensitivity analysis was performed regarding those operational parameters the track engineer can interfere with and from which a control strategy can be shaped, but as such have not been addressed in previous research of the vehicle-switch panel interaction. The here performed sensitivity analysis was combined with a case study providing further validation of the simulation results. Its novelty lays in providing a broad and quantified overview of the individual influencing factors regarding switch panel degradation.

The work in this thesis has clearly illustrated the impact of (flange) lubrication with regard to loading levels and lateral switch wear. In conclusion, the sharp increase in lateral wear as experienced in the case study is related to the interface properties, more specific the absence of flange lubrication at passenger train dominated routes. This result will supported the responsible track engineer to structure an appropriate friction management strategy.

5.2 Switch panel loading response (fit-for-purpose)

An alternative approach to improving the structural behaviour of the switch panel lies in the improvement of the material resistance to the imposed stress and slip levels, selecting the most appropriate available rail grade for use at a given location (fit-for-purpose). This line of approach is followed by the rail grade selection standards, which specify more resistant rail grades to be installed at the more demanding track sections such as curves and switches. However, the damage response of alternative rail grades currently is insufficiently understood, as is supported by field experience, indicating that the expected benefit of improved steels has not generally been associated with a reduction in required maintenance. In order to select the optimum rail grade for a specific loading condition it is required to define the damage response of the optional materials. Within this thesis this was carried out on the basis of rail damage functions, providing vital understanding of the operational performance of rail grades in terms of surface degradation. Burstow (2003, 2004) investigated the damage response of the R220 normal rail grade, characterising this material in terms of the loading history and related RCF damage development. The present study extends this concept from normal to premium pearlitic rail. Establishing part of new RCF damage models for the premium rail grade R370CrHT and the normal grade R260Mn, insight is gained regarding the damage response of these rail grades. For this purpose results from track inspections were assessed in combination with vehicle-track simulations for the considered case.

It is shown that the concept of the rail damage function provides vital understanding of the operational performance of rail grades in terms of surface degradation. However, from the occurring wide range in track loading conditions it is difficult to achieve clear characterization results from track data only. To reach more controlled loading conditions, a rolling-sliding two-disc laboratory set up to define rail/wheel interface wear and RCF response was designed and validated here. The applied test rig configuration allows a contact angle to be set to one of the discs introducing lateral slip. Together with the applied longitudinal slip this simulates the dynamic conditions between wheel and rail when negotiating a curve. Testing within the RCF regime, applying partial slip, this approach is a novelty in RCF damage function development. The validation result suggest that the presented two-disc approach can be used to support future work to establish RCF-damage functions within a well-defined laboratory environment. Determining these functions for a range of rail grades, the individual contribution towards (track) loading response and related rail grade selection can be appreciated.

RCF damage models can be used to support future rail grade selection, switch design, and maintenance. Using these models, the damage response of different grades of rail can be predicted with respect to the dynamical loading conditions. Accordingly measures can be taken, for instance avoiding Ty values operating within the RCF damage regime. With damage functions available for the range of rail grades and known wear number window and distribution for a specific site, rail grade selection can take place in terms of fit-for-purpose (FFP). From the calculated switch panel loading levels it is clearly illustrated how switch panel sustainability can benefit from a fit-for-purpose approach towards rail grade selection.

As illustrated in figure 21, the track engineer can use the mean value of the wear number along a curve or switch section to optimise track maintenance in relation to RCF generation. A daily fatigue

index as suggested by Zacher (2009) can be used by the track engineer to consult e.g. through look up tables. With the applicable RCF damage function, the accumulated fatigue index for the section can be determined from the average daily traffic. This can support a fit-for-purpose rail grade selection upon renewal.

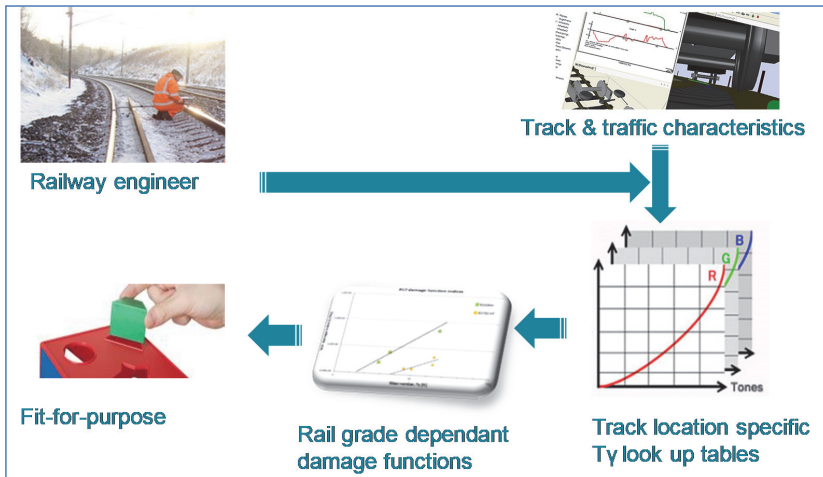


Figure 21: With location specific loading level available and related rail grade damage response understood, fit-for-purpose rail grade selection is supported.

The same approach can also support track engineers in their planning of maintenance activities such as grinding and the decision making process regarding the application of lubrication. Infrastructure managers are able to use these damage models to also assess the impact of changes in train operation (e.g. increased train speed, vehicle types, axle loads) on damage development and the maintenance consequently required.

5.3 Practical implementations of results

Based on the particular findings of this research, NS has decided to fit the radial arm of the recently ordered Intercity new generation (IC-NG, figure 22) bogies with hydro-bushes with FSS characteristics.

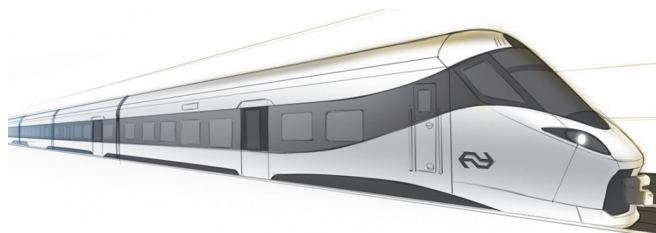


Figure 22: IC-NG to be equipped with hydro bushes, improving track friendliness.

Based on the research findings, NS has also decided to improve the track friendliness of their VIRM double deck fleet, replacing the current conventional radial arm bush with a FSS hydro-bush component. Improving track friendliness in the way proposed there will directly influence the loading and deterioration of Dutch rail infrastructure, reducing track maintenance cost and improving availability. Application of the hydro-bush will reduce the fatigue loading at both wheel and rail. Since the initiation of RCF cracks currently determines the re-profiling interval of the VIRM-4 wheel tread (figure 23), it is expected that the vehicle will also benefit.



Figure 23: Wheel tread with RCF crack damage

Primary based upon the outcome of the study regarding the operational factors (**paper 2**), Dutch rail infrastructure manager ProRail has decided to re-activate their track lubrication strategy at the Amsterdam CS railway yard at which a large number of turnouts were suffering from abnormal lateral switch wear. From the work presented here, the experienced sharp increase in flange wear rate of Dutch intercity trains could also be explained. This insight also supports the train operating company in shaping its lubrication strategy.

6 Concluding remarks and future work

Optimising rail vehicle and track interaction requires a system approach. Many parameters within the vehicle-track system are closely connected but this interconnection is not always obvious. The T_y approach, representing the level of shear forces and slip by the calculated 'wear number' provides a parameter to quantify the occurring loading level as well as expected damage response and therefore was central to the evaluation of the research results. The most important conclusions of this thesis are summarised below.

6.1 Switch Panel loading levels

Track friendliness

- Track friendliness of railway vehicles can be improved significantly when components with frequency-dependent stiffness characteristics are applied at the primary yaw suspension;
- Vehicle curving performance benefits from a low primary yaw suspension stiffness, whereas vehicle running stability requires a high yaw stiffness. This work has proven that it is possible to overcome this paradox by applying a component with frequency-dependent stiffness, combining a low value in the low-frequency regime and a high value in the high-frequency regime.
- Track friendly vehicle concepts can significantly contribute to the structural performance of the switch panel, reducing switch wear loading up to 50%;
- Track friendly vehicle concepts significantly reduce track deterioration cost at narrow radius curves and switches (by respectively 30 and 60%), limiting rail wear and RCF damage;
- Measures to reduce track deterioration at switches and narrow radius curves are currently insufficiently reflected in the cost model overall assessment result. When calculating the overall deterioration cost for the travelled route, the calculation model should include a well-balanced representation of switches and narrow radius curves. This will support the development of future track access charging, stimulating the design and introduction of vehicles with improved track-friendliness;
- The effect of reducing the unsprung mass of a bogie on track degradation was assessed by evaluating the forces between wheel and rail in lateral and vertical direction. It can be observed that reducing the unsprung mass predominantly has resulted in a significant reduction of the lateral track forces, and related T_y . The observed reduction is closely related to the Klingel movement of the bogie. Reduced lateral track forces will lead to reduced track geometry degradation and related maintenance effort and cost.

Operational factors

- Studying the contribution of identified parameters with respect to switch loading and related wear, this research clearly demonstrates the contribution lubrication can have in preventing abnormal lateral switch wear. The level of friction between wheel flange and rail gauge face is dominating the wear loading and related wear behaviour at the switch rail in diverging route. For the assessed situation, lubrication is seen to be the only influencing parameter that will reduce the wear loading to a level that excessive abnormal lateral wear is prevented.
- Other operational parameters that the railway engineer can act on (e.g. vehicle speed, route through the yard, and rail profiles) are seen to influence lateral switch wear loading only marginally.

6.2 Switch panel loading response

- On the basis of a combination of dynamic train-track simulations and regular track inspection results, RCF damage index values have been established for both the normal R260Mn and the premium R370CrHT heat treated pearlitic rail. From these index values the rising RCF-branch of the damage functions of both rail grades was established. RCF damage index values for R260Mn grade rail were found to coincide with the RCF damage function of the normal grade as reported in the literature by Burstow [2003,2004]. These findings support the conclusion that the RCF regime of the Burstow damage function, with T_y values in the domain between the fatigue crack initiation limit and the peak value of 65 N, is applicable to the entire family of normal pearlitic rail grades, including R220, R260 and R260Mn;
- Compared to the normal grade, the established part of the R370CrHT damage function shows an increased fatigue crack initiation limit value together with a reduced slope of the rising part of the function. Application of this grade in the type I mild wear regime, within the operational window of the RCF damage function with T_y values below 65 N, is beneficial to avoid RCF. The increased crack initiation limit will extend the track length for which no RCF initiation will occur. Within the RCF regime itself the initiation of headchecking will require an increased number of loading cycles;
- Case studies on the basis of T_y , reviewing different switch types regarding representative vehicle loading conditions, have illustrated the improvement potential regarding switch panel performance when applying RCF (T_y) damage functions to support rail grade selection. For the reviewed switch types a significant benefit is expected from premium rail application towards the reduction of RCF damage initiation as for lateral wear;
- The new RCF damage functions established in this research provide the tools for a fit-for-purpose rail grade selection approach. Their application allows for a dedicated rail grade selection, adapted to site-specific operational conditions, supporting structural switch panel performance optimisation;
- From the designed and validated rolling-sliding two-disc laboratory set up it is concluded that the presented two-disc approach can be used to support future work to establish RCF-damage functions within a well-defined laboratory environment.

6.3 Future work

- The expected benefits of track friendly design regarding wheel profile life, energy consumption and squeal noise require further quantification.;
- A new Track Access Charging system should be developed for the Dutch network. This system should appreciate the value of track friendly vehicles regarding S&C in terms of cost and availability;
- The impact of reduced unsprung mass of railway vehicles should be further examined especially with regard to the relatively soft sub-structure of the Dutch network;
- The quantitative determination of the descending part of the damage function for premium grade rail requires further research.

- From the presented rolling-sliding two-disc laboratory set up testing can start to determine the RCF damage functions for a range of rail grades(e.g. R350HT, Hypereutectoid and Bainitic rail steel), from which the individual contribution towards (track) loading response and related rail grade selection can be appreciated.
- Further investigation is required into the current process of rail grade selection which now is primarily determined by curve radii, and how this could be transformed to a fit-for-purpose approach when applying available RCF damage functions;
- The RCF damage models predict the number of loading cycles to visible Headcheck initiation in relation to the wear number. Apart from initiation, the subsequent phase of crack development(growth rate) should also be understood in relation to the wear number. This will further support the optimisation of maintenance at the rail running surface;
- From the developed insight in operational parameters an effective wheel-rail lubrication strategy can be designed to reduce lateral (switch) rail wear and wheel flange wear.

Acknowledgements

The research presented in this doctoral thesis was carried out by the author in the period 2014 – 2018 at the Railway Engineering section of the Faculty of Civil Engineering and Geosciences at Delft University of Technology. The work was carried out under the project number T91.1.12475a in the framework of the Research Programme of the Materials innovation institute M2i (www.m2i.nl), with special support from the Dutch rail infra management organisation ProRail.

A special word of thanks to my supervisor Dr. Michaël Steenbergen for his guidance, support, and advice (especially on how to do this work part-time). I would also like to thank my promotor Prof. Rolf Dollevoet for giving me the confidence to start this research project. I have greatly appreciated the support from my colleagues at TU Delft, especially Jacqueline Barnhoorn. Also the support from ProRail and especially from Dr. Ivan Shevtsov, Ruud van Bezooijen, Dr. Arjen Zoeteman and ir. Bart Schotsman is much appreciated. I would like to thank my colleagues at DEKRA Rail who have supported me in a big way: my discussions with ir. Pier Wiersma, the reviews carried out by Ing. Mark Linders, and Dr. Nico Burgelman's modelling support are gratefully acknowledged here.

Furthermore, the openness and dedication I have encountered at the international assembly of railway researchers has inspired and motivated me to contribute in my own way to the academic field of railway research. Without failing others, I would like to mention Prof. Roger Lundén, Prof. Jens Nielsen, Prof. Ajay Kapoor, Prof. Simon Iwnicki, Dr. Frank Franklin, Dr. Katrin Maedler, Dr. Tore Vernesson, Dr. Eric Magel, Dr. Mark Dembowski, and Dr. Rene Hayder. Also, I would like to thank ProRail track engineer Ing. Remco Verloop for our open discussions. B. Bill is thanked for his inspirational companionship during my travels to and from the University. And a final word of thanks to my big love and soulmate Corine and my lovely daughters Hilde and Fien without whom I would be lost.

References

- Alarcón, G. I., Burgelman, N., Meza, J. M., Toro, A., & Li, Z. (2015). The influence of rail lubrication on energy dissipation in the wheel/rail contact: a comparison of simulation results with field measurements. *Wear*, 330, 533-539.
- Andersson, M. Marginal cost of railway infrastructure wear and tear for freight and passenger trains in Sweden, Swedish National Road and Transport Research Institute (VTI), European Transport \ Trasporti Europei n. 48 (2011): 3-23.
- Bolton, P.J. Clayton, P. Rolling-sliding wear damage in rail and tyre steels, *Wear*, 93 (1984) 145-165.
- Bosso, N. Comparison of different scaling techniques for the dynamics of a bogie roller rig, *Vehicle System Dynamics*, 2016.
- Bugarin, M.R. Garcia Diaz de Villegas J.M, Improvement in railway switches, *Journal of Rail and Rapid Transit*, IMechE 2002.
- Bugarín, M.R. Orro, A. Novales, M. Geometry of High-Speed Turnout, *Transportation Research Record – Journal of the Transportation Research Board*, 2261 (2011), 64-72.
- Burstow, M.C. Whole life rail model application and development for RSSB – development of a RCF damage parameter AEATR-ES-2003-832 Issue 1 October 2003.
- Burstow, M.C. Whole life rail model application and development for RSSB (T115) – continued development of an RCF Damage Parameter, AEATR-ES-2004-880 Issue 2 September 2004.
- Burstow, M.C. Experience of premium grade rail steels to resist rolling contact fatigue (RCF) on GB network, *Ironmaking & Steelmaking* (2013), 40:2, 103-107.
- Burstow, M.C. A Model to predict and understand Rolling Contact Fatigue in wheels and rails, proceedings of WCRR 2006, Canada, 2006.
- Coleman, I. The Development of Modelling Tools for Railway Switches and Crossings, Thesis, Imperial College London, Department of Mechanical Engineering, 2014.
- Daves, W. Kubin, W. Scheriau, S. et al. A finite element model to simulate the physical mechanisms of wear and crack initiation in wheel/rail contact. *Wear* (2016) 366–367:78–83
- Dollevoet, R. Li, Z. Arias-Cuevas, O. A method for the prediction of head checking initiation location and orientation under operational loading conditions, *Proc. IMechE Vol. 224 Part F: J. Rail and Rapid Transit*, 2010.
- ERRI B176/3, Benchmark problem – Results and assessment, B176/DT290, Utrecht 1993.
- Essen, H.E. van et.al, Marginal costs of infrastructure use - towards a simplified approach, CE Solutions for environment, economy and technology, Delft, The Netherlands, Final report (2004).
- Fletcher, D. Beynon, J. Development of a test machine for closely controlled rolling contact fatigue and wear testing, *Journal for Testing and Evaluation*, JTEVA, Vol.28, No.4, July 2000, pp. 267-275.

Garnham, J.E. Davis, C.L. Very early stage rolling contact fatigue crack growth in pearlitic rail steels, *Wear* 271 (2011) 100-112.

Gretzschel, M. Jaschinski, A. Design of an active wheelset on a scaled roller rig, *Vehicle System Dynamics*, 2004.

Hiensch et al., Improving track-friendliness of rolling stock, Proceedings of International Heavy Haul Association (IHHA 2015), Australia, 2015.

Hiensch, M. Dirks, B. Horst, J. van der Stelt, J. Rail head optimisation to reach a sustainable solution preventing Railway Squeal Noise, *Inter-Noise 2007*, Istanbul, 2007.

Huang, Y.B. Shi, L.B. Zhao, X.J. et al. On the formation and damage mechanism of rolling contact fatigue surface cracks of wheel/rail under the dry condition. *Wear* (2018) 400–401:62–73.

INNOTRACK Concluding Technical Report, UIC – Paris, 2010. ISBN: 978-2-7461-1-1850-8.

INNOTRACK Project, report D 4.1.5 – Definitive guidelines on the use of different rail grades, 2006.

Ishida, M. Satoh, Y. Development of rail/wheel high speed contact fatigue testing machine and experimental results, *RTRI*, Vol. 29, No. 2, May 1988.

Iwnicki, S.D. Wickens, A.D. Validation of a MATLAB Railway Vehicle Simulation Using a Scale Roller Rig, *Vehicle System Dynamics*, 1998, 30:3-4, 257-270.

Iwnicki, S. et. al, The 'SUSTRAIL' high speed freight vehicle: Simulation of novel running gear design, in 23rd Symposium on Dynamics of Vehicles on Roads and Tracks (IAVSD 2013)2013: Qingdao, China.

Iwnicki, S. D. et. al, Dynamics of railway freight vehicles, *Vehicle System Dynamics*, 2015, Vol. 53, No. 7, 995–1033.

Jaschinsky, A. On the application of similarity laws to a scaled railway bogie model, thesis TU Delft, 1990.

Jenkins, H. Stephenson, J. Clayton, G. Morland, G. Lyon D. (1974). The effect of track and vehicle parameters on wheel/rail vertical dynamic forces. *Railway Eng. J.* 3 (1), 2–16.

Johnson, K.L. Contact mechanics and the wear of metals, *Wear* 190 (1995), pag. 162-170.

Kalker, J.J. Wheel-rail rolling contact theory. *Wear*, 144 (1991) 243-261.

Karttunen, K. Kabo, E. Ekberg, A. A numerical study of the influence of lateral geometry irregularities on mechanical deterioration of freight tracks *Proc IMechE Part F: J Rail and Rapid Transit* (2012) 226(6) 575–586.

Kassa, E. Johansson, G. Simulation of train-turnout interaction and plastic deformation of rail profiles, *Vehicle System Dynamics*, 2006, pag. 349-359.

Kráčalík M, Trummer G, Daves W. Application of 2D finite element analysis to compare cracking behaviour in twin-disc tests and full scale wheel/rail experiments, *Wear* (2016) 346-347.

Lewis, R. and Dwyer-Joyce, R.S. Wear mechanisms and transitions in railway wheel steels. Proceedings of the Institution of Mechanical Engineers, Part J: Journal of Engineering Tribology, 2004, 218(6), 467-478.

Lewis, R. Olofsson, U. Mapping rail wear regimes and transitions, Wear 257 (2004) 721-729.

Lewis R, Dwyer-Joyce RS. Wear mechanisms and transitions in railway steels. Proc. IMechE, Part J: Engineering Tribology, 2004, 218, 467-478.

Lewis, R. et.al, Mapping railway wheel material wear mechanisms and transitions, JRRT328, Proc. IMechE Vol. 224 Part F: J. Rail and Rapid Transit, 2010.

Linders, M. Extension and validation of the VIRM-4 vehicle model, Plurel report/13/120125/004, March 2013.

Lim, S.C. The relevance of wear-mechanism maps to mild-oxidational wear, Tribology international, November 2002, pag. 717-723.

Markine, V.L. Steenberg, M.J.M.M. Shevtsov, I.Y. Combatting RCF on switch points by tuning elastic track properties, Wear 271 (2011) 158–167.

Miner AM, Cumulative damage in fatigue J. Appl. Mechanics, 12 (3) (1945), pp. A-159.

Molatefi, M. Hecht, M. Kadivar, M.H. Critical speeds and limit cycles in the empty Y25-freight wagon, Proc. IMechE Vol. 220 Part F: JRRT67, 2006.

Nash, C. UNification of accounts and marginal costs for Transport Efficiency, 5'th framework project UNITE, Final Report (2003), Institute for Transport Studies, University of Leeds, Leeds, UK.

NEN-EN 13674-1:2011, Railway applications - Track - Rail - Part 1: Vignole railway rails 46 kg/m and above.

Nicklisch, D. et al. Geometry and stiffness optimization for switches and crossings, and simulation of material degradation, Proceedings of the Institution of Mechanical Engineers Part F Journal of Rail and Rapid Transit 224(4):279-292, July 2010.

Nielsen, J.C.O. Pålsson, B.A. Torstensson, P.T. Switch panel design based on simulation of accumulated rail damage in a railway turnout, CM2015, Colorado Springs, USA, 2015.

Öberg, J. E. Andersson, E. Determining the deterioration cost for railway tracks, J. Rail and Rapid Transit, IMechE 2009.

Oswald, R.J. Bishop, G. Optimization of Turnout Layout- and Contact-Geometry Through Dynamic Simulation of Vehicle-Track Interaction, 7th International Heavy Haul Conference, Brisbane, Australia, 2001.

Pålsson, B. Towards optimization of railway turnouts, Licentiate Thesis, Department of Applied Mechanics, Chalmers University of Technology, Goteborg, Sweden, 2011.

Pålsson, P.B. Nielsen, J.C.O. Wheel-rail interaction and damage in switches and crossings, Vehicle System Dynamics, 2012, pag. 43-58.

Pålsson, B. Nielsen J.C.O, Design Optimization of Switch Rails in Railway Turnouts, 9th International Conference on Contact Mechanics and Wear of Rail/Wheel Systems (CM 2012), China, 2012.

Ponter et al. Shakedown analyses for rolling and sliding contact problems, International Journal of Solids and Structures 43 (2006) 4201–4219.

ProRail internal document, Beheer en onderhoudskosten 2014, J. Swiers.

Shackleton, P. and Iwnicki, S. "Comparison of wheel–rail contact codes for railway vehicle simulation: an introduction to the Manchester Contact Benchmark and initial results." Vehicle System Dynamics 46.1-2 (2008): 129-149.

Shackleton, P. Bezin, Y. Crosbee, D. Molyneux-Berry, P. Kaushal, A. Development of a new running gear for the Spectrum intermodal vehicle, Proceedings of the 24th Symposium of the International Association for Vehicle System Dynamics (IAVSD 2015), Graz, Austria, 17-21 August 2015.

Spangenberg, U. Fröhling, D. Mitigating severe side wear on 1:20 tangential turnouts, IHHA2015, Perth, Australia, 21-24 June 2015

Steenbergen M. (2007). The role of the contact geometry in wheel–rail impact due to wheel flats. Veh. Syst. Dyn. 45 (12), 1097-1116.

Steenbergen JMM, Rolling contact fatigue in relation to rail grinding, Wear356-357(2016)110–121

Stock R, Pippan R, RCF and wear in theory and practice – The influence of rail grade on wear and RCF, Wear 271 (2011) 125-133.

Stichel, S. On freight wagon dynamics and track deterioration, Journal of Rail and Rapid Transit, Proc. of IMechE, Part F, Vol. 213, No. F4, London, 1999, p 243-254.

Sun, Y. Cole, C. Boyd, P. A Numerical Method Using VAMPIRE® Modelling for Prediction of Turnout Curve Wheel-rail Wear, CM2009, Italy, September 2009

Tunna, J. Urban, C. A parametric study of the effects of freight vehicles on rolling contact fatigue of rail Proc. IMechE Vol. 223 Part F: J. Rail and Rapid Transit, 2009.

Tyfour, W.R. Benyon, J.H. Kapoor, A. Deterioration of rolling contact fatigue life of pearlitic rail steel due to dry-wet rolling sliding line contact, Wear 197 (1996) 255-265.

Tyfour, W.R. Beynon, J.H. The effect of rolling direction reversal on fatigue crack morphology and propagation. Tribology International (1994) 27:273–82.

UIC. Testing and approving of railway vehicles from the point of view of their dynamic behaviour – Safety – Track fatigue – ride quality. Code 518, Paris, October 2005

Vermeij, I. et al, Optimisation of Rolling Stock Wheelset Life through Better Understanding of Wheel Tyre Degradation, International Journal of Railway Volume 1, Issue 3, 2008, pp.83-88 Zacher, M. Rolling contact fatigue (RCF): models and experiences of DB AG, RTR1/2011 pag. 35-42

Zacher, M. Prediction of gauge corner cracking in rails for rail maintenance, Contact Mechanics, CM2009, Florence, Italy.

Curriculum vitae

Martin Hiensch (E.J.M.)

Education	University of Applied Science – Utrecht (1985 – 1988).
Date of birth	8 September 1965
Place of Birth	Rhenen, the Netherlands
Nationality	Netherlands

Carrier

1991 – now CTO, NSTO, AEA Technology, DeltaRail, Plurel, DEKRA Rail

Senior Consultant and Business development manager in the field of wheel-rail interface.

1988 –1990 Stichting Geavanceerde Materiaalkunde (SGM), Technische Universiteit Twente.

Appended papers

- [1] Hiensch, E.J.M. Wiersma, P. Reducing switch panel degradation by improving the track friendliness of trains, *Wear* 366-367 (2016) 352–358, DOI:10.1016/j.wear.2016.03.031
- [2] E.J.M. Hiensch & N. Burgelman (2017): Switch Panel wear loading – a parametric study regarding governing train operational factors, *Vehicle System Dynamics*, DOI: 10.1080/00423114.2017.1313435
- [3] Hiensch M. Burgelman N. Hoeding W. Linders M. Steenbergen M. Zoeteman A. Enhancing rail infra durability through freight bogie design. *Vehicle System Dynamics* (2017). DOI: <http://dx.doi.org/10.1080/00423114.2017.1421766>
- [4] Martin Hiensch and Michaël Steenbergen, Rolling Contact Fatigue on premium rail grades: Damage function development from field data, *Wear* 394–395 (2018) 187–194, DOI: 10.1016/j.wear.2017.10.018
- [5] Martin Hiensch and Nico Burgelman, Rolling Contact Fatigue: damage function development from two-disc test data, *Wear* 430-431 (2019) 376-382, <https://doi.org/10.1016/j.wear.2019.05.028>

Paper 1

Reducing switch panel
degradation by improving the
track friendliness of trains.



Reducing switch panel degradation by improving the track friendliness of trains



Martin Hiensch^{a,b}, Pier Wiersma^b

^a Delft University of Technology, Section of Railway Engineering, Faculty of Civil Engineering and Geosciences, Stevinweg 1, 2628 CN Delft, The Netherlands

^b DEKRA Rail, Concordiastraat 67, 3551EM, Utrecht, The Netherlands

ARTICLE INFO

Article history:

Received 12 January 2016

Received in revised form

29 February 2016

Accepted 29 March 2016

Available online 12 April 2016

Keywords:

Turnout

Switch panel

Frequency Selective Stiffness

Track friendliness

ABSTRACT

In this paper the performance of primary suspension elements with Frequency Selective Stiffness (FSS) behaviour in bogies is presented with respect to the ability to reduce wear and fatigue damage at the wheel–rail interface, thus enhancing the so-called ‘track friendliness’ of trains. Vehicle behaviour during negotiation of a turnout is evaluated in a case study with the Dutch double stock VIRM-4 train. Assessment of vehicle running behaviour is carried out by means of track–train simulations within the VAMPIRE multibody simulation software. The impact of FSS suspension elements is quantified in relation to wear and rolling contact fatigue damage (RCF) in the wheel–rail interface and regarding ride quality. The research shows that with application of FSS elements at the primary suspension, wear loading of switch and closure rail can be reduced significantly, increasing expected maintenance intervals and rail life. Simulation results demonstrate passenger comfort levels not to be influenced negatively.

© 2016 Elsevier B.V. All rights reserved.

1. Introduction

A railway turnout allows for the switching of rolling stock between two tracks. Turnouts are known operational bottlenecks in the railway network. The nature of the wheel–rail forces, acting as a result of changing contact conditions and route of travel, contribute strongly to this critical behaviour. The negotiation of the so-called ‘Switch panel’ (Fig. 1) in the diverging route of a railway turnout is accompanied by a large lateral displacement of the railway vehicle.

The resulting contact forces and slip levels at the wheel–rail interface cause the switch panel rails to suffer from wear (Fig. 2), plastic deformation and rolling contact fatigue damage (initiation and growth of cracks, Fig. 3). Consequently, the importance of switch inspection and maintenance activities is high (e.g. inspection, grinding, repair welding, replacement), whereas the available maintenance windows are limited. Since switches are key assets at the junction of individual routes, their non-availability often leads to a major disruption of the train service.

In turnouts applied by Dutch infra-manager ProRail, stock and switch rail are historically produced from R260Mn rail grade. The Dutch network is characterised by a route length of about 3000 km, a total track length of about 7000 km, 7300 turnouts and 3000 level crossings. An average gross freight volume of 70 MGT is annually facilitated by the network. The network is used daily by

6550 trains servicing 1.2 million passengers a day. Netherlands Railways (NS) is the largest train operating company, realizing more than 80% of the total train kilometres. With more than 870 coaches currently in operation, the VIRM double stock EMU is the largest fleet of NS.

1.1. Wheel–rail interface performance at the switch panel

The forces and resulting stresses acting at the switch panel running band are determined by the characteristics of the vehicle (e.g. axle load, yaw stiffness), the track (e.g. alignment, stiffness), the interface (e.g. wheel–rail profile combination, lubrication) and operational parameters (e.g. speed). Concentrating on track characteristics, switch panel performance has been investigated in [1, 2], e.g. by optimisation of track geometry through variation of the track gauge, or track stiffness (e.g. rail and under sleeper pads). The suggested gauge widening can be successful for the through route, it is however not effective in mitigating problems in the diverging route. Others [3] have investigated switch rail profile design, optimising rolling radius characteristics to improve switch kinematics.

In addition to track design optimisation, a further contribution reducing switch panel damage could be delivered by the vehicle. Novel running gear design has been studied e.g. in [4], however until now these studies focus on the running behaviour at plain line. The aim of the present study is therefore to assess the impact of improved track friendliness of trains regarding switch panel negotiation.

E-mail address: e.j.m.hiensch@tudelft.nl (M. Hiensch).

<http://dx.doi.org/10.1016/j.wear.2016.03.031>

0043-1648/© 2016 Elsevier B.V. All rights reserved.

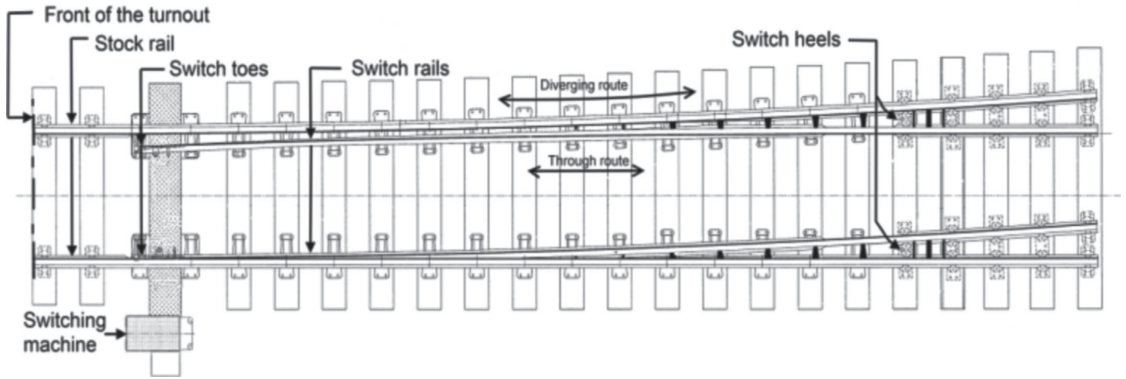


Fig. 1. Turnout switch panel.



Fig. 2. Severely worn and locally spalled switch blade (wear debris visible at sleepers and in ballast).



Fig. 3. RCF damaged stock rail.

When negotiating a turnout in the diverging route, the curving ability of the vehicle design plays an important role in the wheel-rail contact behaviour and the performance of the switch panel over time. To limit wear and rolling contact fatigue (RCF) damage at switches and curves, a low rotational stiffness of the wheelset within the bogie frame is required since this facilitates steering of the wheelset, reducing the lateral forces. However, to guarantee stability on straight track at high speed, a high rotational stiffness is necessary, resulting in high values of primary yaw suspension stiffness design. Consequently vehicle stability on straight track and curving ability in switches and curves impose a conflict upon the vehicle designer.

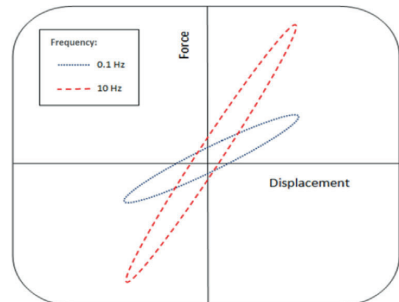


Fig. 4. Typical stress-strain behaviour depending on loading frequency.

1.2. The concept of Frequency Selective Stiffness

Recent developments within bogie design are aiming, among others, at the application of new elastic components with a characteristic that is dependent on the frequency of loading. As was presented in [5] these so-called Frequency Selective Stiffness (FSS) elements can, when applied at the primary yaw suspension, provide the required high stiffness at high loading frequencies to ensure stable running, together with low stiffness at low frequencies, resulting in moderate loading when negotiating a curve or switch. For the application discussed in this article, FSS behaviour is achieved by redesigning the classic steel-rubber component, adding internal chambers filled with hydraulic liquid. Connecting these chambers through a channel, serving as a flow control, adds a damper function to the component. The component stiffness becomes sensitive to the speed at which the fluid is transported from one chamber to another, resulting in a frequency-dependent stiffness (Fig. 4). These elements can often be retro-fitted within the existing train concept by simply replacing the conventional bush (Fig. 5).

The frequency content of the transverse loading of vehicles in curves depends on the curve radius. As compared to normal curves, the loading situation in turnouts can be expected to be more serious in the high-frequency regime.

When the primary suspension experiences a high-frequency loading, the damper function of the FSS element will be blocked, resulting in a stiffness value approximately equal to the conventional primary suspension element. Therefore the behaviour of this element type needs to be examined further. This study will

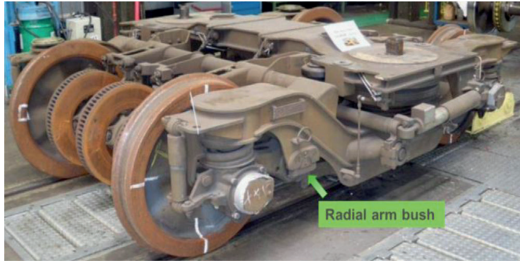


Fig. 5. Location of the primary suspension at the VIRM-4 type bogie.

focus on the potential benefits of the application of FSS, that were demonstrated for larger radius curves, and how these could also apply to switch panel negotiation. The dynamic simulation and evaluation of improved primary yaw suspension stiffness design, related to turnout negotiation, is the main novelty of this work. This information is of interest in understanding if track friendliness of rolling stock could be optimised with respect to turnout negotiation, to reach a more sustainable rail transport system resulting in a win-win situation for the whole system.

1.3. Abbreviations

- RCF: rolling contact fatigue
- FSS: Frequency Selective Stiffness
- PYS: Primary Yaw Stiffness
- T_y : dissipated energy (J/m)
- C_l : viscoelastic bush radial stiffness at low frequency range (kN/mm)
- C_h : viscoelastic bush radial stiffness at high frequency range (kN/mm)
- K_c : damping coefficient (Ns/mm)
- P_{CT} : discomfort level at curve transitions (% of passengers experiencing discomfort)

2. Dynamic simulations input

Assessment of the effect of FSS elements has been carried out by means of vehicle dynamics simulation, calculating contact forces and vehicle accelerations throughout the switch panel. Using the VAMPIRE multibody simulation software, the impact of modification in suspension characteristic has been quantified for a number of wheel-rail interface aspects: wear, RCF and passenger comfort. For validation purposes track inspection of several switches has been performed, documenting the nature and position of wheel-rail contact and rail damage throughout the switch panel. This information was used to support interpretation of the modelling results.

2.1. Track model

The applied track model describes the diverging route through the switch panel of the most common type of turnout applied in Dutch track: crossing angle 1 over 9 (Fig. 6). The cross sectional geometry through the switch panel has been built up from over 120 transverse rail profiles, measured in track at an average worn turnout. The profile measurement interval at the entry of the switch panel, where the rail heads of switch rail and stock rail are machined, was set to 50 mm. Switch geometry design values were further applied to the model (track gauge 1435 mm, no rail

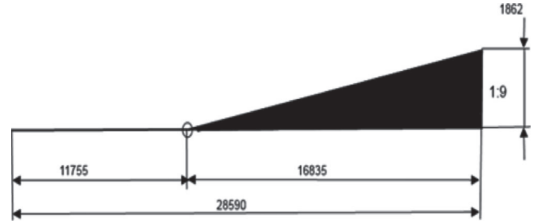


Fig. 6. Layout of 1 in 9 crossing angle switch design, all dimensions in millimetres. Maximum permitted train speed for this switch type (in diverging route) is 40 km/h.

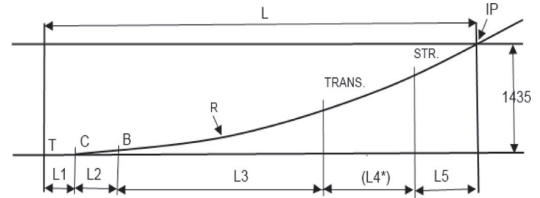


Fig. 7. General set up of switch geometry design.

Table 1

Lengths and radii for the considered 1 over 9 switch, measured along the left hand switch rail.

L1	1250 mm
L2	2055 mm
L3	19,284 mm
L4	0 mm
L5	2112 mm
R	195 m
CB	250 m

inclination). Apart from cross sectional wear, no geometrical disturbances were included in the track model. The rail head profile is UIC 54 E1. The lateral rail to sleeper stiffness is set to a default VAMPIRE value of 43 kN/mm, vertical track stiffness per rail to 50 kN/mm. These values are assumed to be constant throughout the switch.

The general set-up of switch geometry design can be described by the changes in curvature in combination with the lengths of each section. Fig. 7 illustrates these changes for a (left hand) switch design: L1 – length of straight from switch point T to transition curve starting point C, L2 – length of transition curve CB, L3 – length of switch radius R, L4 – length of transition curve from radius R to straight through crossing, L5 – length of straight to common crossing intersection point IP. In order to allow a more rapid build-up of the switch toe thickness, for the evaluated switch a 1:100 kink of the left hand stock rail towards the field side has been designed at point T. Table 1

2.2. Vehicle model

The modelled vehicle is Dutch double stock train type VIRM-4. The vehicle model consists of a front coach with one leading trailer bogie and one motor bogie, both of Dutch bogie manufacturer Stork-RMO design and an intermediate coach with trailer bogies designed by the Schweiz. Industrie-Gesellschaft (SIG). The wheel base is 2500 mm for the trailer bogies and 2750 mm for the motor bogies. The VIRM vehicles have a maximum speed of 160 km/h and axle loads of up to 22 t when fully loaded. At the axles of the motor bogie (axles 3 and 4), traction is simulated by applying a

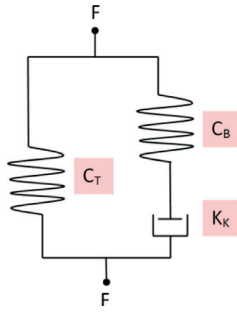


Fig. 8. Viscoelastic model of the FSS element.

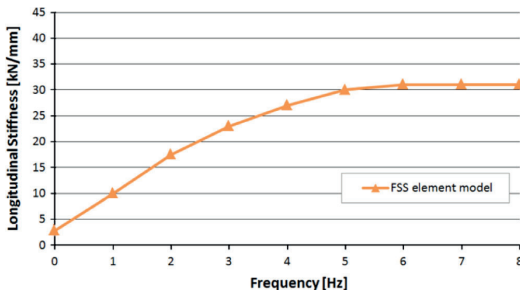


Fig. 9. FSS element stiffness dependency from loading frequency.

constant torque at both axles of 4.14 kN m, resulting in a driving force of 9 kN per wheelset. The vehicle model was initially validated by comparing its resonance frequencies and natural damping coefficients with the measurement results of real life dynamic tests. The model has been further validated by comparing measured vehicle behaviour with simulation output using measured track geometry data [6].

As part of the vehicle model, the radial arm bush was initially modelled as a conventional bush, comprising a constant stiffness value for the full frequency range. To evaluate the impact of FSS, this component was represented by a viscoelastic model (Fig. 8). This model consists of two elements; one linear spring in parallel with a series combination of a linear spring and damper. When this model is loaded, the two elements have a common displacement but the resulting force is determined by the level of maximum stiffness of either element. The output force is depending on the velocity and therefore the frequency of the displacement (low stiffness C_T in the low frequency range; higher stiffness C_B at higher frequencies). At considered operational values, being frequencies of 0.1 Hz to 10 Hz and amplitudes between 0.5 mm and 2 mm, the viscoelastic model receptance is in good agreement with measured receptance during dynamic component testing. Due to mass effects small stiffness variations do occur in relation to loading amplitudes. Fig. 9 presents the average stiffness vs. loading frequency within mentioned amplitude range.

3. Modelling results

Simulation runs were carried out with two versions of the VIRM-4 vehicle model; one equipped with conventional primary suspension and one with primary suspension elements with FSS behaviour. The radial stiffness of the conventional primary

suspension applied in VIRM trailing bogie is 30 kN/mm (linear behaviour) with resulting high Primary Yaw Stiffness (PYS) of 60 MNm/radian. Corresponding to the work presented in [5] the FSS characteristic is set to a static radial stiffness $C_T=2.8$ kN/mm and a dynamic radial stiffness value $C_B=25$ kN/mm. The applied vehicle speed is 40 km/h. The trailing bogie wheel load is set to 72 kN. The applied wheel profile design is UIC S1002, average worn with reduced flange width. The coefficient of friction between wheel and rail is set to $f=0.32$.

3.1. Assessment of RCF and wear

Assessment of wear and RCF behaviour (Head Check development) has been derived from the RCF damage function as presented in [7]. The main parameter in this function is the $T\gamma$ value (or wear number), which is a direct output from the Vampire multibody analysis. The parameter $T\gamma$ represents the dissipated energy between wheel and rail per travelled metre of track and is expressed in Joule per metre (J/m) or Newton (N). $T\gamma$ is determined by the product of tangential force (T) and creepage (γ). As presented in [7], the relation between the occurrence of visible RCF damage and wear number has been empirically established for R220 grade rail material. This RCF damage function has been extensively validated by comparing model predictions to Head Check propagation rate in track. It was found that there is a good correspondence between the model predictions and track observations [8].

3.1.1. $T\gamma$ development along the switch and closure panel

The dissipated energy $T\gamma$, at the wheel–rail contact patch of the leading axle, is presented in Fig. 10. The horizontal axis represents the position in the track. The switch toe is located at $x=40$ m. The left hand turnout is negotiated in the diverging route. The direction of travel is from left to right (the facing direction). For both the switch panel (position 40–48 m) and closure panel (position 48–63 m), $T\gamma$ development is presented for the contact area of the wheel tread/flange root (running surface) and the contact area of the wheel flange (flange). For those locations where simultaneously contact occurs at the running surface of switch rail and stock rail, $T\gamma$ values are summed.

Upon entering the switch, the wheel flange of the leading right wheel first contacts the switch rail at $x=40.5$ m. This is accompanied with a steep increase of $T\gamma$, with a peak at 1 m behind the toe of the switch. This area corresponds to the location where spalling and plastic deformation of the switch rail has been observed during track inspection (see also Fig. 2). When entering the switch, the primary suspension experiences a high-frequency loading. This causes the $T\gamma$ -values during entry of the switch panel to be similar for both types of primary suspension elements. When moving further down the switch panel, the primary suspension loading frequency decreases, resulting in softening of the FSS component. This allows the wheelset to set itself more in radial position, thereby decreasing $T\gamma$ -values. Throughout the switch panel the $T\gamma$ -level of the FSS element displays a growing deviation from the conventional primary suspension $T\gamma$ -level.

Upon leaving the switch panel, at around 12 m behind the switch toe ($x=52$ m), the $T\gamma$ -value at the flange of the leading right wheel, when equipped with the FSS type element, drops 40% with respect to the value of the conventional type (300 N vs. 500 N). This reduction is even stronger moving through the closure panel (from switch heels to front of the crossing nose), with values up to 50%.

The irregular $T\gamma$ -values corresponding to the first 8 m into the switch panel are caused by momentary changes in wheel–rail contact conditions. Small lateral changes of the wheelset relative to the rail cause the wheel–rail contact position to jump between

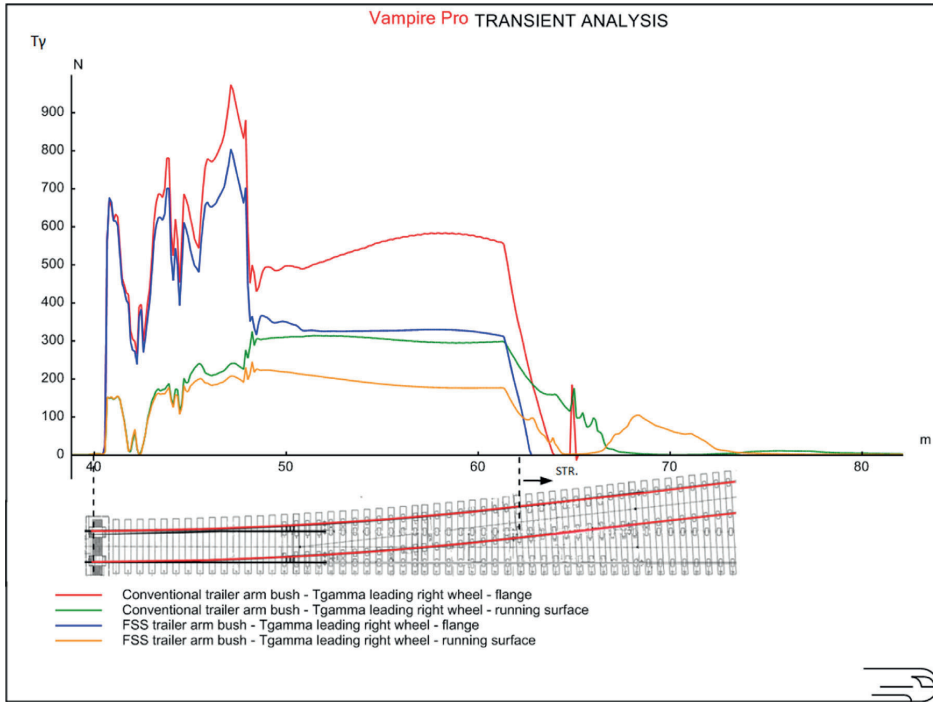


Fig. 10. Wear index $T\gamma$ at the wheel–rail contact area of running surface and flange, at the diverging route through switch and closure panel. Calculated for the leading wheelset of a VIRM-4 train at 40 km/h with conventional and FSS primary suspension elements.

switch rail and stock rail. This causes rapid changes in rolling radius and slip levels and is reflected in the observed sudden changes in $T\gamma$ -values. The observed irregular behaviour is explained from the use of multiple measured rail profiles. Up to 8 m behind the switch toe, successive Mini-prof rail profile measurements were used to describe the switch panel profile development. In particular the switch panel rail profile variation in the diverging route, in length 6 m from the switch entry (switch toe) to the switch heel where the switch rail profile transition has been completed and the switch rail regains a constant (nominal) rail section, has been build up from multiple measured rail cross-sections. The use of measured rail profiles at the switch panel, especially those combining stock and switch rail, will involve small alignment deviations between the successive measurement locations. These deviations and resulting changes in contact position cause the irregular $T\gamma$ behaviour, the overall $T\gamma$ development however remains clear. Beyond these first 8 m the rail is described by one single measured profile, resulting in a more steady wheel–rail contact behaviour.

3.1.2. Yaw angle development

Fig. 11 is presenting the development of the leading wheelset yaw angle through the switch and closure panel. It is observed that the application of FSS elements results in a graduate decrease of the yaw angle. The softening of the FSS component results in a reduction of the wheelset rotational stiffness, allowing a more radial setting of the wheelset in the curve. This improvement in steering ability is accompanied by a reduction of creepage levels which are reflected by the in Fig. 10 observed decrease in $T\gamma$ -values.

3.1.3. Flange contact area

The observed $T\gamma$ -value at the flange of the leading right wheel has been assessed using the RCF-damage function as presented in [7]. According to this RCF-damage function, the wheel–rail flange contact for both PYS component types are in full wear regime throughout the switch and closure panel ($T\gamma > 170$ N). Within the flange contact area no RCF damage is expected to develop for the R260Mn switch rail. This is confirmed by track observations for the conventional design. FSS application reduces the angle of attack of the wheelset, thereby reducing the level of lateral creepage. This results in the observed reduction of $T\gamma$ -values at the flange contact area, indicating a significant decrease in wear loading.

3.1.4. Running surface contact area

The RCF damage function from [7] indicates Head Check damage to develop when $20 < T\gamma < 170$. The observed $T\gamma$ -values at the running surface (wheel tread/flange root contact area) of the leading wheel predict RCF to develop at the switch panel, starting from the switch toe up to 3 m into the switch panel. The running surface at this position in the turnout is located at the stock rail. For the conventional PYS design, head check development at this position is confirmed by track observations (see also Fig. 3). Fig. 10 also shows that after three metres into the switch panel, the wheel–rail contact at the running surface operates in a full wear regime ($T\gamma > 170$ N). This applies to both PYS element types. FSS application however results in a significant decrease in wear loading of the running surface.

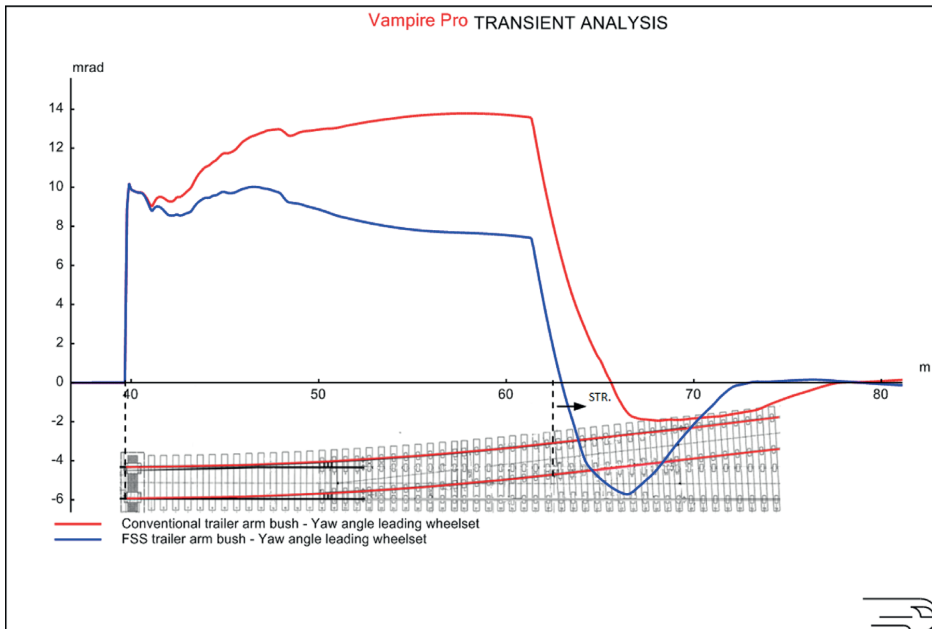


Fig. 11. Yaw angle development at the diverging route through switch and closure panel, calculated for the leading wheelset of a VIRM-4 train at 40 km/h with conventional and FSS primary suspension elements.

3.2. Passenger comfort (P_{CT})

Diverging through a turnout involves a large lateral displacement of the vehicle. The switch design in combination with the vehicle suspension characteristics and train speed determine the resulting discomfort. When regarding the switch panel as a curve transition, the experienced discomfort is found to be related to maximum lateral acceleration, maximum lateral jerk and maximum roll velocity. Passenger comfort has been evaluated by determining the accelerations at front and rear positions of the coaches in the vehicle–track simulations. For this purpose, filtering was applied in accordance with EN 12299:2009, Railway applications – Ride comfort for passengers – Measurement and evaluation. The P_{CT} comfort index values were calculated from the simulation output. The results show that for the assessed type of turnout, the application of FSS suspension elements has no significant impact on passenger comfort. The P_{CT} results (percentage of passengers experiencing discomfort) for the FSS equipped coach are approximately equal to the situation with conventional PYS.

4. Discussion

When negotiating a turnout in the diverging route, the curving ability of the vehicle will play an important role in the wheel–rail contact behaviour and the life-time performance of the switch panel. However, the curving ability of a vehicle, demanding low Primary Yaw Stiffness (PYS), conflicts with the required stability at high speed, demanding high PYS values. The PYS values of VIRM type double deck trains of NS are known to be relatively high, reducing the curving ability of these vehicles significantly. This restricted ability promotes wear and Rolling Contact Fatigue (RCF) damage development in both rail and wheels.

A new type of PYS component with Frequency Selective Stiffness (FSS) behaviour allows low stiffness values in curving to be combined with high stiffness values needed for stability at high speed. The presented research demonstrates that this application is expected to be very beneficial for both the Dutch infra-manager and train operator. From three metres behind the toe of the switch, moving further down the switch panel, a reduced PYS results in a significant decrease of T_y damage values. Comparing FSS behaviour to the conventional PYS design, for the assessed type of turnout, wear loading within the wheel–rail contact area is found to be reduced up to 50% when applying the FSS component.

Assessment of the observed T_y -values indicate the wheel–rail flange contact, for both PYS element types, to operate in a full wear regime throughout the switch and closure panel. No RCF development is to be expected for this contact position. Since the life of the switch rail and closure rail are dominated by wear, the resulting 40–50% reduction in wear loading achieved by FSS application will have a strong impact on maintenance need and cost. Throughout the switch and closure panel and for both PYS component types the contact between the wheel tread/flange root and rail head (running surface) is mainly operating in a full wear regime. RCF damage development is to be expected only at the stock rail running surface, at the first three metres into the switch panel. This is confirmed by track inspection. For the assessed vehicle–turnout combination, the T_y -value of this RCF susceptible area at the stock rail running surface is not influenced by FSS application, indicating unchanged RCF sensitivity.

The simulation results show good agreement with track observations. The location where spalling and plastic deformation of the switch rail has been observed during track inspection corresponds to a steep increase of the T_y -value from the emerging flange contact at the switch toe. This damage seems to be strongly related to the geometrical design of the turnout. Using the turnout

track model to review design optimisation could be an important next step.

5. Conclusions

Assessment of vehicle running behaviour, more specific the evaluation of primary suspension elements with Frequency Selective Stiffness (FSS) behaviour, was carried out by means of track–train simulations within the VAMPIRE multibody simulation software. The study especially evaluated the potential of FSS application to reduce wear and fatigue damage at the wheel–rail interface of a turnout.

The simulations show that track friendliness of trains, when negotiating a turnout, can be improved significantly by the application of FSS elements at the primary suspension level. The research has shown wear loading of switch, stock and closure rail to be reduced up to 40–50%. This reduction also apply to the wheel. The observed reduction in wear loading will result in an improvement of structural performance of the switch panel. Evaluation of passenger comfort through the diverting route of the assessed turnout showed comfort levels not to be influenced by the application of FSS primary suspension elements.

Acknowledgements

This research project is being carried out by the author under the project number T91.1.12475a in the framework of the Research Programme of the Materials innovation institute M2i (www.m2i.nl). The author would like to acknowledge DEKRA Rail for their contribution to the results presented in this paper.

References

- [1] M.R. Bugarin, J.M. Garcia Diaz de Villegas, Improvement in railway switches, *J. Rail Rapid Transit*, IMechE (2002).
- [2] B. Palsson, *Towards Optimization of Railway Turnouts* (Licentiate thesis), Department of Applied Mechanics, Chalmers University of Technology, Goteborg, Sweden, 2011.
- [3] B. Palsson, J.C.O. Nielsen, Design optimization of switch rails in railway turnouts, in: Proceedings of the 9th International Conference on Contact Mechanics and Wear of Rail/Wheel Systems (CM 2012), China, 2012.
- [4] S. Iwnicki et al., The 'SUSTRAIL' high speed freight vehicle: simulation of novel running gear design, *IAVSD13-3*, Z-ID490.
- [5] Hiensch et al., Improving track-friendliness of rolling stock, in: Proceedings of the International Heavy Haul Association, Australia, 2015.
- [6] M. Linders, Extension and validation of the VIRM-4 vehicle model, *Plurel report/13/120125/004*, March, 2013.
- [7] M.C. Burstow, A model to predict and understand rolling contact fatigue in wheels and rails, in: Proceedings of the WCRR, Canada, 2006.
- [8] M. Zacher, Rolling contact fatigue (RCF): models and experiences of DB AG, *RTR1/2011*, pp. 35–42.

Paper 2

Switch Panel wear loading –
a parametric study regarding
governing train operational
factors.

Switch Panel wear loading – a parametric study regarding governing train operational factors

E. J. M. Hiensch & N. Burgelman

To cite this article: E. J. M. Hiensch & N. Burgelman (2017) Switch Panel wear loading – a parametric study regarding governing train operational factors, *Vehicle System Dynamics*, 55:9, 1384-1404, DOI: [10.1080/00423114.2017.1313435](https://doi.org/10.1080/00423114.2017.1313435)

To link to this article: <https://doi.org/10.1080/00423114.2017.1313435>



© 2017 The Author(s). Published by Informa UK Limited, trading as Taylor & Francis Group.



Published online: 20 Apr 2017.



Submit your article to this journal [↗](#)



Article views: 328




View related articles [↗](#)



View Crossmark data [↗](#)

Switch Panel wear loading – a parametric study regarding governing train operational factors

E. J. M. Hiensch^{a,b} and N. Burgelman ^b

^aSection of Railway Engineering, Faculty of Civil Engineering and Geosciences, Delft University of Technology, Delft, Netherlands; ^bDEKRA Rail, Utrecht, Netherlands

ABSTRACT

The acting forces and resulting material degradation at the running surfaces of wheels and rail are determined by vehicle, track, interface and operational characteristics. To effectively manage the experienced wear, plastic deformation and crack development at wheels and rail, the interaction between vehicle and track demands a system approach both in maintenance and in design. This requires insight into the impact of train operational parameters on rail- and wheel degradation, in particular at switches and crossings due to the complex dynamic behaviour of a railway vehicle at a turnout. A parametric study was carried out by means of vehicle-track simulations within the VAMPIRE[®] multibody simulation software, performing a sensitivity analysis regarding operational factors and their impact on expected switch panel wear loading. Additionally, theoretical concepts were cross-checked with operational practices by means of a case study in response to a dramatic change in lateral rail wear development at specific switches in Dutch track. Data from train operation, track maintenance and track inspection were analysed, providing further insight into the operational dependencies. From the simulations performed in this study, it was found that switch rail lateral wear loading at the diverging route of a 1:9 type turnout is significantly influenced by the level of wheel–rail friction and to a lesser extent by the direction of travel (facing or trailing). The influence of other investigated parameters, being vehicle speed, traction, gauge widening and track layout is found to be small. Findings from the case study further confirm the simulation outcome. This research clearly demonstrates the contribution flange lubrication can have in preventing abnormal lateral wear at locations where the wheel–rail interface is heavily loaded.

ARTICLE HISTORY

Received 14 October 2016
Revised 3 February 2017
Accepted 26 March 2017

KEYWORDS

Dynamic train-turnout interaction; switch panel; wear; flange lubrication

1. Introduction

The increasing use of rail for both passenger and freight traffic is demanding a growing effort and cost of track maintenance and, if unchallenged, could become a major constraint in the development of overall railway productivity. Issues with track availability and cost related to maintenance will first present themselves at the more vulnerable bottlenecks in the railway network. From this viewpoint switches and crossings (S&C) clearly stand out,

CONTACT E. J. M. Hiensch  e.j.m.hiensch@tudelft.nl

since a significant part of the annual rail infrastructure budget is already allocated to maintenance and renewal of S&C, illustrating its vulnerability. The Innotrack technical report [1] concludes ‘switch wear’ to be one of the top three main reported track problems.

S&C are important elements in the railway network operation, as they enable trains to change between tracks. Allowing trains to reach their targeted platform, the number of railway switches per route length is especially high at and around railway stations. A railway turnout consists of a switch panel and a crossing panel connected by a closure panel. The designated areas in turnout negotiation are indicated in Figure 1.

The high demand for maintenance at S&C is explained by the nature of its function, design and resulting forces. The dynamic behaviour of a railway vehicle in S&C is complex. From the switch toe (Figure 2), moving down the switch panel, switch- and stock rail profiles are gradually changing. This has an ongoing effect on the contact positions between wheel and rail, the acting rolling radius difference and resulting (tangential) wheelset steering forces. When negotiating a switch in the diverging route, railway vehicles often experience significant lateral displacements. This will cause the wheel flange to come into contact with the rail face. When in flange contact, the level of lateral forces and high slip values can result in significant lateral rail head (side) wear, accumulated plastic strain and problems with crack formation and chipping of material (spalling). Due to the

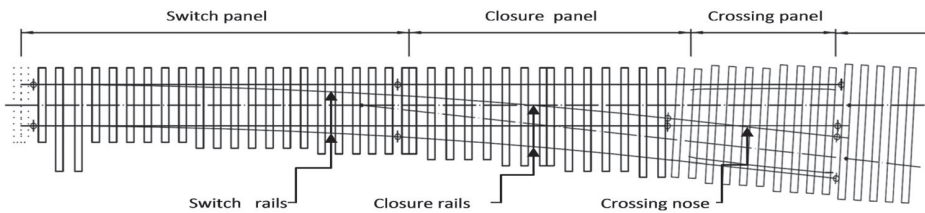


Figure 1. Designated areas in turnout negotiation.

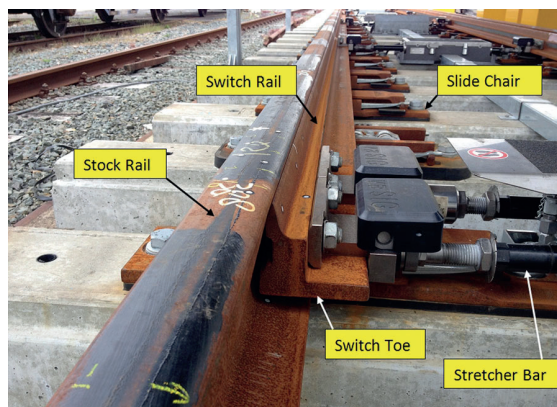


Figure 2. Switch panel components.

negative impact on service life and safety against derailment, severe side or gauge face wear of the switch rail will have significant operational and financial implications.

The Dutch railway network has around 8600 switches in its 7000 km of track. From [2], presenting the cost of operation and maintenance of track in the Netherlands, it can be seen that in 2014 yearly cost for S&C routine maintenance (KO), comprising inspection, service tests, small repairs and replacement of components, is about € 85 million covering 40% of the total annual KO track maintenance budget. Switch maintenance clearly claims a disproportionate amount of the overall budget. The in [1] reported Innotrack analysis of selected lines at Deutsche Bahn (DB) and Banverket (BV) identified the switch maintenance budget breakdown, presented in Figure 3.

Understanding the impact of individual train operational parameters on rail- and wheel degradation is required in order to manage the experienced wear, plastic deformation, crack development and resulting maintenance both at wheels and rail. To examine the effect of single parameter changes to resulting track loading and related material response, parametric studies can be carried out using commercial multi-body software like VAMPIRE[®] to model the dynamic interaction between vehicle and track/wheel and rail. Kassa and Johansson [3] present a parametric study for a Y25 freight bogie with respect to wheel profile, axle load and vehicle speed in relation to contact pressure and wear index along the switch rail at the diverging route. Especially for freight bogies, a large distribution in (worn) wheel profile shape and resulting multiple wheel–rail contact conditions are common as well as a large variation in axle load. Contact pressure and wear index were observed to increase with increasing axle load, the influence of train speed is however small, whereas the influence of wheel profile is significant. It is found that the large contact pressure on the switch rail was mainly due to poor contact geometry conditions. To further study, the influence of scatter in traffic parameters regarding the dynamic interaction between a railway freight vehicle and a turnout, Pålsson and Nielsen [4] performed a parametric study by simulations of vehicle dynamics. They showed that, when to account for wheel profile scatter, equivalent conicity is the wheel profile parameter best correlating to damage in the

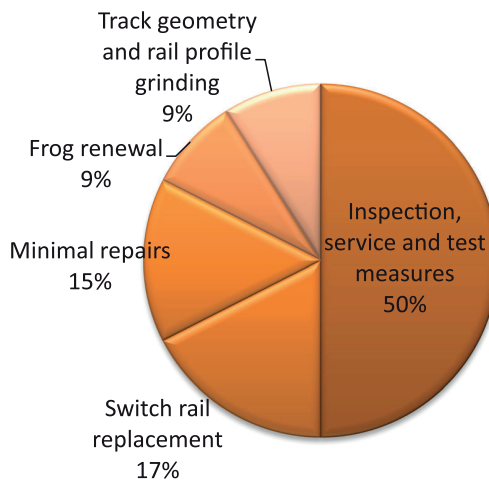


Figure 3. Switch maintenance budget breakdown [1].

switch panel. Beside the diverging route, side wear at the switch panel can also occur in the through route. Results of Spangenberg and Fröhling [5], evaluating severe side wear in a 1:20 turnout, conclude wear at the through route switch rail to be caused by rail profile changes in the switch area resulting in large lateral displacements of the wheelset. Further improvement of the switch panel design for the through route has been studied by Nicklisch et al. [6] and Bugarín et al. [7]. Based on a parametric study, dynamic track gauge optimisation by geometry gauge variation resulted, for the analysed configuration, in a significant reduction of wear and improved behaviour in terms of rolling contact fatigue (RCF).

Other train operational parameters potentially important regarding accumulated damage development, not included in [3], are e.g. direction of traffic, wheel–rail coefficient of friction, traction and mode of train operation (push vs. pull). The objective of the current work is to present a parametric study for the most common type of Dutch turnout (crossing angle 1:9), expanding the parametric scope to include further train operational parameters. However, not directly subject of this study, the effect of worn wheel or rail profiles and axle load is included into the discussion of this article. The level of wear loading at the rail surface resulting from trains negotiating railway turnouts in relation to train-track operational parameters is subject of this study. Additionally, a case study was performed, examining operating conditions at a location with reported severe switch rail wear and cross-checking the parametric study results. Following the specific track yard conditions, two track design parameters were added to the parametric study, examining the effect of track gauge widening and switches in short succession. The main goal of the presented study is to define the dominant switch rail wear influencing parameters in relation to train operation for the considered configuration. This understanding can further assist the track engineer in the optimisation of turnout performance.

The structure of this paper is as follows: after the introduction, Section 2 discusses different regimes of rail wear behaviour. Section 3 presents the modelling set up of vehicle-turnout dynamics. Section 4 presents how the simulation results are analysed regarding wear and fatigue behaviour. The main operational parameters are evaluated in Section 5, presenting the set up and results of the performed parametric study. Section 6 introduces the additional performed case study describing the nature of the occurring problem, documenting its circumstances and presenting results from data analysis and inspection. Overall findings are discussed in conjunction in Section 7 followed by conclusions in Section 8.

2. Rail wear

Due to the acting forces between wheel and rail, wear at the switch panel rail is generally to be expected. Earlier studies regarding the wear behaviour of wheel and rail materials identified different wear regimes, characterised in terms of wear rate and wear debris [8]. The three identified wear regimes were designated mild, severe and catastrophic. Also the occurring wear mechanisms within these regimes were investigated. At normal conditions the acting wear regime will be characterised as ‘mild’ with inter-metallic contact prevented by protective oxide layers [9]. The resulting wear rate is low, the contacting surfaces are smooth, without clear apparent wear debris. With changes to the system, for example, increasing wear loading or unfavourable material pairing, a transition can occur from ‘mild’ to ‘severe’. The wear regime is considered to be ‘severe’ when wear rates are

high and roughness of the wearing surfaces is also high. Analysis of the contact conditions indicated that the transition from mild to severe was caused by the change from partial slip to full slip conditions [8]. A mechanism addressed as ‘delamination wear’ causes the severe wear regime at the wheel–rail contact, marked by deformation followed by crack growth and subsequent material removal. It is mainly generated by adhesion and metal to metal contact. Work from Johnson [10] shows delamination wear to be driven by the process of plastic strain accumulation known as ratchetting. The most evident sign of delamination wear is the existence of lamellar (plate-like) debris particles. Interestingly, the wear within this regime is found to be largely independent of sliding velocity, suggesting that it is controlled by contact stress and limiting traction alone. A second transition to catastrophic wear is considered to be the result of surface temperature effects. Assessment of material respond to cyclic stress can take place by using so-called shakedown maps, presenting the material hardening curves that define the areas with different types of material response. The shakedown map for a general three-dimensional rolling-sliding contact is presented by Ponter et al. [11]. The shakedown limit above which accumulation of plastic strain, that is, ratchetting will occur is seen to increase with decreasing friction coefficient. At coefficient of friction levels < 0.3 , cumulative plastic flow occurs sub-surface. At friction coefficient levels > 0.3 , plastic flow occurs dominantly at the surface. At relative high coefficients of friction (> 0.4), the ratchetting mechanism becomes very localised at the surface. Friction control through railhead lubrication, therefore can assist to move the operational point away from the area of ratchetting, relieving the surface. Other operational parameters addressing the shakedown load factor level and resulting material respond need to be further understood and quantified at an individual level. Damage models based on the calculated energy dissipation can be used for the evaluation of rail wear. This is further discussed in Section 4.

3. Modelling of vehicle-turnout dynamics

The wheel–rail contact is complex due to the relative motion of the two contacting bodies, elastic deformations and friction processes. To solve the contact problem, Kalker [12] developed numerical methods for rolling contact, making these available through his programme CONTACT and later the fast algorithm FASTSIM. Within vehicle system dynamics packages, multi-body software is used to describe both track and vehicles by a number of interconnected rigid or flexible bodies. System behaviour is obtained through analysis of the equations of motion, computing the dynamic movement of the different components, allowing the rail–wheel contact slip and locations to be determined. Then normal contact forces can be determined by for example, means of Herzian formulas and using FASTSIM for the tangential direction [13].

The use of dynamic simulation tools provides the railway engineer with the ability to quantify the impact of changes in design and operational parameters, by considering the complete interaction between vehicle and track. This work requires track and vehicle models to be set up, as well as operational inputs like speed and loading profiles. The simulation software VAMPIRE[®] Pro 6.30 has been used to simulate vehicle dynamics for traffic in the facing and diverging route. The used vehicle model is based on the Dutch VIRM-4 double deck passenger train, currently the largest proportion of the NS fleet. The model consists of a front coach with one leading trailer bogie and one motor bogie and

an intermediate coach with trailer bogies, with a bogie spacing of 20 m. The wheel base is 2500 mm for the trailer and 2750 mm for the motor bogie. VIRM bogies are equipped with trailer arms, connecting the wheelset to the bogie frame. The trailer arm bushes determine the lateral, longitudinal and yaw primary suspension stiffness. The radial stiffness of the conventional primary suspension applied in VIRM trailing bogie is 30 kN/mm (linear behaviour) with resulting high primary yaw stiffness (PYS) of 60 MNm/radian. VIRM-4 trains are reported to suffer from fatigue crack initiation at the running surface (wheel rim). When allowed to grow, these cracks will lead to significant wheel diameter loss during wheel reprofiling aimed to remove these cracks. Therefore, since the year 2010 wheels of VIRM type trains are profiled about every 10 weeks to prevent development of initiating cracks. As a result, wheel profile variation of VIRM-trains is very limited, all very close to the applied design profile being UIC S1002 with reduced flange width. VIRM-4 vehicles have a maximum speed of 160 km/h and axle loads of up to 20 tons when fully loaded. At the axles of the motor bogie (axles 3 and 4), traction is simulated by applying a constant torque at both axles of 4.14 kNm, resulting in a driving force of 9 kN per wheelset. During VAMPIRE[®] simulation runs the vehicle speed remains constant. The vehicle model itself is connected to the rigid ground by a spring/damper. When a torque is applied to the wheels of the model, the driving force will be balanced by this spring/damper, preventing acceleration. Previously validation of the vehicle model has been performed, as described in [14]. Initially by comparing its resonance frequencies and natural damping coefficients with measured accelerations from a wedge test and further validated by comparing measured vehicle running behaviour with simulation output using measured track geometry data.

The multi-body model of the turnout is based upon a mass-spring-damper system. The track model consists of two rails, each attached to the rigid, massless sleeper by spring-damper elements in the lateral direction. The sleeper is connected with two vertical spring-damper elements to the rigid ground. The track model is coupled to each wheelset in the vehicle model (moving track model). The applied track model describes the diverging route through the switch panel of the most common type of turnout applied in Dutch track: crossing angle 1 in 9, as described in [14]. The cross-sectional geometry through the complete switch panel has been built up from over 120 transverse rail profiles, measured in track at an average worn turnout, using the MiniProf Measurement system (Figure 4). The left and right rail profiles are measured individually. The switch toe is set as reference point (0.00). Profiles are measured in the plane of the track and so take into account the rail inclination. The profile measurement interval at the entry of the switch panel, the first meter behind the switch toe, has been set to 50 mm. Further into the switch panel the longitudinal profile discretization has been set to 200 mm and from meter 5 behind the switch toe to 400 mm. To simulate the changing rail profile through the turnout, VAMPIRE[®] performs an interpolation between tabularized wheel-rail contact data of each of the measured rail sections.

Switch geometry design values were further applied to the model (track gauge 1435 mm, no rail inclination). Apart from cross-sectional wear, no geometrical disturbances were included in the track model. The rail head profile is UIC 54 E1. The lateral rail to sleeper stiffness is set to a default value of 43 kN/mm, vertical rail stiffness per rail to 50 kN/mm. These values are assumed to be constant throughout the switch. The timestep in all simulations was 0.1 ms. No cut-off filtering was applied. Results plotting step size is 0.1 kHz

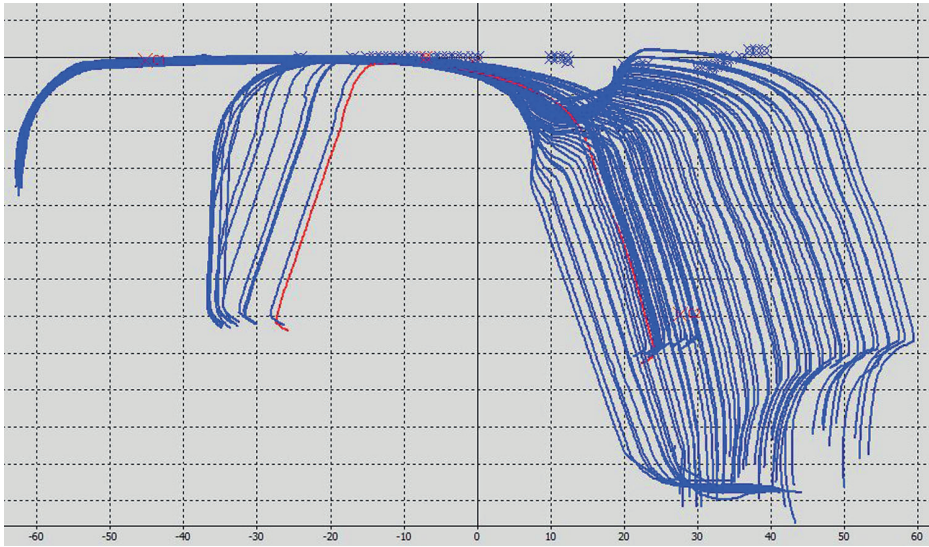


Figure 4. Overview of Miniprof rail cross sectional profiles measured at a section of the switch panel: the combined stock and switch rail serving the diverging route.

for all vehicle speeds. This corresponds to the frequencies proposed in [4] to capture the dynamic interaction for the changing rail profile at the turnout.

4. Wheel-rail damage criteria

Wear and Head Check damage development can be derived from the RCF damage function as presented in [15,16]. The main parameter in this function is the $T\gamma$ value (or wear energy number), which is a direct output from the VAMPIRE[®] multibody analysis. The parameter $T\gamma$ represents the dissipated energy between wheel and rail per travelled meter of track and is expressed in Joule per meter (J/m) or Newton (N). $T\gamma$ is the product of tangential force (T) and creepage (γ). The relation between the occurrence of visible RCF damage in R220 grade rail material is established in the RCF damage function as presented in Figure 5. In this graph, $T\gamma$ is plotted on the horizontal axis. On the vertical axis, the RCF damage

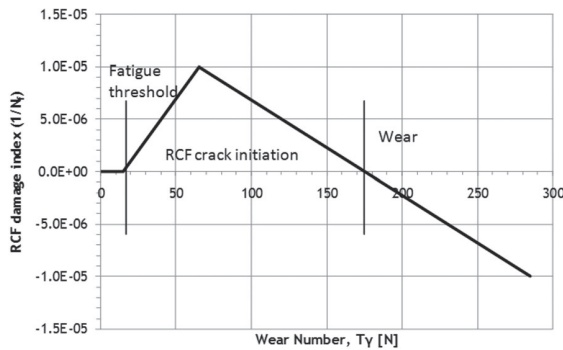


Figure 5. RCF-damage function for rail grade R220 [15,16].

index is plotted. The RCF damage index equals 1 divided by N_f : the number of loading cycles until the first visible Head Check damage occurs.

The RCF damage function has been extensively validated by comparing model predictions to Head Check propagation rate in track. It was found that there is a good correspondence between the model predictions and real-life observations [17]. A similar methodology for prediction of distributions of accumulated rail damage (wear and RCF) in railway turnouts has been presented and demonstrated in [18], involving simulation of dynamic train-track interaction and assessment of expected wear and RCF development.

Besides RCF, also the expected wear behaviour can be determined from the occurring $T\gamma$ value, since the wear load is closely related to this parameter. For the standard rail grade R220 an empirical threshold value has been established above, which wear behaviour transfers from 'mild' to 'severe'. This transition can be expected from $T\gamma > 200$ N, resulting in a significant increase in wear rate and surface roughness. Based on twin-disk testing, Lewis and Dwyer-Joyce [8] present the wear behaviour in relation to $T\gamma$ for the 'severe' wear regime. The wear rate is found to be a linear function of the wear energy number divided by contact patch area ($T\gamma/A$).

Assessment of $T\gamma$ loading distinguishes two contacting areas: the running surface (rail crown/ shoulder) and flange. Due to the high level of slip when in flange contact, wear loading in general here is significantly higher than at the rail crown or flange root contacting area.

5. Sensitivity analyses

A sensitivity analysis has been carried out by means of track-train simulations within the VAMPIRE[®] multi-body simulation software. Studying the contribution of identified parameters with respect to switch loading and related wear, $T\gamma$ values were assessed for the leading wheel. Since lateral wear is the result of wear loading at the flange, for this study $T\gamma$ development only is presented at flange contact. The parametric study was carried out involving train operational parameters that were identified as potentially dominating the resulting wear loading. The operational parameters considered are: vehicle speed, running direction, traction and wheel-rail friction level. Additionally, the influence of track gauge and track yard design was reviewed, in particular, the effect of multiple switches in short succession. Influence of the individual parameters is compared to a reference situation. The considered reference situation, for which only one parameter at a time was varied, consists of

- direction of traffic: diverging route, facing direction;
- connecting track to turnout: tangent;
- vehicle speed: 40 km/h;
- track gauge: 1435 mm;
- traction: active and
- no flange lubrication, wheel-rail friction coefficient set to $f = 0.32$.

To illustrate the overall dynamics at play for the modelled vehicle negotiating the 1:9 switch, the resulting lateral and vertical forces for the reference situation are presented in Figures 6 and 7. For the leading wheel of each bogie almost directly after entering the

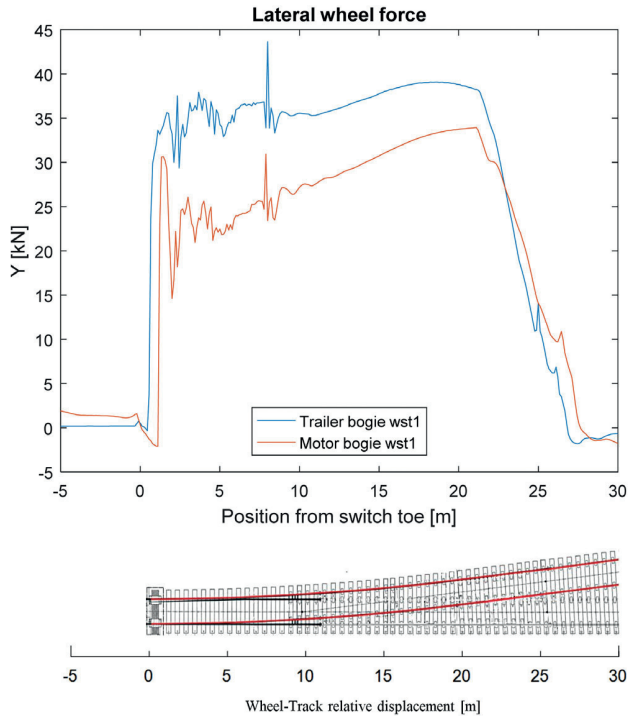


Figure 6. Lateral wheel force of at the leading wheel of the front bogie (trailer) and second bogie (motor).

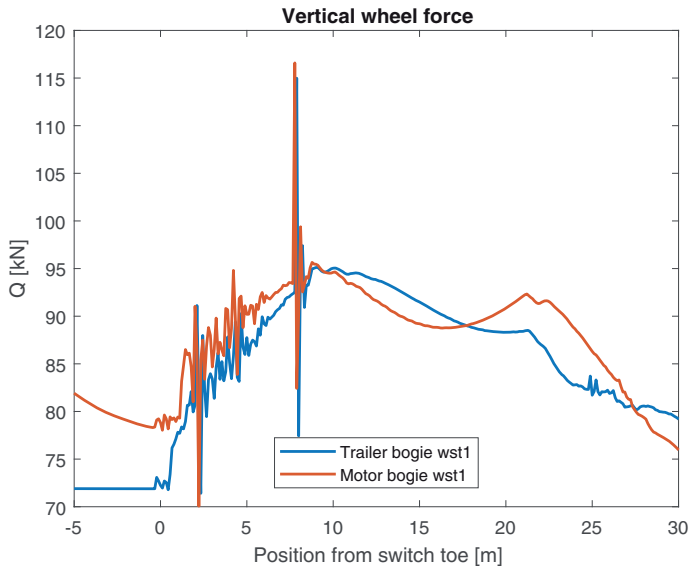


Figure 7. Vertical wheel force of at the leading wheel of the front bogie (trailer) and second bogie (motor).

switch flange contact occurs, resulting in a sharp increase in lateral wheel force. Throughout the switch panel and crossing panel the wheels remain in flange contact, showing a rather irregular behaviour during the first 8 m.

The irregular lateral and vertical wheel force values corresponding to the first 8 meters into the switch panel are caused by discontinuities in the wheel–rail contact conditions. The use of measured rail profiles at the switch panel, especially those combining stock and switch rail, will involve small alignment deviations between the successive measurement locations. These deviations and resulting changes of the wheelset relative to the rail cause the wheel–rail contact position to jump between switch rail and stock rail. This leads to abrupt changes in contact pressure, rolling radius and slip levels and is reflected in the observed sudden changes in Y and Q values, the overall development however remains clear. Beyond these first 8 m, the rail is described by a single measured profile, resulting in a steadier wheel–rail contact behaviour.

5.1. Results

Simulation results are presented and discussed for the assessed parameters.

5.1.1. Vehicle speed

Figure 8 presents the effect of train speed in relation to flange contact T_γ development at the leading wheel of the leading bogie. When negotiating the switch panel, three distinct peaks for T_γ are seen to arise. These occur from changes in contact position and corresponding changes in locations and orientations of contact forces and slip. Upon entering the switch, a first peak for T_γ arises due to the appearing flange contact. A second peak occurs when the wheel load fully transfer from stock rail to switch rail. A third peak arises

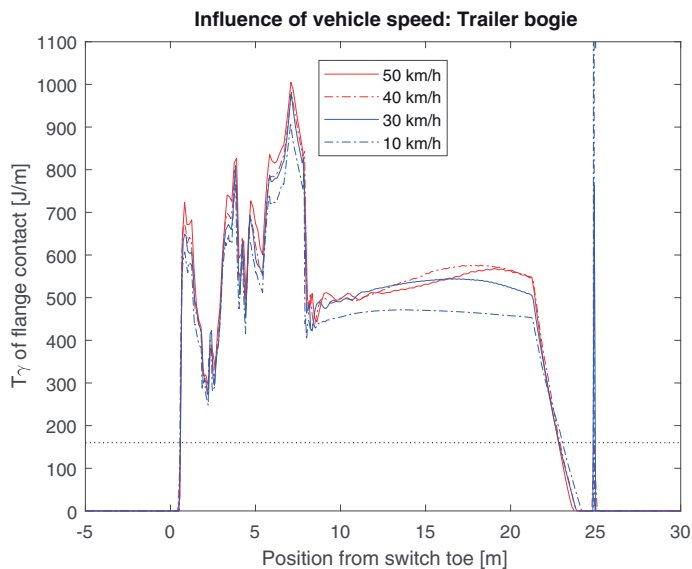


Figure 8. Wear loading for different train speeds. T_γ development at leading wheel of leading bogie.

at the end of the switch rail: at the transition of the machined switch rail profile to the nominal profile.

Figure 8 clearly shows the influence of train speed to be rather small. This observation is in accordance with the findings of the parametric study reported in [3] concluding that, for a give combination of wheel profile and axle load, the influence of train speed on contact pressure is small. Similar VAMPIRE[®] simulation results are reported in [19], presenting a modelled 1:9 turnout and container wagon (22.5 tons axle load). For the presented vehicle speed range of 5–50 km/h, it can be observed that the influence on wear energy development at the flange contact is very limited, this again in correspondence with the present study.

5.1.2. Wheel–rail coefficient of friction

The effect of the wheel–rail friction coefficient within the flange contact is presented in Figure 9.

The friction coefficient is seen to have a significant effect on the level of $T\gamma$ and the corresponding wear loading of switch and closure panel. Decreasing the friction coefficient from $f = 0.32$ to $f = 0.15$ will halve the lateral wear loading at the switch rail gauge face. For the lubricated (low friction) condition, the resulting $T\gamma$ values of 300 J/m for the leading trailer bogie and 200 J/m for the motor bogie indicate the switch rail to operate within the regime of full wear. The expected wear rate however is much lower compared to the non-lubricated (high friction) condition. From the resulting $T\gamma$ values in lubricated condition ($T\gamma \approx 200$ J/m), operation of the closure rails can be expected to be within the regime of mild wear for the leading bogie. For the motor bogie, with $T\gamma$ values for the reviewed configuration varying from 100 to 180 J/m, locally a shift into the RCF/wear regime is to be expected.

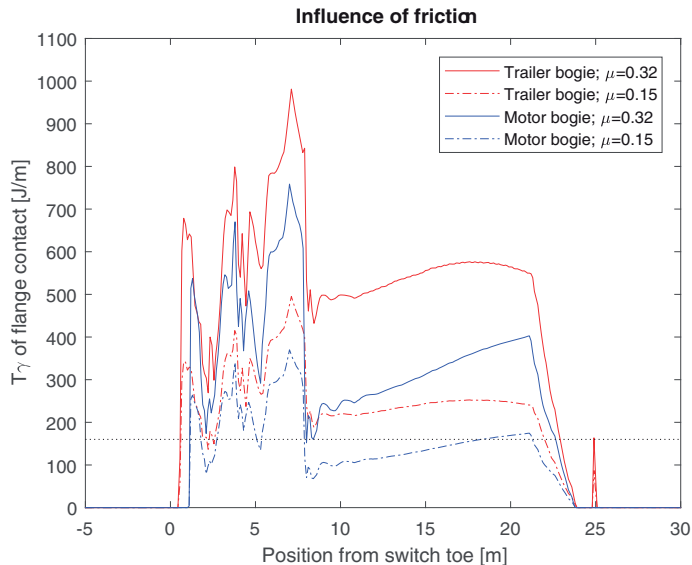


Figure 9. Wear loading in dependency on friction coefficient. $T\gamma$ development at the leading wheel of trailer and motor bogie.

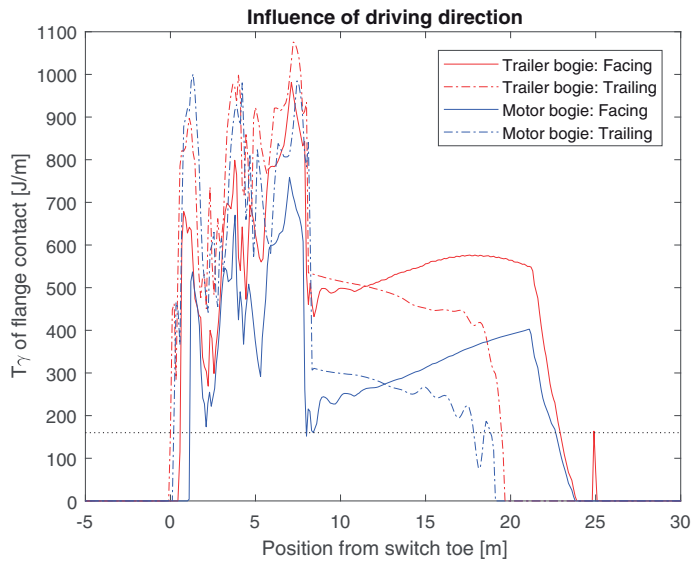


Figure 10. Wear loading for different directions of traffic (trailing/facing). T_γ development at the leading wheel of motor and trailer bogie.

5.1.3. Direction of travel at diverging route

Figure 10 shows the effect of direction of travel at the diverging route, presenting the T_γ development for the leading wheels of first (trailer) and second bogie (motor). When travelling in the trailing direction (running along the point), the wear loading at the switch rail is seen to be 30% higher compared to the facing direction (running towards the point), as can be seen in Figure 10. The wear loading at the closure rail on the other hand is seen to decrease when travelling the diverging route in trailing direction. *Remark:* in both trailing and facing direction the applied vehicle orientation is equal with respect to the direction of traffic: the front coach is followed by intermediate coach.

This effect in wear loading can be explained by the relatively short curved section for this type of switch. When the leading bogie enters the curved section of the turnout, the second bogie will still be in the tangent track section. When going further down the curve the coach will start to rotate with respect to the second bogie, addressing the rotational resistance between these two. The resulting torque will increase the lateral (Y) force at the flange contact of the leading wheelset. When the leading wheelset has passed the switch curve, a similar however less pronounced effect will occur at the flange contact for the second bogie. This effect is illustrated in Figure 11, presenting the lateral (Y) forces when negotiating a curve with radius 195 m, curve length 20 m, without transition curves. It can be observed that for both the leading (trailer) bogie and second (motor) bogie the lateral forces at the leading wheel are gradually increasing.

5.1.4. Track layout, gauge and traction

The effect of the track layout has been considered by connecting the left-hand switch to a right hand curve with 195 m radius without cant, creating an S-shaped curve. The influence of this alignment set-up seems to be small. After negotiating the curve the lateral

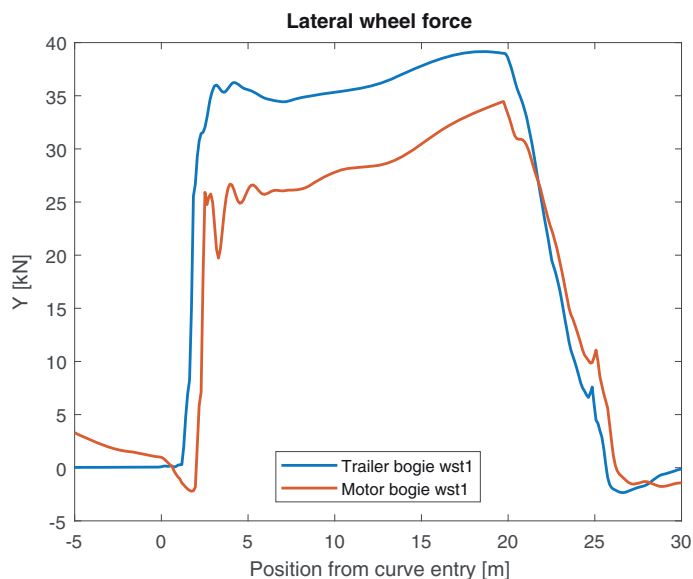


Figure 11. Development of the lateral (Y) forces when negotiating a curve with limited length (20 m).

position of the wheels is out of centre. This has an influence on the position where the wheel flange makes first contact with the switch rail, it however has no significant influence on the level of the wear loading. Increasing the gauge to 1445 mm does not show to have a significant influence on the level of wear loading, nor does traction show a notable effect.

6. Case study

An opportunity to expand the scope of this parametric study occurred when issues with severe switch rail wear were reported at a large number of 1:9 turnouts installed at the ProRail railway yard of Amsterdam Central Station (see Figure 12).

The most extreme case that was reported, was 1 mm of side wear within nine days, resulting in a significant increase in maintenance pressure and related cost for repair and renewal. A corresponding increase in side wear was also reported for the high rail of a number of narrow curves near the station. This abrupt increase in wear behaviour offered the opportunity to study the effect of possible changes in operational parameters to which modelling results can be cross-checked.

6.1. Problem analysis

In order to understand the setting and specific issues related to the observed dramatic change in lateral switch rail wear at the Amsterdam CS railway yard, it was decided to perform a systematic problem analysis. The involved parties were specialists of infrastructure manager ProRail, the responsible maintenance contractor and train-track specialists. The goal was to identify influencing factors and probable causes and deciding upon further



Figure 12. Severely worn switch rail (inspection December 2014).

analysis. The reported problem was first accurately defined, e.g. determining its characteristics and appearance, at what locations does the problem (not) occur, what is the normal value, what is the deviation and since when has the problem occurred. Also it is important to recognise if there have been changes to the system that could affect the (accumulated) wear loading of the switch panel, for example an increase in annual tonnage, change in operating trains and/or different routing of (freight) trains through the railway yard.

During the problem analysis a number of switches from the railway yard, equal in design, were reviewed. Based on maintenance and loading class, some in this group were ranked as ‘severe’ others as ‘mild’, corresponding to the experienced wear rate. From each of these groups switches were selected for further analysis. The reported dominating wear problem manifests itself at the switch panel, more specifically at the switch rail serving the diverging direction. Although for severely wearing switches also the closure rail suffers from excessive lateral wear, the small lateral wear limit value at the switch rail compared to the corresponding limit value for the closure rail determines the switch rail to dominate the resulting maintenance and renewal pressure. Reported switch rail life for the severely wearing switches has fallen to nearly three months. The trend in wear development of these switches is said to show a sharp deviation, which suddenly occurred at the end of 2013 – start 2014. To underpin these reported observations, historical data from these switches were analysed, consisting amongst others of individual switch loading development, accumulated tonnage for both passenger and freight trains, train-type operation and maintenance-related activities.

6.2. Operational data

For the selected switches, the accumulated yearly tonnage was analysed. Since 2010, following a re-routing at the track yard, both some of the ‘mild’ and ‘severe’ wearing switches have experienced a significant change in annual tonnage at the diverging route, together with a reversal of the dominant direction of traffic. This resulted in a 10-fold increase in tonnage in the facing direction and a corresponding decrease in the trailing direction (increasing

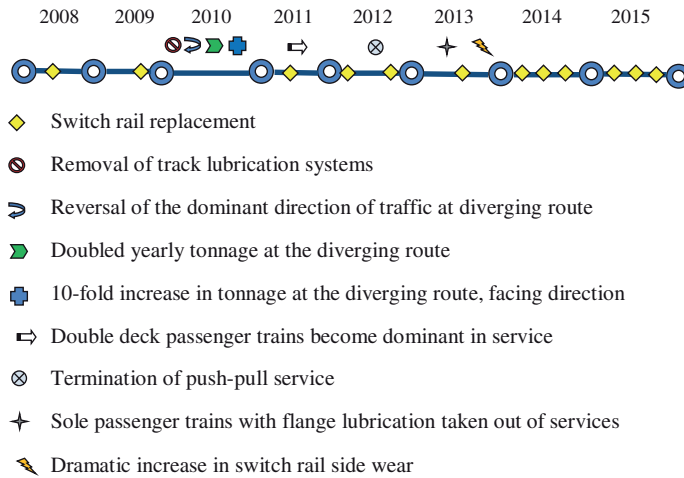


Figure 13. Switch rail replacement dates for one of the ‘severe’ wearing switches (left switch rail, serving the diverging route). Period August 2008 – September 2015.

from 1.2 to 12 MGT/year). Of the switches analysed, the lowest total yearly tonnage in the diverging route, with a very low contribution in the facing direction, belonged to a ‘severe’ wearing switch. Furthermore, contributions from passenger and freight traffic to the total tonnage in the diverging route was analysed. The contribution of freight traffic in the diverging route for one switch (mild wearing) is around 15% of the total tonnage (predominantly in facing direction). The contribution of freight traffic to the total tonnage for the other analyse switches is low, only 3%.

6.2.1. Switch rail lifetime development

The switch rail lifetime development of the selected switches was analysed from the contractor’s maintenance logs. Figure 13 shows how the time interval between replacements has decreased for one of the ‘severe’ wearing switches, illustrating the effect of the increasing wear rate on rail lifetime. Around 2010 several changes occurred, as indicated in Figure 13. These changes are reflected by the replacement interval. During the period 2008 up to and including 2010 the average switch rail life is approx. 17 months. The involved maintenance specialists consider this life span as ‘to be expected’ given the extreme conditions at the Amsterdam CS yard. During the years 2011–2013, after the mentioned change in switch loading and routing in 2010, the average switch rail life is seen to decrease to approx. nine months. From 2014 the average switch rail life suddenly further decreases to approx. three months. For comparison: the in March 2011 installed left switch rail at one of the ‘mild’ wearing switches was to be replaced only in September 2015, after a life span of 53 months. Although over this period, the average annual tonnage in the diverging route for this switch is about 2/3 of that for switch illustrated in Figure 13, the observed difference in switch rail life is still significant.

6.2.2. Related switch maintenance issues

Switch panel maintenance firstly addresses safe passage of the wheels for the switch toe area. The main risk at this location is the development of a gap between switch toe and stock rail,

causing the wheel flange to slip between stock and switch rail and, as a result, forcing the guiding wheel of the wheelset to travel the through route where the other wheel follows the diverging route. This will inevitably lead to a derailment. Regular S&C inspection involves service tests, wear and gauge measurements, checks of slide chairs, rail fastenings, lubricators (when applicable) and ultrasonic inspection. Routine S&C corrective activities involve, for example, manual rail profile maintenance (grinding), manual tamping, repair welding and component replacement. Also, the track alignment of the railway yard will influence the S&C loading and resulting maintenance demand. Due to the limited available space at the Amsterdam railway yard, successive switches are positioned in relatively close distance resulting in small radius connecting curves. This situation in alignment has not changed over the years.

Up and until 2010, track gauge-lubrication installations were present at Amsterdam CS. These installations were in operation at a number of switches and curves, aiming to reduce wear and flanging noise. However, in the experience of the responsible infrastructure manager and maintenance engineers, the cost of maintenance of these installations was considered to be high and effectiveness low due to frequent malfunction (e.g. inaccurate targeting resulting in the passing wheel flanges not to contact the lubricated area and/or absence of lubricant). At the Amsterdam CS railway yard, these track lubrication systems were removed in the year 2010, three years before the observed deviation from the trend in wear rate. When reviewing train operation at Amsterdam CS, it can be observed that the dominating train types over the years were passenger coaches type ICR and DDM in combination with NS locomotives 1700/1800 series (in push-pull service), together with passenger double deck trains of the VIRM type and freight trains (especially coal hoppers) with a range of freight locomotives. From 2010, VIRM-4 trains are gradually starting to dominate the passenger trains tonnage contribution at Amsterdam CS. From 2012, NS locomotives 1700/1800 are gradually removed from Dutch tracks, last visiting Amsterdam CS in the year 2013. Loco's 1700/1800 are the only type of NS trains fitted with flange lubrication. This implies that those switches and curves at Amsterdam CS that are only serving NS trains, passenger routes, do not receive any lubrication from passing wheel flanges. Freight locomotives are equipped with flange lubrication, hence rail at freight routes are (to some extent) expected to receive lubrication.

6.3. Track inspection results

Following the selection of 'severe' and 'mild' wearing turnouts, track inspections were carried out at the selected turnouts. Transverse profile, track gauge and roughness measurements were performed at several positions, together with visual inspections of the running band to assess the presence of RCF damage and lubrication. These results served as further input to the problem analysis. At the date of inspection (4 September 2015), the operational performance time of the inspected four left switch rails was, respectively, 1, 3, 6 and 52 months. During the track inspection, a distinct difference in visual appearance was observed between 'severely' and 'normal' wearing switches. Wear debris were clearly present at the switches with reported 'severe' wear, together with plastic deformation and spalling of the switch rail tip and high roughness of the gauge corner (Figure 14). The gauge corner of the switch with reported low wear rate, possesses a smooth running



Figure 14. Switch panel of ‘severely’ wearing switch (left switch and stock rail). Wear debris present, high roughness of gauge face. No lubrication marks.



Figure 15. Switch panel of ‘mild’ wearing switch (left switch and stock rail). No wear debris observed. At the gauge face remains of lubrication are present.

surface with no debris particles on site. At the switch rail gauge corner of this ‘mild’ wearing switch remains of flange lubrication were observed (Figure 15); the other inspected ‘severe’ wearing switches did not show any traces of flange lubrication.

7. Discussion

The simulations performed in this study have shown that switch rail lateral wear loading in the diverging direction of a 1:9 type turnout, is significantly influenced by the level of wheel–rail friction and to a lesser extent by the direction of travel. The other studied operational parameters, being vehicle speed, traction, gauge widening and track layout, showed no significant impact on the expected wear loading.

Those simulations in this study for which flange lubricated conditions were assumed, with a decreased friction coefficient, showed a local shift of the closure rail response into

the RCF/wear regime when negotiated by the motor bogie. $T\gamma$ loading levels at the leading trailer bogie imply switch and closure rail loading to be predominantly within the regime of mild wear, with no expected RCF damage development. The significance of the wheel–rail friction coefficient regarding wear development was further underpinned by the case study results. The one distinct difference between the investigated ‘severe’ and ‘mild’ wearing switches being the presence of lubrication at the latter.

For the researched track configuration (turnout angle 1:9) and train operation, it is concluded that with respect to wear the dominant influencing factor is the wheel–rail friction coefficient. The identified most probable cause of the observed dramatic change in lateral wear development is a steep increase in the wheel–rail friction coefficient. After dismantling the track lubricators in 2011, no direct wear impact was observed, since the wear loading was kept to an acceptable level due to flange lubrication systems in operation at a number of the frequently visiting locomotives. However, from the moment that these vehicles with flange lubricators were no longer visiting Amsterdam CS (end 2013), the wear rate went up dramatically.

Following a sharp increase in wear loading at the flange contact, beside lateral wear of the rail, also an increase in wheel flange wear is to be expected. Inquiry at the NedTrain chief engineer, responsible for overhaul and maintenance of NS trains, confirmed this expectation. From mid-2014, a significant increase in wheel flange side wear is experienced, especially at intercity type trains VIRM and ICM. It is also confirmed that for these vehicles neither the wheel material quality nor the supplier have changed in recent years. This further underpins the conclusion that the experienced sharp increase in lateral wear is related to the interface properties and has a system wide impact: the absence of flange lubrication at passenger train dominated routes.

From the development in annual tonnage, it can be seen that the doubled tonnage at the diverging route in combination with a reversal in running direction did not result in a dramatic reduction in switch rail life. Not the annual tonnage seems the switch rail life defining parameter here, but much more the occurring wear regime. For the modelled setup, a change in wear regime from severe to mild could only be reached with decreased wheel–rail friction.

From the switch rail life development at Amsterdam CS, the effect of mode of operation (push-pull vs. pull) did not show to have a significant effect on the switch rail wear rate. With push-pull service ending in 2012 (changing to pull only), this change did not coincide with the witnessed sharp deviation in the wear development trend at the end of 2013 – start 2014.

Not included in this study is the effect of worn wheel or rail profiles, nor the effect of axle load. For the performed study, however, profile development seems not a governing factor, since the wheel profile variation of the dominating VIRM trains is very limited. The extremely short switch rail life seen at the case study, resulting in frequently installed new switch rails with new profiles, further indicates the effect of rail profile variations must be small. The limited impact of wheel and rail profile variation is further underpinned by the observation that can be made from the turnout with the main annual freight tonnage. Wheel profiles of freight wagons are known to vary more widely, nevertheless this turnout shows a significantly longer switch rail life. Since the axle load variation for the dominating VIRM passenger train is limited, also the effect of these variations will be limited for the studied configuration.

Following the dramatic wear development a field trial was initiated at Amsterdam CS, installing Head Hardened (HH) switch rails at a number of severe wearing turnouts. Although monitoring is still ongoing, first results confirm the expected HH-switch rail life to increase by a factor four compared to the standard rail grade when applied at these heavily loaded turnouts. For the HH-switch rail the observed wear regime is 'Severe' as well.

The considered modelling reference situation, for which parameters were varied, represents a severe load case which also is limited to only one (however dominant) type of train. In practice the $T\gamma$ loading will show a wider distribution, depending on the parameter combination for the individual event. Given a very unfavourable parameter combination, loading into the severe wear regime could still occur even in lubricated conditions. This implies that reduction of the wheel–rail friction coefficient at the flange contact will reduce the number of occasions at which the wear loading is raised into the severe wear regime. With proper lubrication applied to the configuration considered here, switch rail life is expected to return to levels before the dramatic change in 2013/2014.

8. Concluding remarks and future work

The wear loading at the rail surface resulting from trains negotiating railway turnouts in relation to train-track operational parameters is the subject of this study. A sensitivity study was carried out to understand the impact of possibly influencing train operational parameters regarding wear loading at the wheel–rail interface. This level of loading at the wheel–rail interface very much determines the required maintenance effort and costs. The operational parameters considered are vehicle speed, running direction, traction and level of wheel–rail friction. Additionally, the influences of track gauge and track yard design, in particular, the effect of multiple switches in short succession, were reviewed. Furthermore, a case study has been performed in response to a sharp increase in wear rate, reported at a specific location in the Dutch network. This case study supplied further insight into the system approach regarding wheel–rail management and allowed cross-checking the modelling output.

Based upon the executed problem analysis and turnout-train simulations, it can be concluded that the friction coefficient between wheel flange and rail gauge face is dominating the wear loading and related expected wear behaviour at the switch rail in diverging route. To a lesser extent also the direction of travel in the diverging route is of influence, with the loading level increasing with 30% for the trailing direction. Other studied operational parameters, being vehicle speed, traction and gauge widening showed no significant impact on the level of wear loading. Examining especially the effect of curves and switches in short sequence, track layout did not show to be of any significance to the resulting level of wear loading.

The most likely cause for the abrupt increase in switch rail lateral wear experienced at Amsterdam CS is the complete disappearance of flange lubrication when the sole NS trains equipped with flange lubricators were no longer serving this location. The presented study clearly demonstrates the contribution of flange lubrication in preventing abnormal wear at locations where the wheel–rail interface is severely loaded. Reported recent issues with an increasing wheel flange wear rate of connected trains seem to further underpin this conclusion. The application of flange lubrication, for the reviewed configuration, is expected to lower the wear loading at the wheel-rail interface to a level that operation in

the ‘Mild’ wear regime can be expected for most of the switch and closure rail length in most operational conditions.

Together with a significant reduction in wear loading from flange lubrication, resulting in a shift from severe to mild wear, simulations performed in this study show the rail material respond at the switch and closure panel locally to shift into the RCF/wear regime. Rail grade selection in relation to $T\gamma$ loading levels therefore needs further work to prevent adverse side effects and to identify further optimisation opportunities.

Disclosure Statement

No potential conflict of interest was reported by the authors.

Funding

This research is being carried out by the author under the project number T91.1.12475a in the framework of the Research Program of the Materials innovation institute M2i (www.m2i.nl). Part of the work was funded by ProRail (the Dutch rail infra management organisation). Discussions with Mr. Remco Verloop are gratefully acknowledged.

ORCID

N. Burgelman  <http://orcid.org/0000-0003-4038-8364>

References

- [1] INNTRACK Concluding Technical Report, UIC – Paris, 2010. ISBN: 978-2-7461-1-1850-8.
- [2] ProRail internal document, Beheer en onderhoudskosten 2014, J. Swiers.
- [3] Kassa E, Johansson G. Simulation of train-turnout interaction and plastic deformation of rail profiles. *Veh Syst Dyn.* 2006;44:349–359.
- [4] Pålsson PB, Nielsen JCO. Wheel-rail interaction and damage in switches and crossings. *Veh Syst Dyn.* 2012;50:43–58.
- [5] Spangenberg U, Fröhling D. Mitigating severe side wear on 1:20 tangential turnouts. IHHA2015, Perth, Australia, 21–24 June 2015.
- [6] Nicklisch D, Kassa E, Nielsen J, et al. Geometry and stiffness optimization for switches and crossings, and simulation of material degradation. *Proc Inst Mech Eng, Part F: J Rail Rapid Transit.* 2010;224(4):279–292.
- [7] Bugarín MR, Orro A, Novales M. Geometry of high-speed turnouts. *Transport Res Record – J Transport Res Board.* 2011;2261:64–72.
- [8] Lewis R, Dwyer-Joyce RS. Wear mechanisms and transitions in railway wheel steels. *Proc Inst Mech Eng, Part J: J Eng Tribol.* 2004;218(6):467–478.
- [9] Lim SC. The relevance of wear-mechanism maps to mild-oxidational wear. *Tribol Int.* 2002;35:717–723.
- [10] Johnson KL. Contact mechanics and the wear of metals. *Wear.* 1995;190:162–170.
- [11] Ponter ARS, Chen HF, Ciavarella M, et al. Shakedown analyses for rolling and sliding contact problems. *Int J Solids Struct.* 2006;43:4201–4219.
- [12] Kalker JJ. Wheel-rail rolling contact theory. *Wear.* 1991;144:243–261.
- [13] Shackleton P, Iwnicki S. Comparison of wheel–rail contact codes for railway vehicle simulation: an introduction to the Manchester contact benchmark and initial results. *Veh Syst Dyn.* 2008;46(12):129–149.
- [14] Hiensch EJM, Wiersma P. Reducing switch panel degradation by improving the track friendliness of trains. *Wear.* 2016;366–367:352–358.

- [15] Burstow MC. Whole life rail model application and development for RSSB – development of a RCF damage parameter. AEATR-ES-2003–832 Issue 1 October 2003.
- [16] Burstow MC. Whole life rail model application and development for RSSB – continued development of an RCF Damage Parameter. AEATR-ES-2004–880 Issue 2 September 2004.
- [17] Zacher M. Rolling contact fatigue (RCF): models and experiences of DB AG, RTR1/2011. p. 35–42.
- [18] Nielsen JCO, Pålsson BA, Torstensson PT. Switch panel design based on simulation of accumulated rail damage in a railway turnout. CM2015, Colorado Springs, USA; 2015.
- [19] Sun Y, Cole C, Boyd P. A numerical method using VAMPIRE[®] modelling for prediction of turnout curve wheel–rail wear. CM2009, Italy, September 2009.

Paper 3

Enhancing rail infra durability
through freight bogie design.



Vehicle System Dynamics

International Journal of Vehicle Mechanics and Mobility

ISSN: 0042-3114 (Print) 1744-5159 (Online) Journal homepage: <http://www.tandfonline.com/loi/nvsd20>

Enhancing rail infra durability through freight bogie design

Martin Hiensch, Nico Burgelman, Wouter Hoeding, Mark Linders, Michaël Steenbergen & Arjen Zoeteman

To cite this article: Martin Hiensch, Nico Burgelman, Wouter Hoeding, Mark Linders, Michaël Steenbergen & Arjen Zoeteman (2018): Enhancing rail infra durability through freight bogie design, Vehicle System Dynamics, DOI: [10.1080/00423114.2017.1421766](https://doi.org/10.1080/00423114.2017.1421766)

To link to this article: <https://doi.org/10.1080/00423114.2017.1421766>



© 2018 The Author(s). Published by Informa UK Limited, trading as Taylor & Francis Group



Published online: 11 Jan 2018.



Submit your article to this journal [↗](#)



Article views: 31



View related articles [↗](#)



View Crossmark data [↗](#)

Full Terms & Conditions of access and use can be found at
<http://www.tandfonline.com/action/journalInformation?journalCode=nvsd20>

Enhancing rail infra durability through freight bogie design

Martin Hiensch^{a,b}, Nico Burgelman ^b, Wouter Hoeding^b, Mark Linders^b,
Michaël Steenbergen^a and Arjen Zoeteman^{a,c}

^aTechnical University Delft, Railway Technology, Delft, Netherlands; ^bDEKRA Rail, Utrecht, Netherlands; ^cProRail, Utrecht, Netherlands

ABSTRACT

The extensive usage of railway infrastructure demands a high level of robustness, which can be achieved partly by considering (and managing) the track and rolling stock as one integral system with due attention to their interface. A growing number of infra managers consider, in this framework, the track-friendliness of vehicles that have access to their tracks as a key control parameter. The aim of this study is to provide further insight into potential contributions to track-friendliness, assessed in relation to track deterioration mechanisms and cost, understanding how potential benefits are best to be utilised. Six proposed freight bogie design measures are evaluated with respect to the improvement in curving behaviour, switch negotiation and related track degradation mechanisms. To this purpose a sensitivity analysis has been carried out by means of track–train simulations in the VAMPIRE[®] multi body simulation software. Additionally, the impact on track deterioration costs has been calculated for those track-friendly design modifications identified as most promising. Conclusions show that the standard Y25L freight bogie design displays rather a track-friendly behaviour. Tuning the primary yaw stiffness shows a high potential to further improve track-friendliness, significantly reducing track deterioration cost at narrow radius curves and switches (by, respectively, 30% and 60%). When calculating the overall deterioration cost for the travelled route, the calculation model should include a well-balanced representation of switches and narrow radius curves.

ARTICLE HISTORY

Received 17 March 2017
Revised 30 November 2017
Accepted 16 December 2017

KEYWORDS

Switch panel; frequency selective stiffness; track-friendliness; track deterioration cost; bogie design; RCF damage

1. Introduction

Maintenance cost associated with wear and fatigue damage at the wheel–rail interface are dominating the budget of many infrastructure manager and train operating company, with switch maintenance often claiming a disproportionate amount of the overall budget. The Innotrack technical report [1] concludes ‘bad track geometry’, ‘rail cracks/fatigue’ and ‘switch wear’ to be the top three of reported main track problems. Track geometry degradation is strongly connected to the quality of the support conditions in combination with track forces induced either by trains or temperature. From the occurring wear and fatigue features it is understood that this damage type is strongly connected to track

CONTACT Martin Hiensch  e.j.m.hiensch@tudelft.nl

layout, especially curved track sections. Consequently the curving behaviour of a vehicle, and related level of creep forces, plays an important role in occurring wear and fatigue loading at the wheel–rail interface. Apart from track radii below 2000 m, vehicle curving behaviour is particularly challenged at the diverging route through a turnout. Öberg and Andersson [2] identify three deteriorating mechanisms, together determining the overall track degradation cost. In accordance with the [1] reported main track problems, the identified mechanisms are track settlement, component fatigue of the super structure and wear and rolling contact fatigue of rails. These mechanisms are governed by the static and dynamic wheel forces and levels of creepage between wheel and rail of which magnitudes are mainly determined by vehicle, track, interface and operational characteristics. Measures that act on these forces and creepage levels will have a direct impact on the overall track degradation and related maintenance cost. Examples of track-related measures are, for example, the application of rail profiles with gauge corner stress relieving properties [3], the local tuning of track elastic properties to reduce the dynamic forces on track components such as the crossing point [4], and track alignment optimisation (e.g. intervention on variations in track alignment or level of cant deficiency) as described in [5]. Punctual and proper maintenance regarding the quality of the running surface and track geometry will further contribute as will the monitoring of the borne tonnage, for example, by weigh-in-motion systems located at key points in the network, to control (dynamic) wheel load especially in relation to developing wheel out-of-roundness. An example of interface management aiming to reduce track forces is the application of wheel–rail lubrication. Searching to increase wheel lifetime, alternative wheel profiles have been designed to reduce the acting wheel–rail forces [6]. Recent developments in vehicle bogie design aim, among others, to further reduce wear and fatigue loading of track and wheels. Bogies that fulfil these conditions are considered to behave ‘track-friendly’. From the viewpoint of overall system performance, infrastructure managers will have an interest in the level of track-friendliness of the vehicles that have access to their track.

From the understanding that train characteristics affect infrastructural degradation differently, inducing different levels of cost, train exploitation should be priced accordingly. To increase efficiency in current pricing schemes, the introduction of differentiated track access charges based on wear and tear from different vehicle types has been discussed [7]. Several European rail infra providers (Network Rail, Swiss Federal Railways) have now started to incorporate track-friendliness into their track access pricing schemes. Target here is to allocate the direct cost to individual trains, incidentally stimulating the inflow of track-friendly designs. In this study, in addition to the assessment of track-friendliness with regard to the level of contact forces and track degradation, the impact of the identified track-friendly design modifications on track deterioration also has been monetised, applying the cost calculation model of Öberg and Andersson [2]. For this purpose one of the major freight route in the Netherlands was selected, comparing the deterioration cost per ton-km for each of the different vehicle concepts running on this route.

The objective of the current study is to evaluate a number of railway bogie design measures regarding their contribution to track-friendliness, assessed in relation to track deterioration mechanisms and cost, understanding how potential benefits are best to be utilised. Bogie design improvements related to freight transport and their impact to Dutch track are of special interest here. For this purpose a sensitivity analyses has been carried out by means of track–train simulations within the VAMPIRE[®] multi body simulation

software, also serving as an input to the applied cost calculation model. The novelty of the performed track deterioration study is twofold. Firstly the combination of both a technical and economic assessment regarding track friendly design changes and secondly the focus on critical assets being switches and narrow radius curves. An important result is the finding that within the applied cost calculation model, as introduced in par. 4.2, positive effects from the viewpoint of track availability and overall performance are undervalued.

The structure of this article is as follows: after the introduction, the technical framework is presented in Section 2, discussing vehicle curving behaviour, presenting the identified design modifications, scope of the research and how the simulation results are analysed regarding wear and fatigue behaviour. The dynamic modelling input for the purpose of track-friendliness assessment is introduced in Section 3, with results for both the technical and economic evaluation presented in Section 4. Overall findings are discussed in conjunction in Section 5 followed by conclusions in Section 6.

2. Theoretical framework

In this section vehicle curving behaviour is discussed for the Y25L freight bogie, presenting identified design modifications and how these are analysed regarding wear and fatigue behaviour.

2.1. Vehicle curving behaviour

When negotiating a curve with a moderate radius, the rolling radius difference, built up by the lateral displacement of the conical wheels towards the outside of the curve, will create steering forces. These steering forces, when larger than the yaw resistance of the wheelset, lead to a more radial position of the wheelset. However, in sharper curves in general the wheelsets of railway vehicles suffer from under-steer. Because of the angle of attack lateral slip will be generated at the wheel-rail contact patch, where the guiding wheel of the leading axle normally is dominant with respect to tangential forces and slip levels. Lateral slip of both wheels is directed towards the inner side of the curve. These contact forces and resulting stresses can lead to plastic deformation, wear and rolling contact fatigue (RCF) damage at the rail head and wheel tread (Figures 1 and 2). Consequently, demanded maintenance is high; for example, inspection, grinding, repair welding and rail replacement at track and wheel re-profiling and replacement at the workshop.

Compared to modern-day passenger vehicles, the bogie design of freight vehicles is often more basic, aiming for robustness, not necessarily at improved curving behaviour. In Europe the most commonly used bogie designed for freight wagons is the two-axle bogie type 'Y25L-UIC' (L stands for the French word 'Lourd' which translates in English to Heavy). The bogie Y25L was developed by the French National Railway SNCF and standardised by the (International Union of Railways) UIC. As described in [8] the bogie Y25L primary suspension consists of a set nested coil springs (with a bi-linear characteristic for tare/laden ride) and a single Lenoir link providing vertical and lateral frictional damping (Figure 3). The friction force depends on the vertical load. The longitudinal axle box clearance is 4 mm, unidirectional, allowing a certain yaw angle. After this small amount of longitudinal clearance has been exceeded, the longitudinal stiffness will rise steeply. Therefore the wheelsets can steer themselves in curves as long as the 4 mm clearance is not fully



Figure 1. Wheel tread with RCF crack damage.



Figure 2. Severely worn narrow radius track section with wear debris at ballast and collecting magnet.

consumed. For curves with a radius below 600 m this clearance is exceeded, and relatively poor curving behaviour as well as high lateral wheel–rail forces are to be expected [9]. From the viewpoint of efficiency, freight wagons are often loaded to their maximum, reaching the allowed track axle load which in the Netherlands is 22.5 ton. The bogie Y25L is admitted for axle loads up to 22.5 ton; the maximum running speed for a wagon fitted with these bogies is 120 km/h when empty and 100 km/h when fully loaded. Although in absolute numbers the annual freight transport in the Netherlands is relatively low compared to passenger traffic (respectively, 40 vs. 144 mio. train km), poor narrow curving behaviour in

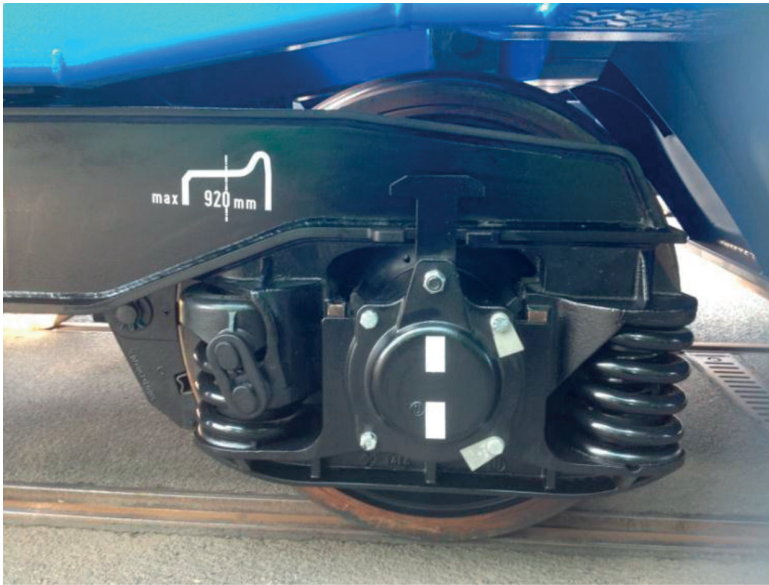


Figure 3. Y-25 primary suspension consisting of a set nested coil springs and a single Lenoir link.

combination with high axle loads can, depending on curve radii distribution, cause a disproportional contribution of freight transport to track degradation. Achieving improved track-friendliness of freight bogies therefore can significantly contribute to improving the whole system performance, resulting in a more sustainable rail transport system. Identification and quantification of performance-based design principles can further support this development.

2.2. Measures to improve track-friendliness

To improve track-friendliness of freight bogies, over the years a vast number of bogie design innovations have been considered and reviewed by the industry. The vast number of Europe's 400,000 strong freight wagon fleet, however, is still fitted with classic bogies. A parametric study of freight vehicle effects on rail surface damage is presented in [10]. Regarding the design of the vehicle it was concluded that the characteristics of the primary yaw stiffness (PYS) significantly influence the resulting rail surface damage. The SUSTRAIL project [11] has studied freight bogie design optimisation of the primary suspension by the use of double Lenoir link primary suspension, allowing opposite longitudinal displacement at the wheelset's both primary suspensions, thus facilitating larger yaw angles of the wheelsets while still utilising standard components. Within [11] further assessment of wheelset guiding design optimisation included the benefit of linkages providing longitudinal stiffness between the axle boxes using a radial arm (also known as 'trailer arms'). These radial arms are connected to the bogie frame by pivot bushes. For this type of suspension, the PYS is dominated by the radial stiffness of the radial arm pivot bush. This rotational stiffness of the wheelset within the bogie frame strongly determines the radial setting of the wheelsets in curves, having a direct effect on the contact conditions,

the level of creepage and the lateral forces at the wheel–rail contact patch. Vehicle stability on straight track and curving ability in switches and curves however impose a conflict upon the vehicle designer. Recent developments in suspension design provide the required high PYS stiffness at high loading frequencies to ensure stable running, together with low PYS stiffness at low frequencies, resulting in moderate loading when negotiating a curve or switch.

This suspension behaviour is achieved through the application of new elastic components with a characteristic that is dependent on loading frequency. As presented in [12] these so-called Frequency Selective Stiffness or ‘hydrobush’ elements can, when applied at the radial arm pivot bush, lead to a significant reduction of rail and wheel surface damage. An overview of further design optimisation measures is presented in [8].

The research presented here focuses on the improvement of switch negotiation and curving performance and related wheel–rail contact stress levels by optimisation of the steering behaviour of Y25L freight wagon bogies. Starting from the above-identified design optimisation measures a parametric study has been set up, investigating the effects of several freight bogie design parameters on rail surface damage. A sensitivity analysis was carried out by vehicle dynamic simulations, performed with respect to the characteristics of primary and secondary suspension, unsprung mass and cross anchor application. Additionally, the impact on track deterioration cost has been calculated for the track-friendly design modifications identified as most promising. Quantifying the claimed benefits of these innovations in bogie design to the overall rail transport will support decision making.

2.3. Assessment of track-friendliness

Assessment of the level of track-friendliness with regard to curving behaviour and switch negotiation is carried out in terms of wear and Head Check damage development, derived from the RCF damage function as presented in [13]. The key parameter in this part of the assessment is the parameter $T\gamma$ (‘T-gamma’), in which longitudinal and lateral tangential

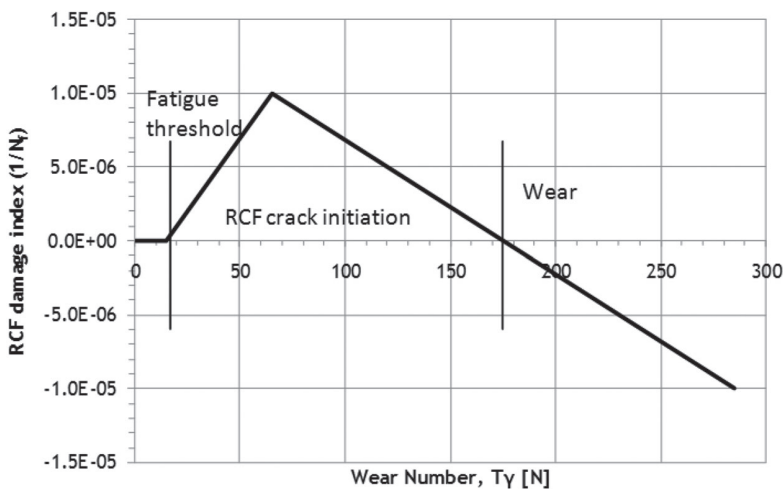


Figure 4. RCF-damage function for rail grade R220 [13].

forces and creepages are combined to calculate the energy dissipated at the wheel–rail contact patch. $T\gamma$ can be used as an output value indicating the expected damage development with respect to wear and RCF development. The relation between the occurrence of visible RCF damage in R220 grade rail material is established in the RCF damage function as presented in Figure 4. In this graph, $T\gamma$ is plotted on the horizontal axis. On the vertical axis, the RCF damage index is plotted. The RCF damage index equals 1 divided by N_f : the number of loading cycles until the first visible Head Check damage occurs. The ‘Wear number’ $T\gamma$ is a direct output from the VAMPIRE[®] multibody analysis. The energy dissipation value $T\gamma$ is determined at the first outer wheel for curves with different radii and for switch panel negotiation. Note that spin moment and spin creepage terms are not included in [13]. The spin contribution, however, is included in the output of the here performed simulations. Quantifying the relative contribution of lateral, longitudinal and spin creepage to the dissipated energy for a 300 m curve radius [14] showed the relative spin contribution to be in the order of 8%, not influencing the overall assessment result. The impact on track geometry degradation have been assessed through simulations on a tangent track, evaluating the level of track forces.

3. Vehicle–track interaction model

Presented in this section are the applied track and vehicle models to assess the track-friendliness of the proposed bogie design modifications.

3.1. Bogie and vehicle models

Based on data presented in [15] a model of the Y25L bogie was set up in VAMPIRE[®], using the also presented simulation and measurement results for purpose of validation. Based on the validated Y25L bogie model, six further bogie vehicle models were set up, in order to assess the following design modifications:

- Bogie with double Lenoir linkage
- Bogie with trailer arms, fitted with conventional bushes
- Bogie with trailer arms, fitted with hydrobushes
- Bogie with reduced secondary lateral stiffness
- Bogie with reduced unsprung mass
- Bogie with cross-anchors and trailer arms, fitted with conventional bushes

For the Y25L bogie design the yaw stiffness is determined by the longitudinal stiffness between the axle boxes and bogie frame. For the longitudinal direction, the primary suspension is modelled as a tri-linear stiffness element (in fact a linear spring element with two bump stops), in parallel with a friction element which produces a friction force proportional to the static and dynamic wheel load. When starting the yaw rotation, the first 4 mm of longitudinal play is consumed at a relatively low stiffness value of approx. 1 kN/mm. After this 4 mm displacement, a nominal longitudinal stiffness value of 10 kN/mm is assumed in accordance to [15]. Three PYS design modifications are analysed here: (1) the double Lenoir linkage, possessing equal characteristics to the single Lenoir with the only difference that the clearance is doubled and the centre position defined as in the middle of

this 8 mm. (2) Application of trailer arms with conventional bush: based upon suspension characteristics from conventional trains with max. 22.5 tons axle load and fitted with bogies with trailer arms, chosen linear longitudinal stiffness is 20 kN/mm. Similarly, the axial stiffness was chosen as 5 kN/mm and the conical stiffness as 1 kNm/mrad. Dynamic stiffening was not included here. And (3) application of trailer arms with hydrobush: applied stiffness values are based upon earlier investigation published in [12] (static stiffness 2.8 kN/mm, dynamic stiffness 15 kN/mm). Within [12] it is described how the frequency dependent effect is implemented into the Vampire model. All design modifications were variants of the Y25L bogie.

In order to quantify the benefits of any new design, a benchmark vehicle has been selected based on Y25L bogies with a coal hopper wagon type HHA. The ‘wagon body’, including everything except bogies, is defined in terms of mass, inertia and centre of gravity, both for the tare and laden condition (7 and 22.5 tons axle load, respectively). The wagon body rests on the bogie’s secondary springs. Simulations were carried out in tare and laden condition. The coefficient of friction between block braked wheels and rail is set to $f = 0.45$, in correspondence to [10].

3.2. Track models

3.2.1. Switch loading

The assessment of switch loading was carried out using a track model of the diverging route through a switch panel, with vehicle speed set to 40 km/h. The most common type of turnout applied in Dutch track has been selected. This turnout has a crossing angle 1 over 9, with switch radius 195 m as presented in [12].

3.2.2. Curving

The track input for curving behaviour assessment consists of a set of right-hand curves with radii 250, 500, 750, 1000, 1500, 2000 and 2500 m. The cant is set to 50 mm for the radii from 250 m to 1000 m, to 30 mm for 1500 m, and to 0 mm for 2000 m and 2500 m. For each simulation the operational speed is set to a value that results in a cant deficiency of 30 mm. Track irregularities following ERRI B176 type low [16] were applied to the track curving track models, promoting earlier friction break-out of wheelsets and bogie (rail inclination 1:40, track gauge 1435 mm). Runs were performed with the UIC 54E5 (anti-head check) rail profile and new (unworn) S1002 wheel profiles.

3.2.3. Track degradation

Assessment with regard to the level of vertical and lateral track forces, and resulting impact to track geometry degradation, has been carried out using 1000 m of as-measured tangent track in the Netherlands with consisting shortwave vertical and lateral track irregularities. The Power Spectral Density (PSD) of measured track irregularities as a function of wavelength show the track geometry recording data not to comprise lateral wavelengths below 6 m and vertical wavelengths below 8 m. The simulated train speeds varied with a maximum of 100 km/h when fully laden and 120 km/h when tare. Runs were performed with the UIC 54E1 rail profile, and new (unworn) S1002 wheel profiles.

4. Evaluation

4.1. Technical criteria

Over 200 simulation runs were performed for this part of the study. All simulations have been executed in VAMPIRE Pro[®], version 6.30. All simulation results have been compared with the simulation results for the Y25L reference bogie. Only those results that produced noteworthy differences are discussed in detail.

4.1.1. Primary yaw stiffness

In this section the effect of PYS design modifications is discussed with respect to switch negotiation, curving behaviour and dynamic wheel forces.

4.1.1.1. Switch negotiation. Figure 5(a–d) present the dissipated energy $T\gamma$ development for the different PYS design variations at contact patch areas of the first wheelset during switch negotiation. The horizontal axis represents the position in the track. The switch toe is located at $x = 40$ m. The left-hand turnout is negotiated in the diverging route. The direction of travel is from left to right (the facing direction). For both the switch panel (position 40–48 m) and closure panel (position 48–63 m), $T\gamma$ development is presented for

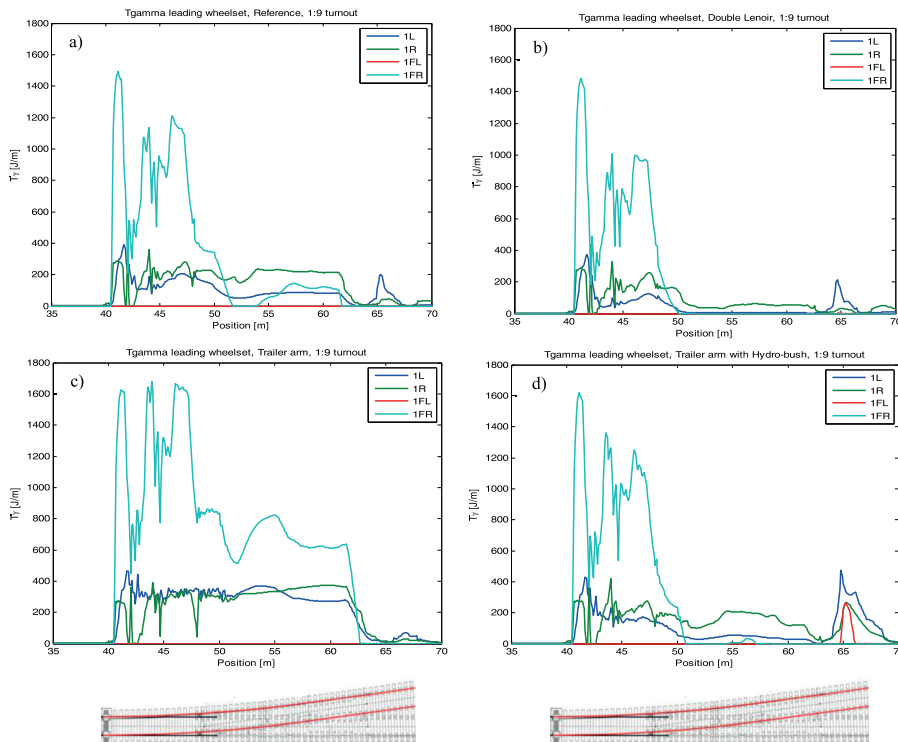


Figure 5. $T\gamma$ development for the different PYS design variations at the contact patch areas of the first wheelset during switch negotiation. Reference (a), double Lenoir (b), trailer arm with conventional bush (c), trailer arm with hydrobush (d). The right wheel (R) is guiding, 1R/L: wheel tread/flange root contact, 1FR/FL: flange contact.

Table 1. Rail damage development type, based on $T\gamma$ loading of the guiding right wheel during 1:9 switch negotiation in diverging route.

Modification	Switch panel contact area		Closure panel contact area	
	Flange	Tread/flange root	Flange	Tread/flange root
Y25 – reference	Wear	Wear	RCF	Wear
Double Lenoir	Wear	Wear	Below damage threshold	RCF
Trailer arm – conventional bush	Wear	Wear	Wear	Wear
Trailer arm – Hydro bush	Wear	Wear	Below damage threshold	Wear

the contact area of the wheel tread/flange root (left wheel:1L, right wheel:1R) and the contact area of the wheel flange (1FL, 1FR). For those locations where simultaneously contact occurs at the running surface of switch rail and stock rail, $T\gamma$ values are summed. Summation of $T\gamma$ for simultaneous contacts can unwillingly influence the resulting evaluation outcome. However, for the here evaluated situation the load transfer length with simultaneous contact is very short compared to the total length of the switch panel and therefore summation does not influence the resulting prevalent switch panel damage mode (wear or RCF).

Upon entering the switch, the wheel flange of the leading right wheel comes into contact with the switch rail at approximately 0.5 m behind the switch toe. This results in a steep increase of $T\gamma$. When comparing the $T\gamma$ peak values, it can be seen that these are not influenced by the examined PYS design measures. Significant differences, however, can be observed at the wheel tread/flange root contacting area of the switch panel and at both the contacting area of flange and wheel tread/flange root of the closure panel.

Flange contact at the closure panel becomes negligible for the design variants double Lenoir and trailer arm with hydrobush, eliminating side wear loading at this location in track. The application of trailer arms with conventional bushing leads to an increase of PYS compared to the reference situation with resulting $T\gamma$ values during switch negotiation well above 200 N, placing its operational window entirely in the region of ‘Wear’. By applying the damage function as shown in Figure 4, the expected effect of the individual modifications can be understood more clearly. Table 1 presents for each modification the expected damage development at switch and closure panel, based on the operational wear number from the guiding right wheel.

4.1.1.2. Curving behaviour. Figure 6 presents the simulation results for the different PYS design variations and different curve radii. It shows the quadratic mean (RMS) $T\gamma$ value of the outer wheel of the leading wheelset, determined in the full curve. For each design modification these RMS $T\gamma$ values are plotted against the curve radius. The results in Figure 7 show that improved curving behaviour, compared to the Y25L reference bogie, only occurs for radii below 750 m. This positive effect is only present for two of the evaluated design modifications; the double Lenoir and trailer arm with hydrobush, and to a lesser extend for the reduced secondary horizontal stiffness. The best narrow radius curving performance is shown by the double Lenoir design, with resulting $T\gamma$ values below the damage threshold value down to the 500 m radius curve. As was the case with switch negotiation, it can be seen here that the trailer arm bogie design with conventional bush results in increased $T\gamma$ values due to the increased PYS. For the assessed operational conditions, the influence of the cross anchor is negligible.

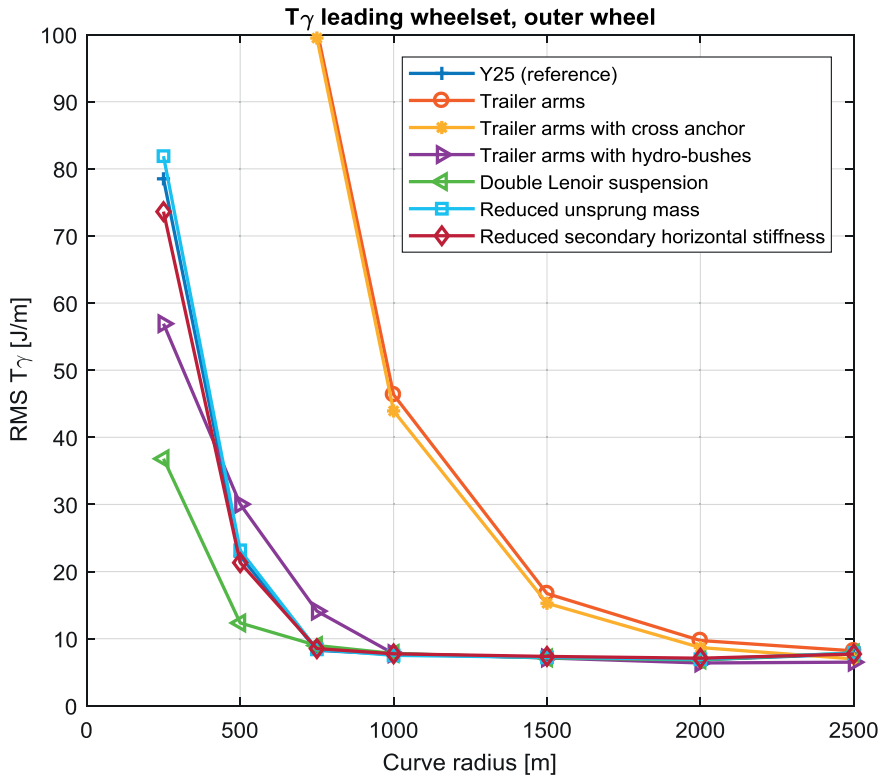


Figure 6. T_γ development for the different design variations and curve radii.

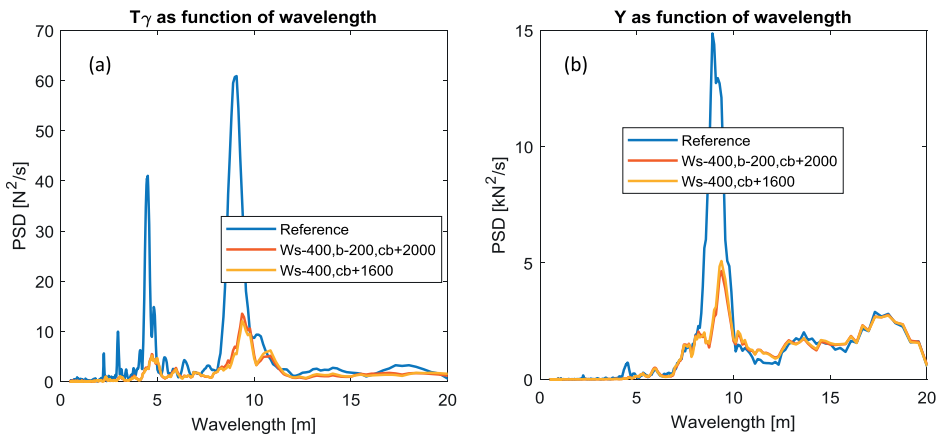


Figure 7. T_γ and lateral force (Y) as a function of the wavelength of the leading wheelset for the reference bogie, bogie with reduced unsprung mass and bogie with reduced sprung and unsprung mass.

The impact of a rubber ring mounted between the Y25L bogie frame and the lower part of the centre pivot was examined by introducing a lateral stiffness to the centre bowl set to 0.2 kN/mm, corresponding the limit value proposed at the EU Seventh Framework

Programme SPECTRUM presentation ‘Suspension simulation of a rail freight vehicle for LDHV goods’ (Paris, 8th April 2015). Initially developed for stability improvement, here the potential for curving improvement was examined. The resulting $T\gamma$ values for switch negotiation are shown not to be significantly influenced by this design modification, it has only a minor influence on curving behaviour.

A cross anchor is a pair of linkages applied diagonally between the wheelsets. These wheelsets, when yawed by the wheel–rail contact forces, will assume a radial position. Providing diagonal linkages between the wheelsets of the Y25L reference bogie is however not useful, since the combination of these linkages with the single Lenoir dampers would prevent all longitudinal movements of the wheelsets relative to the bogie frame. Therefore, in this research the cross anchor is limited to a combination with the design with trailer arms and conventional bush. The resulting $T\gamma$ values do not show a significant influence of this design measure on running behaviour; for the switch negotiation nor for curving, the found $T\gamma$ levels are corresponding to those for the trailer arm without cross anchor.

4.1.1.3. Track degradation. Developments in bogie design are seen to also target the bogie mass for which a reduction can be achieved, for example, by the inboard bearing wheelset concept and hollow axles considerably reducing the unsprung mass together with a low weight bogie frame design. The effect of reducing the unsprung mass of the bogies on track degradation is investigated by examining the forces between wheel and rail in lateral and vertical direction. Reduction of the unsprung mass is implemented in the vehicle model by reducing the mass per wheelset with 400 kg; additionally the mass per bogie frame is reduced with 200 kg. This results in a mass reduction of 1000 kg for each bogie (approx. 20% reduction) and implies 2000 kg of extra freight. To illustrate the effect of the individual changes in mass of bogie frame (sprung) and wheelset (unsprung), simulations have been carried out for the following three configurations (all variants retaining 22.5 tons axle load): (1) Reference Y25, (2) mass of each wheelset reduced with 400 kg (Ws-400) and bogie frame reduced with 200 kg (b-200) adding 2000 kg of extra freight to the wagon and (3) mass of each wheelset reduced with 400 kg (Ws-400) adding 1600 kg of extra freight.

As mentioned in Section 5.2 the track section applied for this analysis is tangent track with measured track irregularities. The applied vehicle speed is 90 km/h, laden. For the laden condition 22.5 ton axle load is applied. The power spectral density of $T\gamma$ as a function of the wavelength is presented in Figure 7(a). It can be seen that a reduction of the unsprung mass results in a significant reduction in $T\gamma$ loading. The dominating wavelength of 9 m corresponds to the wavelength of the Klingel motion of a Y25 wheelset. The lateral forces (Y) power spectrum is presented in Figure 7(b). Reducing the unsprung mass predominantly has resulted in a significant reduction of lateral track forces and associated $T\gamma$. Reduced lateral track forces can expectedly lead to a reduction in track geometry degradation and related maintenance effort and cost. For the vertical track forces, the observed reduction is much smaller.

As mentioned in Section 3.2, the track geometry input data used for assessment of wheel–rail forces does not comprise lateral wavelengths below 6 m and vertical wavelengths below 8 m. It should therefore be noted that track geometry as registered by a measurement coach is not a fully adequate parameter to determine the effect of unsprung mass

on track degradation. The unsprung mass has a significant effect on the vertical dynamic wheel–rail force for wavelengths that are shorter than or in the same order of magnitude as the wheel circumference, which is about 3 m. This implies that the unsprung mass plays a crucial role in the degradation rate of points and other switch parts, of insulated joints and potentially of welded connections with insufficient straightness. These components are key assets in the performance of a railway network. For conventional train speeds, the first derivative of the trajectory of the gravity centre of the unsprung mass may exhibit a discontinuity, implying wheel–rail impact conditions (see ref. [17]). This is also true in lateral directions. It has been demonstrated in [17] that in these cases the dynamic contact force is proportional to the mass, which is consistent with both theoretical and field results for P1 peak forces from the literature [18]. The level and frequency content of the dynamic contact force have a direct relationship to the degradation rate of concerned railway structural assets, even apart from the parameter $T\gamma$ and induced wear/RCF. It is therefore useful to strive for minimum inertia of unsprung bogie parts.

4.2. Economic criteria

Öberg and Andersson [2] have presented a track deterioration cost calculation model, able to differ between vehicle types based on their characteristics and tendency to deteriorate tracks. The model applies the marginal cost methodology, aiming to determine the additional cost per extra vehicle unit by determining the impact of that vehicle. This model is applied to the present study, assessing the impact of the proposed track-friendly designs regarding track deterioration costs. As a case study, a dedicated freight corridor was selected. The first step in calculating the deterioration cost is to determine the marginal cost level currently for infrastructure in the Netherlands. Next step is to compose a set of VAMPIRE[®] tracks models, representative for the studied corridor. From the executed simulation runs, input data to the deterioration model is acquired, consisting of Ty wear numbers, guiding forces and dynamic wheel loads. Finally, the deterioration cost per ton-km for each vehicle concept is calculated.

The European 5th frame project UNITE [19] defines marginal social cost as the costs of an additional transport unit (train km for rail). Marginal infrastructure cost is the cost to infrastructure managers of additional traffic, principally maintenance and renewal but potentially also other aspects of operating cost. To calculate marginal costs all impacts have to be determined and calculated, and finally these impacts must be monetised. Marginal cost calculation methods can be very complicated, time-consuming and have high data requirements. A simplified method to determine marginal costs is presented in [20], using average variable costs as a substitute for marginal costs. The proposed simplified approach may provide a lower degree of accuracy compared to the more sophisticated approaches but has the advantage of being relatively easy to apply. In many cases the simplified approach can serve to provide a quick indication of the marginal cost level. For this study the proposed simplified method is used as a set-up for the marginal infrastructure cost calculation. In order to limit the complexity of the study, cost for congestion, air pollution and noise are not considered. Required input data regarding infrastructure cost for maintenance and control is derived from [21]. From this input the calculated marginal cost for ProRail track amounts to 0.0031 €/gross ton kilometres. This is in line with the actual

ProRail track access charge for a 650 ton train which in 2013 was set to 0.0035 €/gross ton kilometres.

4.2.1. Dynamic simulations

The selected route, from Roosendaal to Oldenzaal, is 205 km in length with 30% consisting of curved track with a radius below 2000 m. A representative set of track models is designed, covering the various track radii and switches with associated cant. The applied speed profile is based on the maximum allowed line speed for loaded wagons at the different route sections (applied minimum is 40 km/h, maximum 100 km/h). Evaluated vehicle concepts are Y25L reference, Y25L with double Lenoir, Y25L with trailer arm fitted with hydrobush and Y25L with reduced unsprung mass. All concepts are fully laden to 22.5 ton axle load. The applied wheel profile is UIC S1002. To account for the effect of geometrical disturbances regarding wheel–rail forces and corresponding marginal costs, lateral and vertical track irregularities have been generated according to the method provided in report ERRI B176 [22]. To excite frequencies up to 90 Hz, the applied wavelength range is 0.1–200 m. The applied rail profiles are UIC 54E1 on tangent track and UIC 54E5 in curves. The lateral rail to sleeper stiffness is set to a default value of 43 kN/mm, vertical rail to sleeper stiffness to 50 kN/mm. The wheel–rail friction coefficient is set to 0.45. The dynamic simulations direct output consists of the average wear number ($T\gamma$) for the outer wheels (both leading and trailing axle) and quasi-static wheel loads (both vertical and lateral). Also the dynamic wheel load contributions for the frequency content up to 20 Hz and between 20 and 90 Hz are obtained from the VAMPIRE[®] simulations output. For this purpose, in accordance with UIC code 518 [23], vertical and lateral dynamic wheel forces are filtered after which the 99.85 percentile values are determined.

4.2.2. Impact analysis

The track deteriorating cost calculation model presented by Öberg and Andersson [2] is based on two damage models. The first one, a damage model developed in the 1980s by the ORE (Office of Research and Experiments) is the base for the first two terms in Equation (1), respectively, related to track settlement and super structure component fatigue. The third term of the formula, related to wear and RCF, is based upon the Whole Life Rail Model as developed and experimentally validated by Burstow [13].

For the calculation of the cost of track deterioration the total marginal cost is considered as a mean value of the whole network. The overall cost of track deterioration is composed of the individual share of each deteriorating mechanism. Öberg and Andersson propose a distribution of these mechanisms applicable for the Swedish rail network. Typical for the rail network in the Netherlands is the relative soft sub-structure which, in comparison to the Swedish situation, is expected to raise more issues with track settlement. This is reflected in the distribution applied to the present study, with track settlement responsible for 35% of the marginal cost, component fatigue for 25% and the remaining 40% allocated to wear and RCF of rails. From the calculated marginal cost and applied distribution in deteriorating mechanisms, the marginal average cost coefficients are calculated in relation to the Y25 reference bogie. These coefficients are then used to calculate the marginal cost for the other vehicle concepts. To the initial model of Öberg and Andersson lateral track shift forces were included in the settlement mechanism by adding the term (Y_{tot}^3) to first

Table 2. Track deteriorating cost calculation terms.

Notation	
e_R	Marginal cost for curve zone R (€/ton km)
k_1	Marginal average cost coefficient for track settlement
k_2	Marginal average cost coefficient for component fatigue
k_{34}	Marginal average cost coefficient for rail head wear and RCF
m	Mass of vehicle (ton)
n_a	Number of axles
n_w	Number of wheels
Q_{tot}	Total vertical wheel load (kN)
$T\gamma$	Wear energy number (J/m)
Y_{tot}	Total lateral wheel load (kN)
Y_{qst}	Lateral quasi static wheel load (kN)
$Y_{<20}$	Lateral dynamic wheel load contribution processed by a 20 Hz low-pass filter (kN)
Y_{20-90}	Lateral dynamic wheel load contribution with frequency content between 20 and 90 Hz (kN)

term of Equation (1) (Table 2).

$$e_R = \begin{cases} \frac{k_1}{n_a} \sum_i^{n_a} (Q_{\text{tot}}^3 + Y_{\text{tot}}^3) + \\ \frac{k_2}{n_a} \sum_i^{n_a} \left(\sqrt{Q_{\text{tot},i}^2 + Y_{\text{qst},i}^2} \right)^3 + \\ \frac{k_{34}}{m} \sum_i^{n_w} f(T\gamma)_i \end{cases}, \quad (1)$$

$$Q_{\text{tot}} = Q_{\text{qst}} + Q_{<20} + Q_{20-90}. \quad (2)$$

4.2.3. Marginal cost calculation results

The marginal cost for rail wear and RCF are presented in Figure 8. These cost are strongly determined by the PYS and related wear energy number $T\gamma$ and consequently are seen to increase with decreasing curve radius. The single Lenoir link design, as applied to the Y25L reference bogie and the bogie with reduced unsprung mass, allow the wheelsets to steer radially in curves with radii of 750 m and up. For radii below 750 m the marginal cost for bogies with the single Lenoir design is seen to rapidly go up. The improved yaw stiffness behaviour in narrow radius curves for the double Lenoir and hydrobush design results in decreased $T\gamma$ levels in the curve range with radii < 750 m, resulting in significant marginal cost reductions compared to the reference bogie. The frequency-dependent stiffness of the hydrobush design, however, is seen to significantly influence its marginal cost development. Especially in larger radius curves and in tangent track with higher vehicle speeds, the introduced track irregularities cause the primary suspension to operate in its relatively high dynamic stiffness range, which results in an increase of $T\gamma$ and the related marginal cost compared to the reference bogie. The hydrobush respond to track irregularities and resulting increase in stiffness also results in a marginal cost increase for the other two deterioration mechanisms (track settlement and component fatigue). Important is to mention that the here applied hydrobush stiffness characteristic has not been specially designed for the Y25L bogie. Further tuning of the hydrobush stiffness probably can reduce the marginal cost level for tangent track and large radius curves. From the

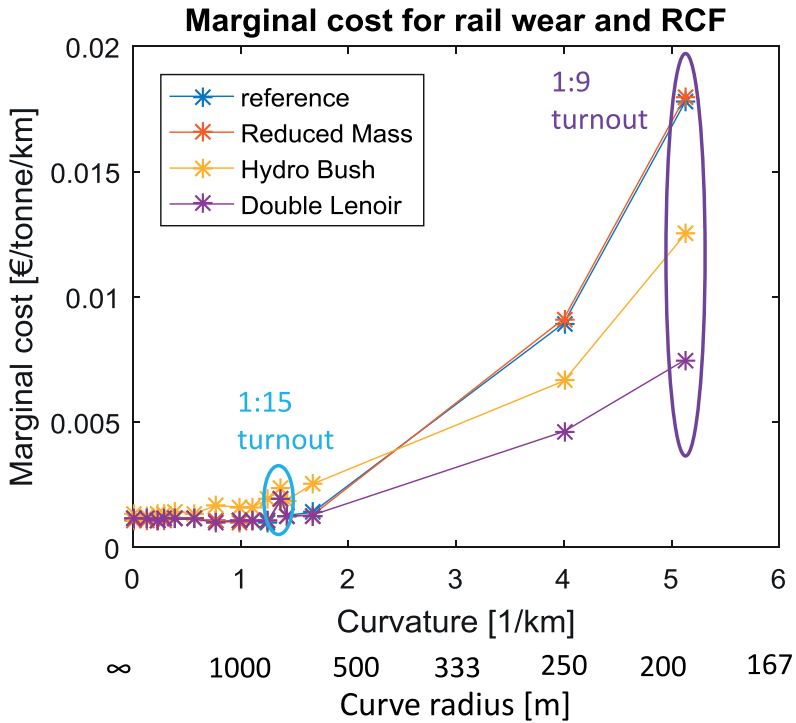


Figure 8. Marginal cost development for wear and RCF in relation to the different bogie designs.

working principle however, it seems unlikely that for the operational conditions considered here an overall cost level equal to or below the reference situation can be achieved. Compared to the Y25L reference bogie, an improvement in running stability can be expected from the hydrobush design when running at higher speeds (> 120 km/h) and when running with empty wagons. Potential beneficial aspects have not been incorporated in this study.

From Figure 8 it is understood that the vehicle concepts with improved PYS behaviour (double Lenoir link and trailer arm with hydrobush) behave more cost friendly in switches and narrow radius curves ($R < 750$ m). However, since this curve range only represent a small part of the total route, the impact on the overall cost savings is limited. In tangent track and large radius curves the double Lenoir performs equal to the reference: due to its improved behaviour in narrow radius curves it results in a cost reduction for the total route of 1.8%. The hydrobush performs noticeably worse in large radius curves and on tangent track, resulting in a marginal cost increase for the total route of 26%.

When calculating the total cost for the selected route, using Equations (1) and (2), the vehicle concept with reduced unsprung mass provides a 2.8% reduction in cost compared to the reference Y25L bogie design. For a 650-ton freight train, a locomotive with seven maximum loaded wagons, travelling the route Roosendaal – Oldenzaal, this results in a cost saving of 12 euro's. At the same time the reduced unsprung mass allows an additional load of 2 tons per wagon, resulting for this particular train in an additional 14 tons freight to be transported.

5. Discussion

In this section the results are discussed regarding the assessment of track degradation mechanisms and related track degradation cost calculation.

5.1. Technical

5.1.1. Switch negotiation

The track loads resulting from simulations in the switch panel demonstrate ‘wear’ to be the dominant damage type for the assessed 1:9 turnout. This is the case for the Y25L reference design, as well as for the assessed design modifications. Clearly the $T\gamma$ peak values occurring when entering the switch panel cannot be reduced by lowering the PYS value. However, at the closure panel, with curve radius 195 m, a significant difference is observed for two of the assessed design modifications, being the double Lenoir linkage and the trailer arm with hydrobush. For these modifications, wheel–rail wear at the flange (gauge face) becomes negligible. Simultaneously the $T\gamma$ level at the wheel tread/flange root contacting area is reduced, shifting from ‘wear’ into the ‘RCF’ region for double Lenoir, where the hydrobush loading level remains in ‘wear’. The other investigated design modifications (trailer arm with conventional bush, reduced secondary lateral stiffness, reduced unsprung mass and the cross anchor application) did not result in a significant optimisation in switch loading.

5.1.2. Curving behaviour

For the assessed operational conditions, the reference Y25L bogie displays excellent curving behaviour for curves above 750 m radius, keeping operational $T\gamma$ levels below the RCF damage threshold. At the curve radius of 500 m $T\gamma$ values are seen to sharply increase, resulting in RCF damage development for all evaluated designs except the double Lenoir design which remains below the RCF damage threshold. Although the trailer arm with hydrobush design results in reduced $T\gamma$ values compared to the reference bogie, its $T\gamma$ level at 500 m curve radius indicates operation within the RCF region. At 250 m radius, both double Lenoir and hydrobush design modifications are experiencing RCF damage development. Of the other investigated design modifications, only the reduced secondary lateral stiffness leads to improved curving, although minor.

5.1.3. Track degradation

The effect of reducing the unsprung mass of the bogie on track degradation, has been assessed by evaluating the forces between wheel and rail in lateral and vertical direction. It can be observed that reducing the unsprung mass predominantly has resulted in a significant reduction of the lateral track forces, and related $T\gamma$. The observed reduction is closely related to the Klingel movement of the bogie. Reduced lateral track forces will expectedly lead to reduced track geometry degradation and related maintenance effort and cost.

5.2. Economic

The marginal cost are clearly the highest at switches and narrow radius curves: for the reference situation the cost at switches is about 12 times the cost at tangent track. For switches,

the double Lenoir design results in a 60% marginal cost reduction for rail wear and RCF compared to the Y25L reference. For the trailer arm with hydrobush a 30% reduction is observed. However, since these switches and narrow radius curves represent only a small portion of the total route length, performance at large radius curves and tangent track is decisive in the overall cost level for the route. This is illustrated by the calculated cost reduction for the route for the double Lenoir being only 1.8%. To account for the degradation of switches and narrow radius curves, being the most vulnerable railway assets both in cost and operation, simply reviewing the overall marginal cost calculation for the route is clearly not sufficient. In [24] reduction in the Variable Usage Charge was calculated for the Spectrum trackfriendly bogie design, using a calculation method that mainly rewarded overall curving behaviour, not considering the travelled route. Resulting variable cost reductions are in the same order of magnitude as those here observed at narrow radius curves and switches.

Because the Y25L reference bogie design possesses a very low PYS at curves with radii from 600 m and up, the impact of the hydrobush element is limited. Significant benefits from this element, however, can be expected when applied to bogie designs with relatively high static PYS values. Not comprising lateral wavelengths below 6 m and vertical wavelengths below 8 m, it should be noted that the evaluated track geometry as registered by the measurement coach at ProRail track currently is not a fully adequate parameter to determine track degradation forces and cost. The significance of these wavelength limits should be further quantified.

6. Conclusions

The potential of proposed design measures regarding the improvement of curving behaviour and switch negotiation of railway freight bogies and related track degradation mechanisms have been studied. For this purpose, a sensitivity analysis has been carried out by means of track–train simulations in the VAMPIRE[®] multi-body simulation software. Curving behaviour of the standard Y25L freight bogie design, with respect to expected wear and RCF development, is shown to be rather good, keeping operational $T\gamma$ levels below the RCF damage threshold for a large range of radii. Only for the evaluated curve radii of 500 and 250 m, RCF development can be expected for the standard Y25L design. Two of the six evaluated bogie design modifications, being the double Lenoir linkage and the trailer arm with hydrobush, both targeting the PYS characteristics, deliver a distinctive contribution to track-friendliness of the Y25L freight bogie. For the assessed conditions the double Lenoir modification expands the curve radii range with $T\gamma$ operational levels below the RCF damage threshold to 500 m. Improved switch negotiation is observed for both the double Lenoir and trailer arm with hydrobush design modification, especially for the closure panel in which, for the assessed situation, flange wear is almost eliminated. Reducing the unsprung bogie mass has shown to reduce the lateral track forces, which will expectedly lead to a reduction in track geometry degradation. Other evaluated design modifications did not significantly contribute to improving track-friendliness under the evaluated conditions.

The improved behaviour at narrow radius curves ($R < 750$ m, switches 1:9) of the vehicle concepts with double Lenoir link and trailer arms with hydrobush provide, respectively, 60% and 30% marginal cost reduction for rail wear and RCF compared to the reference

Y25L bogie. However, since this curve range only represents a small part of the total route, the resulting marginal cost in the executed corridor study is dominated by tangent track and large radius curve sections. Although not significantly contributing to the calculated overall cost, measures decreasing the track deterioration for switches and narrow radius curves, being the more vulnerable track elements, are expected to be beneficial from the viewpoint of track availability and overall performance. Currently, this seems insufficiently reflected in the overall assessment result. When calculating the overall deterioration cost for the travelled route, the calculation model should include a well-balanced representation of switches and narrow radius curves. This will support the development of future track access charging, stimulating the design and introduction of vehicles with improved track-friendliness.

Acknowledgements

This research is being carried out by the author under the project number T91.1.12475a in the framework of the Research Program of the Materials innovation institute M2i (www.m2i.nl). The authors wish to acknowledge the support of ProRail.

Disclosure statement

No potential conflict of interest was reported by the authors.

Funding

Part of the work was funded by ProRail (the Dutch rail infra management organisation).

ORCID

Nico Burgelman  <http://orcid.org/0000-0003-4038-8364>

References

- [1] INNOTRACK Concluding Technical Report, UIC – Paris; 2010. ISBN: 978-2-7461-1-1850-8.
- [2] Öberg J, Andersson E. Determining the deterioration cost for railway tracks. *Proc Inst Mech Eng F J Rail Rapid Transit*. 2009;223(2):121–129.
- [3] Dollevoet R, Li Z, Arias-Cuevas O. A method for the prediction of head checking initiation location and orientation under operational loading conditions. *Proc Inst Mech Eng F J Rail Rapid Transit*. 2010;224:369–374.
- [4] Markine VL, Steenbergen MJMM, Shevtsov IY. Combatting RCF on switch points by tuning elastic track properties. *Wear*. 2011;271:158–167.
- [5] Karttunen K, Kabo E, Ekberg A. A numerical study of the influence of lateral geometry irregularities on mechanical deterioration of freight tracks. *Proc Inst Mech Eng F J Rail Rapid Transit*. 2012;226(6):575–586.
- [6] Vermeij I, Bontekoe T, Liefing G, et al. Optimisation of rolling stock wheelset life through better understanding of wheel tyre degradation. *Int J Railw*. 2008;1(3):83–88.
- [7] Andersson M. Marginal cost of railway infrastructure wear and tear for freight and passenger trains in Sweden, Swedish National Road and Transport Research Institute (VTI). *Eur Transp*. 2011;48:3–23.
- [8] Iwnicki SD, Stichel S, Orlova A, et al. Dynamics of railway freight vehicles. *Veh Syst Dyn*. 2015;53(7):995–1033.
- [9] Stichel S. On freight wagon dynamics and track deterioration. *Proc Inst Mech Eng F J Rail Rapid Transit*. 1999;213(F4):243–254.

- [10] Tunna T, Urban C. A parametric study of the effects of freight vehicles on rolling contact fatigue of rail. *Proc Inst Mech Eng F J Rail Rapid Transit*. 2009;223:141–151.
- [11] Iwnicki S, Bezin Y, Orlova A, et al. The ‘SUSTRAIL’ high speed freight vehicle: simulation of novel running gear design). 23rd symposium on Dynamics of Vehicles on Roads and Tracks (IAVSD 2013) 2013; Qingdao, China.
- [12] Hiensch EJM, Wiersma P. Reducing switch panel degradation by improving the track friendliness of trains. *Wear*. 2016;366–367:352–358.
- [13] Burstow MC. Whole life rail model application and development for RSSB – continued development of an RCF Damage Parameter. AEATR-ES-2004-880. 2 September 2004.
- [14] Alarcón GI, Burgelman N, Meza JM, et al. The influence of rail lubrication on energy dissipation in the wheel/rail contact: a comparison of simulation results with field measurements. *Wear*. 2015;330–331:533–539.
- [15] Molatefi M, Hecht M, Kadivar MH. Critical speeds and limit cycles in the empty Y25-freight wagon. *Proc Inst Mech Eng F J Rail Rapid Transit*. 2006;220.
- [16] ERRI B176 RP1. Preliminary Studies and Specifications, Utrecht, the Netherlands; 1989.
- [17] Steenbergen M. The role of the contact geometry in wheel–rail impact due to wheel flats. *Veh Syst Dyn* 2007;45(12):1097–1116.
- [18] Jenkins H, Stephenson J, Clayton G, et al. The effect of track and vehicle parameters on wheel/rail vertical dynamic forces. *Railw Eng J*. 1974;3(1):2–16.
- [19] Nash C. UNification of accounts and marginal costs for Transport Efficiency, 5th framework project UNITE, Final Report. Institute for Transport Studies, University of Leeds, Leeds, UK; 2003.
- [20] van Essen HE, Boon BH, den Boer LC, et al. Marginal costs of infrastructure use – towards a simplified approach, CE Solutions for environment, economy and technology, Final report. Delft, The Netherlands; 2004.
- [21] ProRail internal document. Beheer en onderhoudskosten 2014, J. Swiers.
- [22] ERRI B176/3. Benchmark problem – Results and assessment, B176/DT290. Utrecht; 1993.
- [23] UIC. Testing and approving of railway vehicles from the point of view of their dynamic behaviour – Safety – Track fatigue – ride quality. Code 518. Paris; October 2005.
- [24] Shackleton P, Bezin Y, Crosbee D, et al. Development of a new running gear for the spectrum intermodal vehicle). Proceedings of the 24th symposium of the international association for vehicle system dynamics (IAVSD 2015); 17–21 August 2015; Graz, Austria.

Paper 4

Rolling Contact Fatigue on
premium rail grades:
Damage function development
from field data.



Rolling Contact Fatigue on premium rail grades: Damage function development from field data



Martin Hiensch^{*}, Michaël Steenbergen

Delft University of Technology, Section of Railway Engineering, Faculty of Civil Engineering and Geosciences, Stevinweg 1, 2628 CN Delft, The Netherlands

ARTICLE INFO

Keywords:

Rolling Contact Fatigue (RCF)
Wear
Damage function
Rail grade selection
Premium rail

ABSTRACT

The concept of the rail damage function provides vital understanding of the operational performance of rail grades in terms of surface degradation. The present study extends this concept from conventional to premium pearlitic rail. This is done on the basis of both simulations of dynamic train-track interaction and field observations. Rolling Contact Fatigue (RCF) damage index values for the conventional R260Mn and the premium R370CrHT grade rail are established, describing the behaviour of the associated damage functions. Defining the individual rail grade damage response to operational loading levels, the potential of the RCF-damage function to support the process of rail grade selection and track maintenance is further discussed.

1. Introduction

Rail surface damage development and related costs of inspection and maintenance are a major concern to infrastructure managers. Control measures aiming to prevent or reduce damage development may target the wheel-rail interaction forces, limiting them through optimisation of the wheel-rail interface geometry or by stimulating the use of so-called track-friendly vehicles which produce reduced forces on the track. An alternative approach is the improvement of the material resistance to the imposed stress and slip levels. This line of approach is followed by the rail grade selection standards applied by most infrastructure managers, which specify more resistant rail grades to be installed at more demanding track sections such as curves. Beside the installed rail grade also the execution of maintenance measures (such as grinding or lubrication) can have a strong impact on the service life of rails [16]. This is supported by field experience, indicating that the expected benefit of improved steels has not generally been associated with a reduction in required maintenance. Based on the experience that Rolling Contact Fatigue (RCF) became a problem only after the normal rail for a specific site was replaced by premium rail, Burstow [1] concludes that premium grade rail steels may not always be the best solution to prevent track damage and that careful consideration of track geometry, operating conditions and traffic is necessary when considering the most appropriate rail grade to select for use at a given location. Ref. [2] reports that the response of the rail grade with respect to RCF development depends on the track test conditions. Further understanding of rail grade performance as a function of operational loading conditions is therefore vital to support the process of rail grade

selection. Rail damage models can be used as an asset management tool to analyse specific track sections, assessing the likelihood of RCF crack initiation and wear on the basis of given loading conditions.

In the literature, work has been undertaken to develop a simple parameter capable of describing damage development in terms of RCF as a function of the loading history. Burstow [3] has found the wear energy number (T_γ) to provide the best correlation between the output of RCF damage simulation work and observed crack location in the field. T_γ describes the mechanical energy dissipated in the wheel-rail contact patch, thus available for initiating damage at the contact surface on the rail. He presents a material specific damage function, derived from track inspections in combination with vehicle-track simulations. The function describes the relationship between the wear energy number and RCF crack initiation fatigue damage, by translating the calculated T_γ into a fatigue damage term, being the number of loading cycles to visual crack initiation. Currently this methodology has been applied only for analysis of sites containing the 'normal' grade rail R220 (according to the European norm [4]), although it can be expected that the concept itself works equally well for other material grades. There is however no validated damage model available for any other rail grade. In order to develop such models, the characterisation of different rail materials needs to be performed in terms of the T_γ loading history and related damage development. The objective of the present study is to establish the RCF damage functions for the normal R260Mn and premium R370CrHT grade rail. In analogy to Ref. [3], the damage indices will be determined from track inspections in combination with vehicle-track simulations for the track sections under consideration.

^{*} Corresponding author.

E-mail address: e.j.m.hiensch@tudelft.nl (M. Hiensch).

The structure of this article is as follows: after the introduction, the theoretical framework is presented in chapter two, discussing rail RCF damage assessment in general. Chapters three and four contain the core of this work, with a discussion of the setup of field observations and vehicle-track simulations in the first chapter, and the relationship between results and track damage in the second chapter. Chapter five discusses the engineering relevance of damage function application in track design and maintenance, followed by conclusions in chapter six.

2. Assessment of RCF damage on rails in general

‘Wear’ is a damage phenomenon being inherently present in each rail-wheel contact, with surface material (oxides) being removed even at the lowest loading levels. Fatigue damage however will initiate only when the cyclic loading level exceeds the material fatigue limit. Assessment of the material response to cyclic loading can take place using so-called shake-down maps, presenting the material hardening curves that define the areas with different material response types in dependence to the peak Hertzian pressure, the material yield stress under pure shear and the traction coefficient [5]. Fatigue damage will develop when individual loading cycles result in the accumulation of plastic strains, exhausting the material resistance to further plastic deformation. This type of material response, known as plastic ratchetting, occurs when loading levels surpass the plastic shakedown limit. The development of fatigue damage at the surface can be slowed down or even entirely prevented by removal of material from the surface due to wear. The development of RCF at the rail-wheel interface depends therefore on the balance between crack initiation and wear rate. Fatigue crack initiation is governed by the process of ratchetting. The wear rate depends on the tangential force in combination with the occurring slip in the contact patch. Damage models incorporating the competing damage mechanisms of wear and fatigue crack growth can be used for the evaluation of rail wear and RCF initiation.

The damage energy model as developed by Burstow was first proposed in [6]. It describes the relationship between the wear energy number T_γ and RCF crack initiation fatigue damage. The parameter T_γ represents the work performed by the frictional shear stresses in the moving wheel-rail contact patch, usually considered per travelled unit distance along the track [15]. This performed work is equivalent to energy dissipated in the contact patch, and is commonly expressed for a unit length of 1 m, giving rise to T_γ being expressed in the unit [J/m] or [N]. The wear number T_γ is calculated from the sum of the lateral and longitudinal products of shear forces (T_x and T_y) and creepages (γ_x and γ_y) at the wheel/rail interface. The wear number is a standard output from vehicle dynamics software. From the model the calculated T_γ is translated into a fatigue damage index; the number of loading cycles to visual crack initiation. This ‘RCF damage index’ expresses the number of cycles before visible RCF cracks can be expected on the rail head. Burstow suggests, for reasons of feasibility, a minimum surface length of approximately 2 mm, stating that cracks to be visible at this length must have developed beyond the initiation stage and some crack growth must have taken place. For each contact location the fatigue damage from individual loading cycles can be summed using Miner’s rule for variable amplitude fatigue loading [7]. When the fatigue life is exhausted, this results in visible RCF damage when the RCF damage index limit is reached.

The behaviour of the overall RCF damage function (shown at the bottom in Fig. 1) is determined by the individual linear damage functions regarding both wear and RCF (at the top in Fig. 1). At damage levels below the fatigue threshold (zone a) no RCF develops. For the rising slope of the damage function (zone b) RCF damage develops due to plastic ratchetting. At higher levels of energy dissipation the wear rate is seen to increase, removing RCF damage as indicated by the descending slope (zone c). When the damage function becomes negative (zone d), initiation of RCF damage is entirely suppressed by wear.

Wear mechanisms and transitions shape the course of the damage function. For rail materials these mechanisms have been studied by Bolton and Clayton with the help of two-disk testing [8]. To allow for a direct comparison between materials, Bolton and Clayton were the first to plot

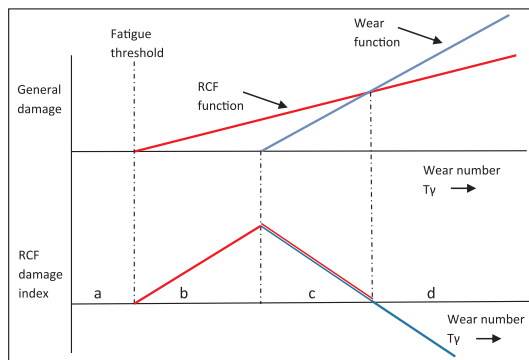


Fig. 1. Wear and RCF as competing mechanisms of rail surface degradation.

the wear rate against the wear number divided by the contact patch area (T_γ/A). From the occurring wear rate, the contact surface appearance and the amount of wear debris occurring during the two-disk testing, three different wear regimes were identified. They were referred to as mild (type I), severe (type II) and catastrophic (type III), associated to increasing contact pressure and slip percentage. Examining side-worn rail samples from curved track sections, Bolton and Clayton conclude the type II wear regime to be most closely related to the rail crown and the gauge corner region, whereas type III wear is usually concentrated at the gauge face due to relatively high slip levels in flange contact. Burstow [3] associated mild wear to the RCF-dominated regime (the rising part of the damage function in Fig. 1), with the transition from mild to severe wear to the change to the wear-dominated regime (the falling part). Lewis et al. [9,10] suggest this mild to severe transition to be associated with the onset of full sliding contact conditions.

Burstow [6] has demonstrated that the RCF damage index methodology can predict the damage level quite well when applied to sites where the RCF generating forces are determined by track irregularities and quasi-static curving. However, in the development of the model a number of assumptions have been made. Burstow mentions the limited number of applied wheel profiles as well as his use of only one single vehicle model, restricting the distribution of contacts and loading conditions. Also the condition of the track geometry at the time of the site survey has been assumed constant over its entire service life. These assumptions will affect the reliability of the model. Nonetheless, good correlations are reported between predictions and field observations of track sites with RCF.

3. Set-up of the damage function determination

In order to derive RCF damage functions for different rail grades, results from track inspections have been assessed in combination with results of vehicle-track simulations for the considered cases. Damage index values have been determined from the accumulated damage to the first visible RCF cracks. In this paragraph the successive individual steps of the analysis are discussed.

3.1. Field observations

Two track sites were selected, denoted here as site A and B. Track geometry details are presented in Table 1. The maintenance history of both sites shows that they are susceptible to the formation of RCF in the form of headchecking. From the difference in curve radii and installed cant between these sites different operating T_γ values are to be expected. This allows for the determination of a wider damage index range in the damage function. For purpose of comparison both sites were visually inspected prior to rail replacement. The RCF development at site A (Fig. 2) was found uniformly distributed over the entire curve. At site B, in the part of

Table 1
Track geometry details (*partly 1200 m).

	Site A	Site B
Curve radius (m)	1000*	2450
Cant (mm)	80	60
Max. Speed (Km/h)	120	140
Length full curve (m)	1200	1150
Avg. daily tonnage (0.10^3 t)	31.5	48.1



Fig. 2. High rail running surface at site A – situation prior to rail replacement (traffic direction to the right; depicted rail length about 0.36 m).

the curve with a constant radius, RCF was not uniformly distributed but clustered in ‘patches’. This suggests a variation in local contact stresses, likely associated to track geometry. At the high rail of both sites A and B, two different rail grades were installed in series; the normal grade R260Mn and premium grade R370CrHT, with a length of 180 m length each. A monitoring program was started from the moment the new rail was installed. During the first year, this comprised visual inspection of the running band each second month, along with measurements of hardness, rail profile and crack depth (eddy current). After the first year the inspection interval was extended to four months.

Since the RCF crack initiation model applies damage summation, it requires loading information in terms of the composition of the daily passing rolling stock. To this purpose strain gauges were installed in the track, measuring the number of passing axles, the axle loads and the train speed. From the recorded wheel base and bogie spacing for each passing vehicle also the vehicle type could be identified.

3.2. Vehicle dynamics simulations

Train registrations clearly showed the loading at both sites to be dominated by the same three train types; two passenger intercity trains and a particular freight configuration, together representing 70% of all axle passages and born tonnage. Although not serving the same route, the train type distribution for both sites was similar. The three dominant vehicle types were modelled using the simulation software VAMPIRE® Pro 6.30. The main dynamic parameters for the two operating passenger vehicles are listed in the Annex of this paper (Table 3). The main parameters of the freight vehicle are presented in Ref. [14]. Vehicle dynamics simulations were performed for quasi-static curving conditions, based upon the track geometry design values. Further dynamic simulations were performed for the track with irregularities as measured by a recording train during the period of field testing. Because of the fact that the wheels of passenger vehicles are frequently reprofiled, vehicle simulation runs were performed with the new (unworn) S1002 wheel profile. Freight vehicle simulation runs were performed with an average worn S1002 wheel profile, selected from profile measurements performed at a number of freight wagons in service. The rail inclination was set to 1:40 and the design track gauge was 1435 mm. The applied rail profile was UIC 54E1 as defined in the norm [4].

The coefficient of wheel-rail friction was set to $f = 0.32$. This is a representative value in accordance with Ref. [13], which specifies the assessment of the running characteristics of railway vehicles for the European network. The vehicle speed and loading condition to be applied in the simulations were derived from the strain gauge measurement results. The vehicle speed was set identical for both passenger train types; 120 km/h at site A and 130 km/h at site B. The freight train speed for both sites was 90 km/h. No traction was applied. Simulations for all vehicle types were carried out in loaded condition. As mentioned earlier the selected three vehicle types together establish 70% of all axle passages and born tonnage. The remaining 30% of the total tonnage, mainly from different commuter train types, has been included in the simulations by simply adding their tonnage to that of the two dominant passenger train types.

3.3. Damage summation

The considered damage loading period started at the moment of rail renewal, ending at the moment of first visible RCF crack detection with a minimum surface length of approximately 2 mm. For the total number of vehicles of each type that has passed the considered site during this period, the T_Y damage summation is performed for each wheelset on each vehicle. Summation of the damage has been carried out with respect to the position in the curve (x), the contact position on the rail head (y) and the contact patch area and ratio (a/b).

4. Test results and implementation in the damage model

The results of track inspections, vehicle dynamics simulations and damage summation are presented in this section, together with the interpolated part of the damage function that follows from this input. Subsequently, the further behaviour of the damage function for premium rail is extrapolated on the basis of work performed by Bolton and Clayton [8] regarding rolling-sliding wear.

4.1. Field observations

From the inspection, a clear difference in the accumulated tonnage until visible crack initiation could be established between the normal and premium rail grade, as can be seen in Table 2.

Shortly after installation the premium rail grade is observed to develop a fine network of superficial cracks (‘craquelure’, Fig. 3). However, visible cracks that develop beyond the initiation stage are found on the premium grade at a much later stage. At site A, RCF develops uniformly over the entire section, independent of the rail grade. Differences in the delay until RCF initiation at site A were dominated by the rail grade but also a difference between the two R370CrHT locations is observed. Similar to the situation prior to rail replacement, RCF at site B develops more locally, with damage clustering in patches. At site B, differences in the delay until RCF initiation were found to depend on rail grade and the position in the curve. Visible headcheck development is illustrated in Fig. 4. Eddy current measurements indicate these cracks to be about 0.3 to 0.4 mm in depth. From profile measurements performed 18 months after rail installation the premium rail grade at track B showed hardly any wear nor deviation from the

Table 2
Accumulated tonnage to visible crack initiation for different measurement locations.

	Accumulated tonnage until visible crack initiation (0.10^6 t).	
	Track site A	Track site B
R260Mn	5,8	8,8 (750 m) ^a
R260Mn	n.a.	14,5 (430 m) ^a
R370CrHT	20,1	35,0 (540 m) ^a
R370CrHT	11,9	33,5 (990 m) ^a

^a Relative position of the measurement location, corresponding to travelled distance (m) as presented in Fig. 5.

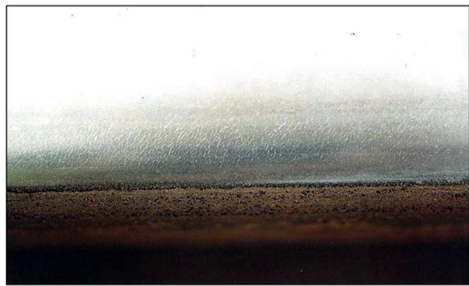


Fig. 3. Fine network of superficial cracks (craquelure) on the premium rail grade (site B). Direction of traffic is to the left, depicted rail length is about 0.1 m.

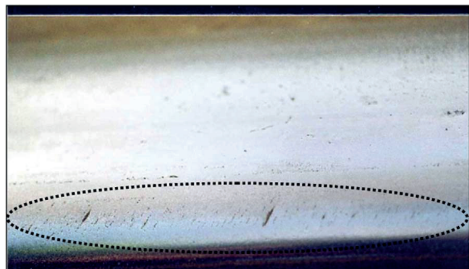


Fig. 4. Visible headchecking at the rail shoulder (within indicated zone, approx. 3–5 mm in length), site B, grade R370CrHT. Direction of traffic is to the left, depicted rail length is about 0.1 m.

design profile, confirming a mild wear operating regime.

4.2. Vehicle dynamics modelling

For the purpose of this study only results at the high rail are evaluated, both for the design track geometry (quasi-static curving conditions) and for the situation with measured track irregularities. For site A the most striking result is that, apart from the leading wheels of the bogies from both passenger type vehicles, none of the other vehicle contact positions during quasi-static curving surpass the fatigue crack initiation limit value of the R220 damage function. Neither the freight vehicle nor the trailing wheels of the passenger vehicles seem to contribute to the observed RCF damage at this site. Evaluating vehicle dynamics in relation to curving behaviour with track irregularities, T_γ development for site A does not show local variations and the average level is equal to the quasi-static curving. At site B the T_γ loading levels for quasi-static curving are below - or just touch - the R220 fatigue crack initiation limit for all vehicle type contact positions, suggesting no significant RCF damage development (Fig. 5a). However, when evaluating vehicle dynamics with measured track irregularities the track geometry variations result in a local steep increase of T_γ , surpassing the threshold value at a number of track segments (Fig. 5b). Further evaluation shows this increase to be due to especially lateral irregularities and a number of a sharp local deviations in the curve radius. For site B, T_γ loading levels vary distinctly due to the track geometry variations; therefore damage summation for this curve should be position-dependent. From Fig. 5 the general T_γ level during quasi-static curving and the level during curving for the measured track geometry are seen to differ, mainly due to differences between design and measured cant.

4.3. Damage summation

The contact patch area and its location on the railhead are evaluated

for the outer wheels and compared to the location where RCF initiation is observed. At track site A, both for quasi-static curving and for curving behaviour with track irregularities, the railhead contact positions of the leading outer wheels of both passenger vehicles correspond to the RCF initiation area. This indicates that the fatigue damage from the individual loading cycles can be summed and related to the observed damage. The observed running band and calculated wheel-rail contact positions are presented within Fig. 6. During quasi-static curving the contact patch locations of the two intercity type vehicles remain unchanged, each represented in Fig. 6 by one shaded marker. For the curving situation with measured track geometry both passenger vehicles show a spread in contact conditions due to the presence of track geometry variations. This is illustrated by two shaded markers for each train, designating the extremities of the contact band.

At site B, wheel-rail contact at the RCF initiation zone only occurs for a discrete number of positions throughout the curve. These coincide with major local deviations in lateral alignment and in curve radius. The observed shifting of the contact location towards the rail shoulder results in a sharp local increase of T_γ for all evaluated vehicle types, as visible in Fig. 5b. These locations were found to be the first ones where RCF damage started to develop. The contact patch distribution for the vehicle response to track geometry variations indicates that only the leading wheels contribute to the observed head check generation.

4.4. Damage function development - interpolation

Damage function indices for the different rail grades have been determined from the observed period to RCF damage initiation in combination with calculated T_γ loading levels, loading positions and corresponding loading frequencies. T_γ levels for quasi-static curving conditions were applied to site A. For site B, T_γ levels were applied from simulations including track irregularities. The resulting indices are presented in Fig. 7 as a function of the wear number. The square (\square) box markers indicate the established R260Mn behaviour. The diamond (\diamond) shape markers denote this dependency for the R370CrHT rail grade. The RCF damage function as established by Burstow [6] for the here presented section is shown by the black line. The dotted line represents the established R370CrHT damage function within this area. The damages indices obtained for the R260Mn rail grade can be observed to coincide with the RCF damage function of R220. This is in accordance with observations made by Zacher [11], who showed that gauge corner cracking predictions based upon the R220 damage function matched remarkably well to that of the R260 grade rail. These findings further support the conclusion that the RCF regime of the R220 damage function can be applied to the entire family of normal pearlitic rail grades including R260 and R260Mn.

The observed spread in accumulated tonnage until visible crack initiation for R370CrHT rail grade at site A, as shown in Table 2, and the related spread in the RCF damage index value for the calculated wear number can be explained from locally varying operational conditions. Changes in track geometry developing over time are expected to lead to larger deviations of the quasi-static T_γ levels calculated for site A as compared to site B, for which track geometry variations were included from the beginning. Also the T_γ level at site A is situated near the expected peak of the damage function, which means that both a periodical decrease or increase of T_γ will lead to an increase in accumulated tonnage until visible crack initiation. At site B, situated in the rising part of the function, the effect of T_γ fluctuations on accumulated tonnage until visible crack initiation will be more levelled off. Moreover, accuracy can also be affected by the chosen inspection interval and seasonal influences.

4.5. Damage function development – extrapolation

The expectation for the remaining part of the damage function can be based on the work performed by Bolton and Clayton [8] regarding rolling-sliding wear damage. The fatigue crack initiation limit, the starting point of the rising slope, is determined by the mechanical properties to resist

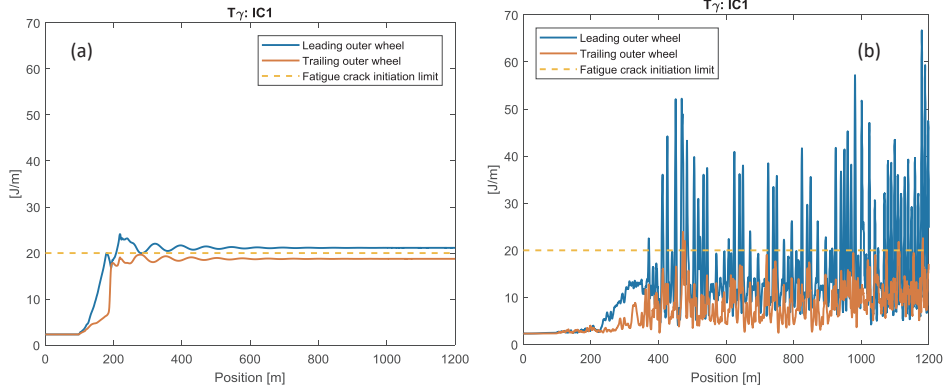


Fig. 5. T_γ development of the IC1 passenger type vehicle at the first 1000 m of site B during quasi-static curving (a) and for the situation including variations in track geometry (b).

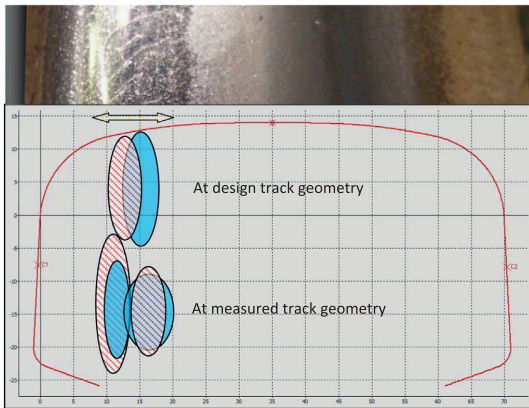


Fig. 6. Site A, R260Mn, 21 months after installation – detail of the running band with arrow indicating the position of the observed RCF damage. The calculated contact location and size at the extremities of the contact band for the leading wheels of both passenger type vehicles are marked for the quasi-static curving condition and for the situation with included track geometry variations.

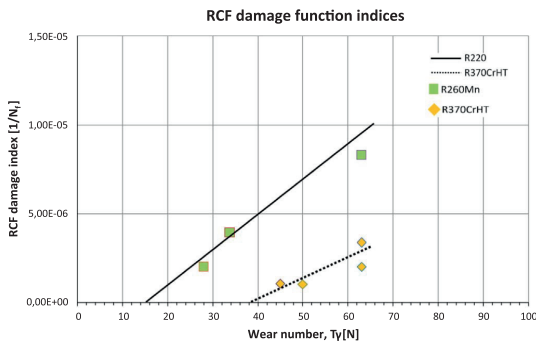


Fig. 7. RCF damage index values for the normal R260Mn and premium R370CrHT grade rail as a function of the wear number, derived from site A and B. The black line represents the ascending part of the R220 damage function from Burstow [6]. The dotted line represents the established R370CrHT partial linear damage function.

fatigue initiation. Pontre [5] shows the shakedown limit above which fatigue damage will develop depends on the material yield strength in shear. From its higher yield shear strength and resulting higher shakedown limit an increase in the RCF initiation limit wear number value can be expected for R370CrHT as compared to R220. The starting points of the individual damage functions in Fig. 7, as determined from the established index values, confirm this expected behaviour. Burstow [3] associates mild wear with the rising part of the damage function. For the type I mild wear regime Bolton and Clayton find the wear rate to be independent on examined rail steels. This indicates the ascending slope of the damage function for the different materials to be determined by its early stage RCF crack growth properties. Garnham and Davis [12] conclude the prior-austenite (PA) grain boundary dimensions and shapes to play a significant role with respect to initial RCF crack initiation growth rates, particularly if defined by regions of pro-eutectoid (PE) ferrite. With initial crack propagation restricted to the boundaries of the deformed PA grains at the surface, microstructural properties define this very early crack growth behaviour. Premium rail grades are characterized by a low level of intergranular ferrite. Microstructure crack-retarding properties of premium rail are further optimised through a very small lamellar spacing achieved by heat treatment. Small cracks (during initiation and first stages of crack growth) are sensitive to lamellar spacing, since the lamellar structure possesses excellent crack-retarding properties thereby decreasing the transgranular crack growth rate. The less steep ascending slope of the R370CrHT damage function reflects its improved crack delaying properties and improved resistance to plastic deformation as compared to the normal grade rail. With RCF crack initiation increasingly suppressed with increasing wear rate Burstow [3] associates the transition from mild to severe wear with the transition from the RCF to the wear regime, the peak of the damage function. For the type II wear rate, Bolton and Clayton have found considerable differences between the various rail steels and concluded these to be dependent on the intrinsic material properties. The type II wear rate for the individual rail steels are found to be a linear function of T_γ/A. The reduction factor in wear rate was observed to increase with increasing material hardness, indicating a less steep descending slope of the R370CrHT material damage function as compared to R220. To a lesser extend this also seems to apply to R260Mn. The exact geometry of the descending slope of these rail grades however needs to be further defined and validated.

The transition from type I to type II wear occurs at operational conditions well beyond the fatigue crack initiation / shakedown limit. This transition seems to be determined by the level of the frictional work destroying the protective oxidation layer and to a lesser extent by the resistance to plastic deformation. Since the oxidation rates of normal and premium rail grades are expected to be relatively similar, one may speculate the transition zone creepage value of these grades to be in the same

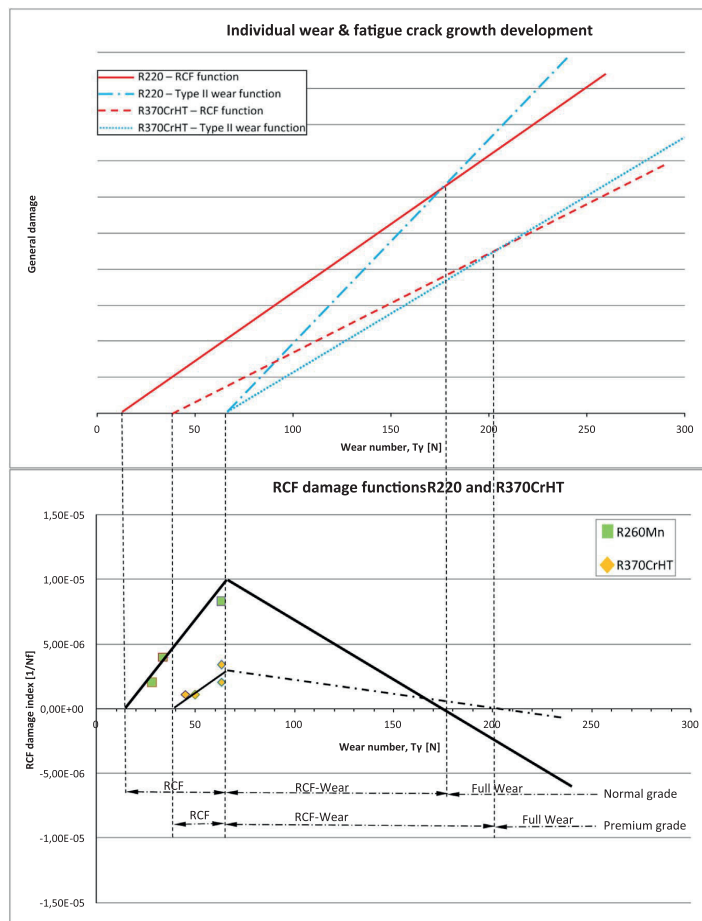


Fig. 8. The individual wear and fatigue crack growth development for R220 as derived from Burstow [6], together with those for R370CrHT as determined in this study (top); RCF damage functions for both R220 and R370CrHT rail grades (bottom). The starting point and development of the downward slope of the R370CrHT damage function (stripe-dotted line) remain speculative.

order. This expected behaviour is confirmed by presented transition zone creepage values by Bolton and Clayton [8]. At contact stresses typical for moderate curving (1300 MPa, [12]) these show little to no difference for the different rail materials, indicating under these conditions the damage function peak for all examined rail grades to be positioned at a similar wear number. These insights can be used to further estimate the R370CrHT damage function within the regimes of simultaneous RCF-wear and of full wear. Fig. 8 presents the individual R220 damage functions derived from Burstow [6] together with those determined for R370CrHT. The starting point of the RCF function is determined by the mechanical material properties to resist fatigue initiation, whereas the slope reflects the early stage RCF crack growth properties. Transition from the regime of RCF to wear is assumed to start at the same T_γ level for both materials with the slope of the descending wear function proportional to the hardness. Since the type II wear function is not yet defined, the starting point and geometry of the descending branch of the R370CrHT damage function remain speculative.

5. Discussion: engineering relevance and outlook

The R370CrHT RCF damage function has implications with respect to rail grade selection in design situations. Compared to the normal grade, the increased fatigue crack initiation limit value of the R370CrHT damage

function indicates a reduction in RCF susceptibility, preventing RCF initiation for an extended range of track curving conditions. The reduced slope of the ascending part of the R370CrHT damage function will, under equal loading conditions, result in a significant increase in expected time to visible RCF damage initiation as compared to normal grade rail. Although not validated, the reduced RCF index peak value will have a further beneficial effect on the loading frequency until visible RCF.

Wear number (T_γ) loading levels and frequencies for any particular site are required in order to apply the RCF damage function to select the optimal rail grade to be installed or to forecast headcheck development. A daily fatigue index as suggested in [11] can be used by the track engineer, to consult e.g. through look up tables. The T_γ magnitude is found to depend strongly on the curve radius together with vehicle curving characteristics. The contact patch distribution at the evaluated conditions, affecting damage summation, indicates that only leading wheels contribute to the damage summation. Especially at the examined larger radius curve ($R = 2500$ m) the operating T_γ levels and contact patch distribution are significantly influenced by the intensity of track geometry variation. This behaviour needs to be reflected within the track-train specific look up and can be addressed for example by taking into account the (mean) track quality number as obtained by the track geometry recording train. Due to the wide range of influencing factors (e.g. wear of wheel profiles, friction conditions), the accuracy of the theoretical model is valuable only to a certain extent. To

support rail grade selection in practice an overall description of the RCF damage function for the different rail grades therefore seems to be sufficient.

RCF damage models can support rail grade selection, switch design and rail maintenance planning. Using these models, the damage response of different rail grades can be predicted given the dynamic loading conditions. Accordingly, measures can be taken e.g. avoiding operational T_y values within the RCF damage regime. The mean value of the wear number along a curve or switch section can be used to optimise track maintenance in relation to RCF generation. With the applicable RCF damage function the accumulated fatigue index for the section can be determined from the average daily traffic. This can support e.g. the planning of maintenance activities such as grinding or rail grade selection upon renewal. Damage models can also be used in an engineering environment to assess the impact of changes in train operation (e.g. increased train speed, vehicle types, axle loads) on the expected damage development and, consequently, required maintenance.

6. Conclusion

On the basis of a combination of dynamic train-track simulations and regular track inspection results, RCF damage index values have been established for both the normal R260Mn and the premium R370CrHT heat treated pearlitic rail. From these index values the rising RCF-branch of the damage functions of both rail grades has been established. RCF damage index values for R260Mn were found to coincide with the RCF damage function of the R220 grade as reported in the literature by Burstow [6]. In line with work by Zacher [11] these findings support the conclusion that the RCF regime of the R220 damage function, with T_y values in the domain between the fatigue crack initiation limit and the peak value of 65 N, is applicable to the entire family of normal pearlitic rail grades, including R260 and R260Mn. Compared to the normal grade, the established part of the R370CrHT damage function shows an increased fatigue crack initiation limit value together with a reduced slope of the rising part of the function.

It can be concluded from the established part of the R370CrHT

damage function that application of this grade in the type I mild wear regime is beneficial to avoid RCF. The increased crack initiation limit will extend the track length for which no RCF initiation is expected. Within the RCF regime itself the initiation of headchecking will require an increased number of loading cycles. Within the operational window of the RCF damage function with T_y values below 65 N, the application of premium grades such as R370CrHT can therefore be expected to result in a significant reduction of the maintenance need.

The quantitative determination of the descending part of the damage function for premium grade rail requires further research. A difficulty here is the wide range in operational loading conditions (e.g. due to variation in vehicle type, wheel profiles, vehicle speed, traction and adhesion levels). To obtain more controlled conditions, laboratory two-disk testing could be applied to both establish and validate the damage functions for the different materials.

The RCF damage functions have significant engineering relevance. Their application allows for a dedicated rail grade selection, adapted to site-specific operational conditions. They can be used either in plain track and in the design of special parts of the rail network, such as switches and crossings. Assessment of the Wear number (T_y) loading levels and frequencies for a particular site provides careful consideration when selecting the most appropriate rail grade for use at a given location, assisting the track engineer towards a fit-for-purpose decision. This can be expected to significantly affect the life-cycle costs.

Acknowledgements

This research is being carried out under the project number T91.1.12475a, in the framework of the Research Program of the Materials innovation institute M2i (www.m2i.nl). Part of the work was funded by ProRail (the Dutch rail infra management organisation) (10.411). The authors would like to thank Nico Burgelman for his support regarding the simulation work, preparing the run-files and the output.

Annex

See Table 3.

Table 3
The main dynamic parameters for the two operating passenger vehicles.

Mass - metric tons (MT)		IC 1	IC2
<i>Car body secondary mass</i>			
Tare	MT	30	38
Laden	MT	35	46
Crush	MT	40	49
distance between bogie pivots	m	19	20
<i>Centre of gravity (laden)</i>			
CG long. offset	m	0,06	0,11
CG lat. Offset	m	0,01	0,01
CG height above rail	m	1,98	2,25
<i>Primary suspension mass</i>			
Bogie (motor)	MT	2,6	3,3
Wheelset	MT	1,7	1,7
longitudinal offset wheelset	m	2,5	2,5
CG height above rail	m	0,5	0,5
Wheel radius (new)	m	0,46	0,46
Wheel radius (fully worn)	m	0,42	0,42
Wheelset roll/yaw inertia	MTm ²	0,8	0,8
<i>Primary vertical dampers</i>			
Linear rate	(MNs/m)	0.027	0.025
distance primary damper to pivot	m	0,6	0,7
<i>Primary suspension</i>			
longitudinal stiffness	(N/m)	4*10e7	4*10e7
vertical stiffness	(N/m)	1.15*10e6	1.15*10e6
Airspring stiffness (laden) linear	MN/m	0388	0413

References

- [1] M. Burstow, Experience of premium grade rail steels to resist rolling contact fatigue (RCF) on GB network, *Ironmak. Steelmak.* 40 (2) (2013) 103–107.
- [2] R. Stock, R. Pippan, RCF and wear in theory and practice – the influence of rail grade on wear and RCF, *Wear* 271 (2011) 125–133.
- [3] M. Burstow. Whole life rail model application and development for RSSB (T115) – continued development of an RCF damage parameter, in: Engineering Research Programme 2004, Rail Safety & Standards Board.
- [4] NEN-EN 13674-1:2011, Railway applications - Track - Rail - Part 1: Vignole railway rails 46 kg/m and above.
- [5] A.R.S. Ponter, et al., Application of the kinematical shakedown theorem to rolling and sliding point contacts, *J. Mech. Phys. Solids* Vol. 33 (4) (1985) 339–362.
- [6] Burstow M. Whole Life Rail Model Application and Development for RSSB – Development of an RCF Damage Parameter, AEATR report, AEATRES- 2003–2832 Issue 1, October 2003.
- [7] A.M. Miner, Cumulative damage in fatigue, *J. Appl. Mech.* 12 (3) (1945) A-159.
- [8] P.J. Bolton, P. Clayton, Rolling-sliding wear damage in rail and tyre steels, *Wear* 93 (1984) 145–165.
- [9] R. Lewis, U. Olofsson, Mapping rail wear regimes and transitions, *Wear* 257 (2004) 721–729.
- [10] R. Lewis, R.S. Dwyer-Joyce, Wear mechanisms and transitions in railway steels, *Proc. IMechE, Part J: Eng. Tribol.* 218 (2004), pp. 467–478.
- [11] M. Zacher. Prediction of gauge corner cracking in rails for rail maintenance, *Contact Mechanics, CM 2009*, Florence, Italy.
- [12] J.E. Garnham, C.L. Davis, Very early stage rolling contact fatigue crack growth in pearlitic rail steels, *Wear* 271 (2011) 100–112.
- [13] EN 14363:2016, Railway applications. Testing and Simulation for the acceptance of running characteristics of railway vehicles. Running Behaviour and stationary tests.
- [14] Molatefi M., Hecht M., Kadivar MH. Critical speeds and limit cycles in the empty Y25-freight wagon, *Porc. IMechE Vol. 220 Part F: JRR67*, 2006.
- [15] G.I. Alarcón, N. Burgelman, J.M. Meza, A. Toro, Z. Li, The influence of rail lubrication on energy dissipation in the wheel/rail contact: a comparison of simulation results with field measurements, *Wear* 330 (2015) 533–539.
- [16] M.J.M.M. Steenbergen, Rolling contact fatigue in relation to rail grinding, *Wear* 356–357 (2016) 110–121.

Paper 5

Rolling Contact Fatigue: damage
function development from
two-disc test data



Rolling contact fatigue: Damage function development from two-disc test data

Martin Hiensch^{a,b,*}, Nico Burgelman^b

^a Delft University of Technology, Section of Railway Engineering, Faculty of Civil Engineering and Geosciences, Stevinweg 1, 2628 CN Delft, the Netherlands

^b DEKRA Rail, Concordiastraat 67, 3551 EM, Utrecht, the Netherlands

ARTICLE INFO

Keywords:

Rolling contact fatigue
Wear
Damage function
Two-disc laboratory testing
Rail grade selection

ABSTRACT

The concept of the rail damage function provides vital understanding of the operational performance of rail grades in terms of surface degradation. Previously, material specific damage functions have been derived from measurements in track combined with vehicle-track simulations. However, from the occurring wide range in track loading conditions it is difficult to achieve clear characterisation results from track data only.

To reach more controlled loading conditions, a rolling-sliding two-disc laboratory set up could be applied. The validation of a two-disc test approach in order to define rail/wheel interface wear and RCF response is the topic of the here presented study.

1. Introduction

Rail damage functions describe the operational performance/degradation of the rail running surface in dependence on the loading conditions imposed by the railway vehicle and rail grade. When damage functions are available for a wide range of rail grades, the track engineer can select the most appropriate rail grade for use at a given location, considering the loading levels and loading frequencies for that particular site.

Work has been undertaken in developing a parameter capable of describing damage development associated with RCF. Burstow [1] has found the wear energy number ($T\gamma$) to provide the best correlation between RCF damage simulation work and observed crack location in the field. $T\gamma$ is a measure of the energy dissipated within the wheel-rail contact, describing the amount of energy which would be available for initiating and propagating damage at the rail head. A material specific damage function is presented in Ref. [1], derived from track observations in combination with related vehicle-track simulations. The in Ref. [2] presented study extends this concept from conventional pearlitic rail to premium rail. From the occurring wide range in loading conditions in track (e.g. due to different vehicle types, wheel profiles, vehicle speed, traction, adhesion levels), it is difficult to achieve clear characterisation results from track observations only. To obtain more controlled conditions, experimental two-disc machines are used in laboratories to investigate the wheel-rail interface, substituting the rail by

one of the discs. This approach could be applied to both establish and validate the damage functions for the different materials and to understand the relationship between material properties and the RCF damage index to serve future rail grade development. The validation of the two-disc test approach in order to define rail/wheel interface wear and RCF response to $T\gamma$ loading levels is the topic of the here presented study.

The development of a two-disc test rig for testing rolling-sliding contact under closely controlled conditions has been presented in Refs. [3,4]. It has been shown that the set-up allows the contact to be examined over a wide range of loads, speeds and slip ratios. RCF and wear behaviour of rail and wheel materials have been studied by means of two disc testing, among others in Refs. [5,6]. Initiation and growth of RCF cracks has been achieved during these tests, showing that the initiation of surface cracks to take place if the surface layer accumulates uni-directional plastic strain higher than the strain to failure. Other researches [15,16] demonstrated how factors such as rolling direction, angle of attack and contact pressure distribution affects the RCF of wheel/rail materials. Daves et al. [17] presents a two-dimensional wheel/rail contact model predicting the crack growth direction considering stick-slip behaviour of wheel/rail contact. Related metallographic investigations of a rail on a full scale test-rig suggest that the angle of the deformation lines decides if a crack grows parallel to the surface and will be removed as wear particle in further contacts or develops as a crack following the deformation line. In search of

* Corresponding author. Delft University of Technology, Section of Railway Engineering, Faculty of Civil Engineering and Geosciences, Stevinweg 1, 2628 CN, Delft, the Netherlands.

E-mail address: e.j.m.hiensch@tudelft.nl (M. Hiensch).

<https://doi.org/10.1016/j.wear.2019.05.028>

Received 7 November 2018; Received in revised form 16 May 2019; Accepted 23 May 2019

Available online 28 May 2019

0043-1648/ © 2019 Elsevier B.V. All rights reserved.

improved lifetime performance many two-disc studies focus on describing the wear behaviour with regard to specific loading conditions. The aim of this study is to determine if the RCF-damage function can be derived from two-disc testing, addressing both the RCF and wear dominated regime.

Since two-disc machines often are scaled models, scaling factors of the involved physical laws need to be determined and respected in order to validly analyse the phenomena considered. Different researchers [7–9] have studied the effect of scaling and simulation of the wheel-roller contact instead of the wheel-rail contact. With respect to the creep forces, Jaschinsky [7] concludes shape similarity of the contact ellipse to be important when the creep forces are not saturated. $T\gamma$ is found to scale proportional to the normal force. In Ref. [10] Bosso conducts a comparison between the different scaling methods/factors, discussing the kinematic problem for the finite radius of the roller (frictional forces and creepage). It is concluded that the contact forces and displacements in the field of contact of all methods show satisfactory results compared to the output obtained from a full-scale model. Comparing the stress and strain state produced in a 1/30 scale twin-disc tests to the full scale wheel/rail experiments calculated by the finite element method [14] concludes that larger disc diameters are beneficial, reducing the influence of surface roughness and wear. The contact mechanics of the rail-vehicle motion is discussed in Ref. [11], presenting the development of the theory of rolling contact. It is concluded that when the traction-slip distribution inside the contact area is significant, Kalker full theory and FASTSIM calculations of the tangential forces and creepages are required to assess wear damage. Calculation of the tangential forces and creepages within the rolling-sliding contact at two-disc testing is discussed in Ref. [12], stressing the importance of preventing excessive profile wear of the two-discs since this will result in the contact pressure to lose its peak at the centre, resulting in the Hertzian theory not to be applicable anymore. With a developing ‘ball-groove’ conformal contact the use of Hertz + Kalker’s FASTSIM code would lead to inaccurate results, requiring e.g. Kalker’s NORM + TAN boundary element-based computer code.

The paper outline is the following. After the introduction in chapter one, the test rig design, scaling issues and consequent disc geometry and loading choices in test rig set-up will be discussed within chapter two. Chapter three presents the calculated equivalent $T\gamma$ levels with respect to slip ratios (longitudinal and lateral), normal load and friction levels using the FASTSIM algorithm for wheel-rail contact evaluation. The test protocol is presented in chapter four, discussing the control of the operational settings and executed measurements. Within chapter five the resulting RCF development will be presented for the different operational settings, providing the index values required to establish the RCF damage function. Evaluation of the test runs within chapter five also includes metallurgical analysis of the running surfaces, especially the micro-structure deformation levels and the development of the contact conditions. Discussion and conclusions are presented respectively within chapter six and seven.

2. Two-disc machine set-up

All tests have been conducted on the specially developed rolling-sliding two-disc machine at DEKRA Rail. Previous tests on this machine focused on the development of rail surface materials and alternative rail profiles, investigating friction characteristics and their contribution to squeal noise reduction [13]. This machine features two separately driven discs. With the here applied rotational speed in the order of 1000–1100 RPM, the resulting contact speed is 45–50 km/h.

Within Fig. 1 the set-up of the two-disc machine is shown. The rear (rail) disc, including bearings and engine, is mounted on a moveable support. This support is moved by a pneumatic cylinder, through a force transducer, which is in line with the disc-disc contact. Each disc is driven by a separate motor with frequency controller. At one of the driving axles the torque is measured, allowing to determine the

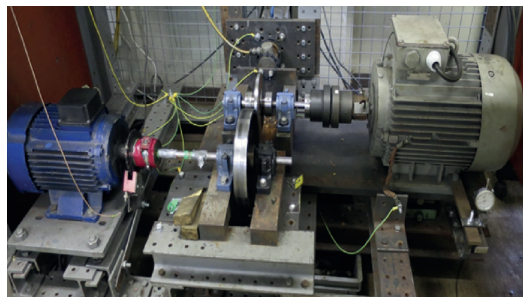


Fig. 1. Two-disc testing machine overview.

tractional effort and thereby the coefficient of friction active between the two discs (see chapter 3). Maintaining a set difference in circumferential speed between the wheel and the rail disc results in a longitudinal slip level. The wheel disc is acting as driving disc (maintaining the higher circumferential speed). Continuously measuring the rotational speed of both discs, a proportional–integral–derivative controller (PID) provides a control loop feedback mechanism to retain the desired longitudinal slip set-point. Measurement error for the torque is $\pm 3\%$. The rotational speed is measured with an accuracy of $\pm 1\%$ however the circumferential velocity can be influenced due to wear. For this reason the diameter of each disc is frequently re-measured.

The applied test rig configuration allows a contact angle to be set to one of the discs introducing lateral slip. Together with the longitudinal slip this simulates the dynamic conditions between wheel and rail when negotiating a curve. Lateral slip can be induced by lifting the support of the moveable disc on one side. This way, an angular difference in the planes of both discs is induced, causing a lateral slip of maximum 2%. During the here performed tests an angular rotation of 2 mrad (0.2% lateral slip) was maintained between the two discs. Initial alignment of the two discs has been carried out with help of a specialist 3-D laser measuring arm, with a specified accuracy of ± 0.013 mm.

2.1. Disc-specimens

The aim of the work is to validate the two-disc approach for RCF-damage function development. The chosen approach is to derive the RCF-damage index values for a rail grade for which the RCF damage function already has been established from field observations; the pearlitic normal rail grade from Ref. [1]. For this purpose rail discs have been manufactured from a normal grade rail type R220 (Fig. 2). Markings have been applied to identify the individual rail disc sections initially located at the head, web and foot of the rail.

The rail disc diameter is 177 mm, the transverse plane is curved (radius 12 mm). The wheel disc is manufactured from medium-carbon steel C 45 (material nr. 1.0503). To improve the shape stability of the running surface the wheel disc has been hardened (heated to 840 °C

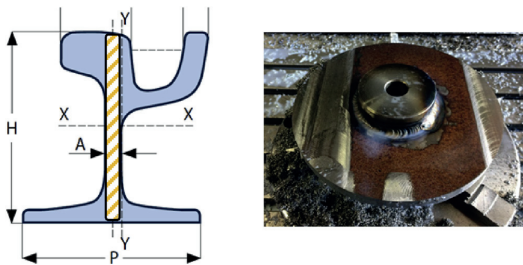


Fig. 2. Rail disc manufactured from a new UIC 59R2 profile rail, grade R220.

than quenched in oil). The transverse plane of the wheel disc diameter is flat. The wheel disc diameter is 240 mm.

3. Contact loading

Regarding the effect of scaling and simulation of the wheel-rail contact Jaschinsky [7] concludes exact similarity of the contact ellipse to be important with respect to the creep forces when these are not saturated. The shape of the contact ellipse is defined by the contact ellipse ratio a/b with a representing half of the contact width and b half of the contact length.

The ratio of the contact ellipses as well as the normal contact stress can be determined by the Hertz theory [11]. The aim is to choose the curvature of the discs together with the normal load in such a way that during testing the resulting contact patch dimensions and normal contact stress correspond to those that occur in track. To this end a representative train-track configuration has been selected which is known to develop RCF damage (Headcheck) in track; a Dutch VIRM intercity vehicle negotiating a 1200 m radius curve. Relevant track and vehicle details are presented in Ref. [2]. The calculated contact ellipse ratio a/b for this track-vehicle configuration, derived from the in Ref. [2] performed train-track simulations, is 2.7 with the mean contact stress being 1050 MPa. The in chapter 2 presented disc curvatures together with disc material properties (elastic modulus and Poisson's ratio) and an applied normal load of 900 N results in an a/b ratio and mean contact stress similar to the calculated vehicle-track reference situation.

The occurring friction coefficient can be calculated from the normal force (F_n), the longitudinal slip and the torque (T). If full slip occurs, the friction coefficient is equal to $\frac{T}{rF_n}$, with r being the radius of the disc. At low (partial) slip the coefficient of friction can be calculated using the Herz + FASTSIM algorithm. This algorithm is used to derive the figure below (Fig. 3), allowing the active coefficient of friction during testing to be determined from the graph.

Starting from the level of friction coefficient, creepages, normal load and disc curvature, the resulting value of wear index T_γ can be calculated using the FASTSIM algorithm [11] for wheel-rail contact evaluation. Since [7] concludes T_γ to scale proportional to the normal force an equivalent T_γ for a full size wheel can be calculated from the T_γ for the two disc set up (Fig. 4).

As explained by Ref. [6] the initiation of surface cracks takes place if

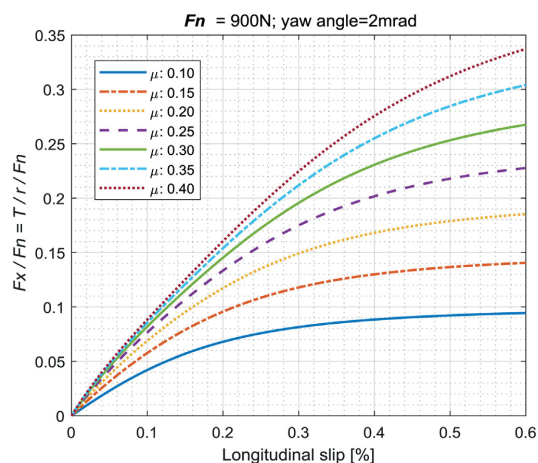


Fig. 3. Traction force relative to the normal force ($F_x/F_n = T/r/F_n$) as a function of longitudinal slip and friction coefficient. The graph is valid for a set angular rotation between the two discs of 2 mrad.

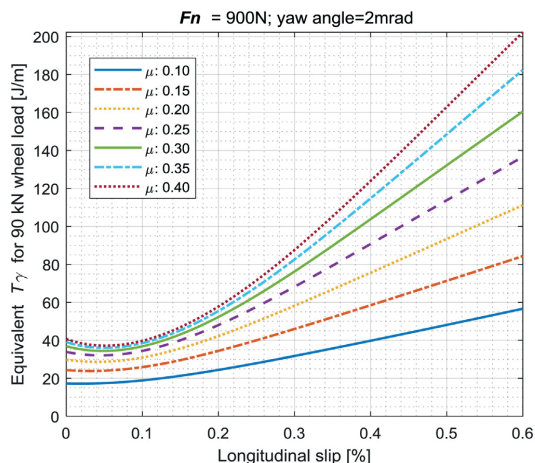


Fig. 4. Equivalent T_γ for 90 kN wheel load as a function of longitudinal slip and friction coefficient. The graph is valid for a set angular rotation between the two discs of 2 mrad.

the surface layer accumulates uni-directional plastic strain higher than the strain to failure. In rolling-sliding contacts, the amount of this accumulation is a function of the coefficient of friction, the maximum contact pressure and the shear yield strength of the material. Tyfour et al. also showed the initiation of fatigue cracks is connected to dry rolling-sliding test runs with relatively high levels of friction, positioning the maximum shear stress at the contact surface. Crack propagation is triggered when subsequent wet rolling-sliding test runs are applied. Due to lubrication the coefficient of friction will drop, relocating the maximum shear stress below the contact surface. At the same time fluid will be trapped within the cracks, stimulating crack propagation due to hydrostatic pressure build up and lubrication of the crack faces, both resulting in increased stresses at the crack tip. Since the purpose of the here performed study is to establish the RCF life as the number of rail-disc cycles required to initiate a fatigue crack only dry rolling-sliding tests have been performed.

4. Testing procedure

Prior to the start of each test run the contact surface roughness of both discs is measured as well as the surface cross sectional profile, after which the surfaces are cleaned using an degreasing agent. To provide initial strain hardening below the contacting surfaces a run-in period of 3000 dry cycles is applied with 1000 N of normal load and zero longitudinal slip. Subsequently longitudinal slip is applied. After the torque/friction has stabilized the resulting coefficient of friction is determined. Based upon the measured coefficient of friction the slip percentages are set and adjusted during testing accordingly to those that the desired T_γ loading value is achieved.

4.1. Assessing RCF-life

The 'RCF damage index' expresses the number of cycles before visible RCF cracks can be expected on the rail head. Burstow [1] suggests, for reasons of feasibility, a minimum surface length of approximately 2 mm, stating that cracks to be visible at this length must have developed beyond the initiation stage and some crack growth must have taken place. Similarly RCF life for the roller rig is defined as the number of rail disc rolling-sliding cycles required to initiate a fatigue crack of a visible length. With the 1:5 scale of the two-disc machine a crack length of 0.40 mm is applied here.

4.2. Crack detection/metallographic analysis

During the actual test-run operation the running surface is monitored after every 20.000 rail disc cycles (approx. 15 min of run time). Monitoring of the running surface consists of visual inspection using a stereo microscope. Early crack detection is further supported by Eddy current measurements. During each test run the rotational speed of both discs, the normal load and torque are continuously sampled. Every 100.000 cycles measurements regarding surface roughness and cross profile are repeated. After completion of the full test, surface roughness and profiles are again measured, after which the rail disc can be sectioned and prepared for metallographic analysis and hardness measurements.

5. Results and analysis

Index values with regard to the R220 RCF-damage function have been derived for two loading levels of T_γ . One selected level ($T_\gamma = 65 \text{ J/m}$) is positioned at the peak of the function, marking the transition from the RCF dominated region to the region of mixed RCF-Wear. From Ref. [1] the corresponding index value to this position is 100.000 cycles (Fig. 14). The other test loading level is chosen at $T_\gamma = 120 \text{ J/m}$ for which [1] indicates 200.000 cycles to visible RCF damage. Test results at the two applied T_γ loading levels are summarized in Table 1 and Table 2.

5.1. Surface crack detection

Surface crack development has been visually determined (Fig. 5). Surprisingly cracks at the rail disc running surface are seen to initiate only at the rail disc running surface positioned within the former rail head. At the here tested loading levels no cracks are seen to develop within the disc circumference machined from the rail web or foot area (Fig. 6).

5.2. Running band development

Due to wear and plastic deformation the shape of the rail disc running band is seen to widen during testing. At the T_γ loading level of 65 J/m the running band maintains a uniform appearance over the circumference of the rail disc. However, during testing at 120 J/m a wavy pattern is seen to appear; a repetitive widening of the contact band. This wavy pattern develops evenly over the rail disc circumference. Again cracks are only seen to appear within the rail disc circumference machined from the rail head. With the formation of this wavy pattern cracks no longer form uniformly over the running band but are seen to form in clusters, suggesting local differences in loading. These patches of cracks appear mainly in the wider parts of the running band however individual cracks are seen also at some of the narrow sections.

Table 1
Testing conditions and results for T_γ loading level = 65 J/m.

	Test number		
	1	2	3
Roughness (Ra) rail/wheel.	Initial: 0.26/0.69 End: 0.34/0.35	Initial: 0.21/0.66 End: 0.32/0.32	Initial: 0.22/0.62 End: 0.38/0.32
Friction coefficient, [run nr.]	0.40 [1]/0.18 [5]/0.18 [9]/0.18 [13]	0.40 [1]/0.25 [3]/0.23 [5]	0.40 [1]/0.23 [4]/0.22 [6]
Longitudinal slip (%), [run nr]	0.25 [1]/0.42 [5]/0.42 [9]/0.42 [14]	0.25 [1]/0.27 [3]/0.30 [5]	0.25 [1]/0.30 [4]/0.32 [6]
Lateral slip (%)	0.20	0.20	0.20
Normal load (N)	900	900	900
Contact area (mm ²) initial/end	0.74/1.29	0.94/1.25	0.96/1.35
Contact ratio (a/b) initial/end	3.0/1.2	2.3/1.4	2.3/1.3
RCF life (cycles to visual surface crack length of 0.40 mm)	0.6 mm crack length after 280.000 cycles	100.000	120.000

Table 2
Testing conditions and results for T_γ loading level = 120 J/m.

	Test number	
	1	2
Roughness (Ra) rail/wheel.	Initial:0.25/0.67 End:0.44/0.45	Initial:0.34/0.67 End:0.46/0.45
Friction coefficient, [run nr.]	0.45 [1]/0.29 [2]/ 0.21 [5]/0.20 [11]	0.45 [1]/0.35 [2]/ 0.23 [3]/
Longitudinal slip (%), [run nr]	0.40 [1]/0.50 [2]/ 0.65 [5]/0.65 [11]	0.40 [1]/0.50 [2]/ 0.64 [7]/0.69 [10]
Lateral slip (%)	0.20	0.20
Normal load (N)	900	900
Contact area (mm ²) initial/end	0.67/0.88	0.97/1.9
Contact ratio (a/b) initial/end	3.7/2.8	2.4/0.6
RCF life (cycles to visual surface crack length of 0.40 mm)	220.000	200.000

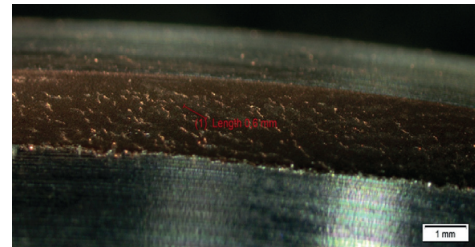


Fig. 5. Rail disc circumference initially located within the rail head area showing cracks at the running surface (load: T_γ 65 J/m, 280 k cycles). This part of the circumference is further referred to as 'area H'.

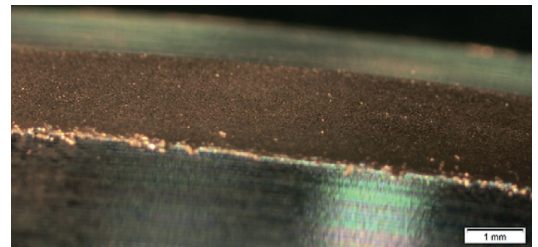


Fig. 6. Rail disc circumference initially located within the rail web area showing no cracks at the running surface (load: T_γ 65 J/m, 280 k cycles). This part of the circumference is further referred to as 'area W'.

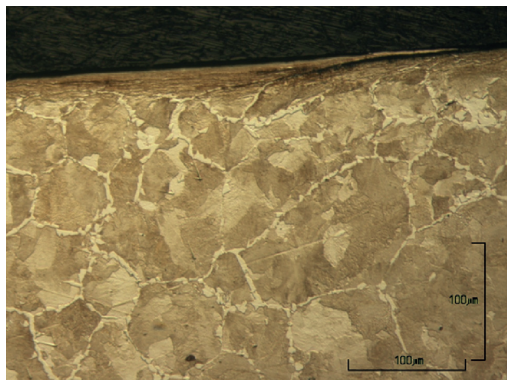


Fig. 7. Crack morphology of a flake, longitudinal cross section – area H (load: T_y 65 J/m, 280 k cycles).

5.3. Metallographic analysis

From the rail disc running surface at area H (head) and area W (web) both longitudinal and lateral cross sections were prepared for metallurgical examination. The morphology of the observed surface cracks at area H is characterized as a ‘flake’ (Fig. 7). The observed damage is similar to the in Ref. [6] presented damage after only dry cycle testing. Accordingly to Ref. [6] RCF crack development is caused when a dry cycle test sequence is followed by wet rolling sliding cycles. From the rail disc transverse cross section (Fig. 8), the deformation at the running surface as a result from the applied lateral slip can be observed.

The microstructure analysis shows clear differences between the rail disc material from the rail head (H) and rail web (W). Area H possesses a pearlitic structure with a network of ferrite positioned at the pre-austenite grain boundaries. Contrary to the microstructure of area H, the microstructure of transversal cross section of area W shows a significant higher percentage of free ferrite, displaying a dominant orientation (Fig. 9). This orientation is very likely to be the result of the rolling process during rail production. The observed difference in microstructure is reflected by the material hardness, measured at the non-deformed base material. The average micro hardness value at the rail web (W) is 266 HV(500 g) against 300 HV(500 g) at the rail head (H). From the differences in hardness and microstructure a difference in wear behaviour is to be expected. This is confirmed by the executed rail

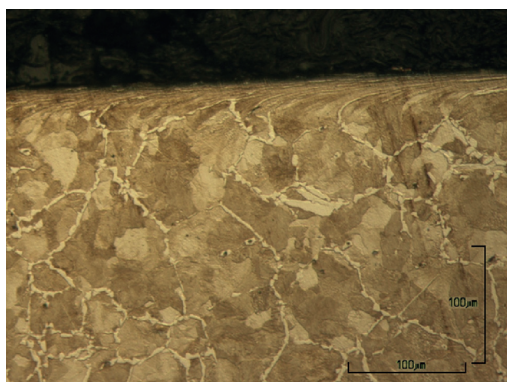


Fig. 8. Transverse cross section over the rail disc running surface, area H (load: T_y 65 J/m, 280 k cycles).



Fig. 9. Microstructure at area ‘W’(transverse cross section). The rail web material shows a texture composed of pearlite (brown) and lines of free ferrite (white). (For interpretation of the references to colour in this figure legend, the reader is referred to the Web version of this article.)

disc cross profile measurements, showing a difference in profile wear between the different circumferential sections. After 280 k cycles the measured maximum vertical wear at area H is 0.7 mm against 1.2 mm at area W. The increased wear rate at area W can explain for the absence of cracks in this part of the disc circumference, shifting the damage response within this section into the fully wear dominated regime.

5.4. Contact conditions

From the performed miniprof profile measurements the development of the contacting surfaces has been established. As shown in Fig. 10 the rail disc profile gets flatter and asymmetric. The asymmetry is caused by plastic deformation. It has been confirmed that high part of the profile develops with the direction of slip. The wheel disc does not show any significant change in profile.

Due to the shape of the rail disc profile, the contact pressure distribution and the T_y cannot be evaluated using FASTSIM. Therefore, Kalker full theory [11] has been applied, using our own Matlab implementation. Figs. 11 and 12 show the resulting contact pressure distribution. It can be seen that the maximum contact pressure decreases

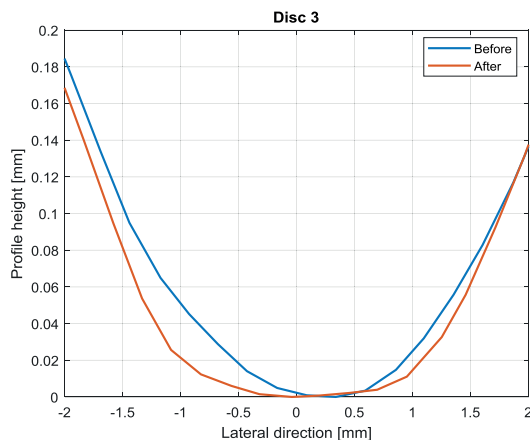


Fig. 10. The lateral profile of rail disc 3 before and after testing.

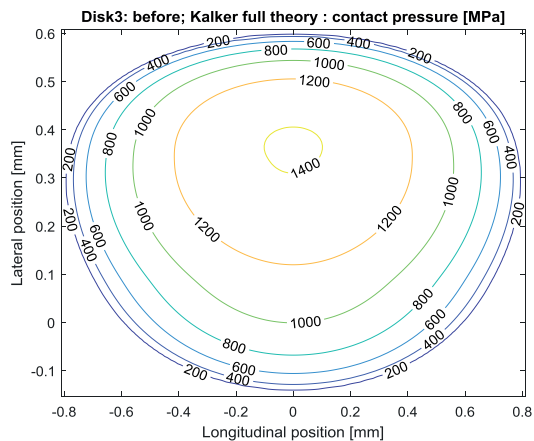


Fig. 11. Contact pressure of disc 3 before testing, as calculated using Kalker full theory.

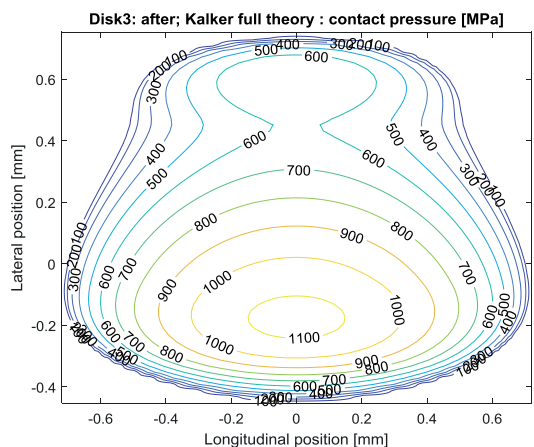


Fig. 12. Contact pressure of disc 3 after testing, as calculated using Kalker full theory.

during testing. However, the equivalent T_γ , as calculated using Kalker full theory, remains unaffected by the change in contact pressure distribution. Therefore Figs. 3 and 4 remain valid and may be used throughout the test for estimating the friction coefficient and calculating the T_γ at specified settings of the test setup.

5.5. Validation result

Damage function indices for the different T_γ loading levels have been determined from the observed cycles to the initiation of visual surface cracks with a length of 0.40 mm. The resulting indices are presented in Fig. 13. The RCF damage function of the R220 rail grade as established by Burstow [1] is shown by the black line. For the examined wear numbers (65 and 120 J/m) the rail disc indices established by two-disc testing can be observed to be in the same order of magnitude as that of the normal grade rail RCF damage function.

6. Discussion

RCF and wear behaviour of rail and wheel materials has been

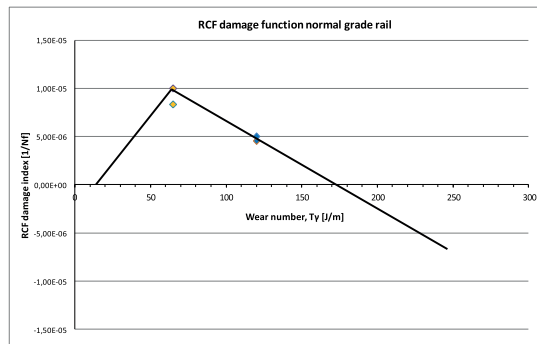


Fig. 13. Damage function indices at loading levels T_γ 65 and 120 J/m established with two-disc testing, depicted within the RCF damage function of normal grade rail as established by Burstow [1].

studied by means of two-disc testing also in the past. Many of these earlier studies focus on describing the wear behaviour with regard to specific loading conditions, usually applying longitudinal slip only. The aim of this study is to validate a two-disc test approach supporting future description of the full range of the RCF damage function, addressing both the RCF and wear dominated regime. The applied test rig configuration allows a contact angle to be set to one of the discs thus introducing, beside longitudinal slip from the set difference in circumferential speed, also lateral slip to simulate the dynamic conditions between wheel and rail when negotiating a curve.

Regarding test rig design, scaling issues and consequent design and loading choices in the test rig set-up are important especially from the viewpoint of contact patch ratio and normal contact stresses. The curvature of the discs together with the normal load are chosen in a way that the resulting contact patch dimensions, and normal contact stress during testing correspond to those that occur at Headcheck sensitive track locations.

Equivalent T_γ levels are calculated with respect to slip ratios (longitudinal and lateral), normal load and friction levels using the FASTSIM algorithm for wheel-rail contact evaluation. Depending on the development of the coefficient of friction between the two discs and the targeted value of T_γ the set longitudinal slip is adjusted. The applied range varied from a minimum value of 0.25% to a maximum of 0.69%. For all executed tests the level of friction coefficient is seen to stabilize at around 0.2 indicating this to be independent of the here applied values of longitudinal slip. Higher values of longitudinal slip are seen to result in an increase of the resulting surface roughness. Due to wear and deformation at the running band the rail disc profile is seen to change during testing. With increasing T_γ loading level an increase in wear rate can be observed. The equivalent T_γ , as calculated using Kalker full theory, remains unaffected by the observed change in profile and corresponding contact pressure distribution.

Similar to the RCF damage model of Burstow [1] which is based on visual crack length initiation in track, the RCF life for the roller rig is defined as the number of rail disc rolling-sliding cycles required to initiate a fatigue crack of a visible length. With the 1:5 scale of the two-disc machine a crack length of 0.40 mm is applied here.

Machining the disc from a rail resulted in part of the circumference to be positioned at the initial rail head, part in the web and part in the foot to the rail. Unlike the rail disc running surface positioned within the former rail head, the disc circumference from the web area is showing no crack initiation. From the differences in microstructure and hardness between the rail head and rail web material a difference in wear resistance is to be expected. This is confirmed by the executed rail disc cross profile measurements, with web wear rate being 1.7 times that of head wear. The higher wear rate at the web section can explain

for the absence of cracks in this part of the disc circumference, shifting the damage response within this section into the fully wear dominated regime.

For the examined wear numbers (65 and 120 J/m) the RCF damage function indices established by two-disc testing can be observed to be in the same order of magnitude as that of the normal grade rail RCF damage function as established by Burstow [1]. With increased T_γ and related wear loading a wavy pattern is seen to develop at the rail disc. Further investigation is required to understand the full impact of this development regarding testing conditions.

The RCF damage functions have significant engineering relevance. Their application allows for a dedicated rail grade selection, adapted to site-specific operational conditions. They can be used either in plain track and in the design of special parts of the rail network, such as switches and crossings and can be expected to significantly affect the life-cycle costs. The track engineer can use RCF damage functions to optimise track maintenance in relation to RCF generation. From track and traffic characteristics the mean value of the wear number T_γ along a curve or switch can be calculated. From these calculations track location specific T_γ look up tables can be set up. With the applicable RCF damage function, the accumulated fatigue index for the section can be determined from the average daily traffic. This can e.g. support a fit-for-purpose rail grade selection upon renewal. A validated method for a controlled quantitative determination of the RCF damage function will provide a solid base for a future optimisation of rail grade design, selection and maintenance. The two-disc laboratory set up allows RCF index values to be determined with more accuracy and higher resolution compared to field testing. This will allow RCF damage models to be derived with higher resolution, resulting in a more detailed understanding of the RCF behaviour of individual rail grades.

7. Conclusion

RCF-damage function indices have been established using a rolling-sliding two-disc laboratory set up. The applied test rig configuration allows both longitudinal and lateral slip to be introduced into the contact, corresponding to the dynamic conditions between wheel and rail when negotiating a curve. For purpose of laboratory set-up validation, performed tests investigate the damage response of the normal rail grade R220. For this rail grade the RCF-damage function is already available from field observations [1].

For the examined wear numbers the RCF damage function indices established by two-disc testing can be observed to be in the same order of magnitude as that of the normal grade RCF damage function as established from field observations. The validation result suggest that the two-disc approach can be used to support future work to establish RCF-damage functions within a well defined laboratory environment.

8. Future work

Further validation work could aim at T_γ loading levels within the regime of full wear ($T_\gamma > 170$ J/m). The development of the running band especially during testing at higher loading levels and how this

could affect the loading conditions needs to be further investigated. Two-disc testing can start to determine the RCF damage functions for a range of rail grades, from which the individual contribution towards (track) loading response and related rail grade selection can be appreciated.

The initiation of cracks/flakes during testing is seen to only occur at the rail disc running surface positioned within the former rail head, the disc circumference from the web/foot area showed no crack initiation. This difference in response to loading levels needs to be further investigated.

Acknowledgement

The authors would like to thank ProRail and especially ir. Bart Schotsman for supporting this work.

References

- [1] M. Burstow, Whole life rail model application and development for RSSB (T115) – continued development of an RCF damage parameter, Engineering Research Programme, Rail Safety & Standards Board, 2004.
- [2] M. Hiensch, M. Steenbergen, Rolling Contact Fatigue on premium rail grades: Damage function development from field data, *Wear* 394–395 (2018) 187–194 <https://doi.org/10.1016/j.wear.2017.10.018>.
- [3] D. Fletcher, J. Beynon, Development of a test machine for closely controlled rolling contact fatigue and wear testing, *Journal for Testing and Evaluation*, JTEVA 28 (4) (July 2000) 267–275.
- [4] M. Ishida, Y. Satoh, Development of rail/wheel high speed contact fatigue testing machine and experimental results, *Q. Rep.* 29 (2) (May 1988).
- [5] R. Lewis, et al., Mapping railway wheel material wear mechanisms and transitions, *JRR328, Proc. IMechE, Part F: J. Rail and Rapid Transit* 224 (2010).
- [6] W.R. Tyfour, J.H. Beynon, A. Kapoor, Deterioration of rolling contact fatigue life of pearlitic rail steel due to dry-wet rolling sliding line contact, *Wear* 197 (1996) 255–265.
- [7] A. Jaschinsky, On the Application of Similarity Laws to a Scaled Railway Bogie Model, thesis TU Delft (1990).
- [8] M. Gretzschel, A. Jaschinski, Design of an active wheelset on a scaled roller rig, *Veh. Syst. Dyn.* 41 (5) (2004) 365–381, <https://doi.org/10.1080/00423110412331300336>.
- [9] S.D. Iwnicki, A.D. Wickens, Validation of a MATLAB railway vehicle simulation using a scale roller rig, *Veh. Syst. Dyn.* 30 (3–4) (1998) 257–270.
- [10] N. Bosso, Comparison of different scaling techniques for the dynamics of a bogie roller rig, *Veh. Syst. Dyn.* 37 (sup1) (2016) 514–530, <https://doi.org/10.1080/00423114.2002.11666259>.
- [11] J.J. Kalker, Wheel-rail rolling contact theory, *Wear* 144 (1991) 243–261.
- [12] R. Stock, R. Pippan, RCF and wear in theory and practice—the influence of rail grade on wear and RCF, *Wear* 271 (2011) 125–133.
- [13] Hiensch, M. Dirks, B. Horst, J. van der Stelt, J. Rail Head Optimisation to Reach a Sustainable Solution Preventing Railway Squeal Noise, *Inter-Noise*, Istanbul, 2007 2007.
- [14] M. Kráčalík, G. Trummer, W. Daves, Application of 2D finite element analysis to compare cracking behaviour in twin-disc tests and full scale wheel/rail experiments, *Wear* (2016) 346–347.
- [15] W.R. Tyfour, J.H. Beynon, The effect of rolling direction reversal on fatigue crack morphology and propagation, *Tribol. Int.* 27 (1994) 273–282.
- [16] Y.B. Huang, L.B. Shi, X.J. Zhao, et al., On the formation and damage mechanism of rolling contact fatigue surface cracks of wheel/rail under the dry condition, *Wear* 400–401 (2018) 62–73.
- [17] W. Daves, W. Kubin, S. Scheriau, et al., A finite element model to simulate the physical mechanisms of wear and crack initiation in wheel/rail contact, *Wear* 366–367 (2016) 78–83.